Charles University

Faculty of Science

Study Programme: Biochemistry

Study Branch: Biochemistry

Bc. Kristýna Tomášová

Telomere Length in Colorectal Cancer

Telomerová délka u kolorektálního karcinomu

Diploma thesis

Supervisor: prof. RNDr. Marie Stiborová, Dr.Sc.

Consultant: MUDr. Pavel Vodička, CSc.

Prague 2019

Čestné prohlášení

Prohlašuji, že jsem tuto diplomovou práci vypracovala samostatně pod vedením školitelky prof. RNDr. Marie Stiborové, Dr.Sc. a konzultanta MUDr. Pavla Vodičky, CSc. a všechny použité prameny jsem řádně citovala.

V Praze, dne …….

.....

Kristýna Tomášová

Acknowledgments

I would like to express my gratitude to prof. RNDr. Marie Stiborová, DrSc., my supervisor, for her patient guidance and kind advices throughout my studies. Especially, I would like to extend my deep gratitude to MUDr. Pavel Vodička CSc., his wife MUDr. Ludmila Vodičková, CSc., Ing. Veronika Vymetálková, Ph.D., and the whole Department of the Molecular Biology of Cancer, Institute of Experimental Medicine Czech Academy of Sciences, where the research has been conducted and where I have carried out also my bachelor thesis. Special thanks go to my colleague Mgr. Michal Kroupa, who works on telomere research as well and who has motivated and supported me through this journey.

The research in this thesis would have taken far longer to complete without the encouragement from many others. I am particularly grateful for the assistance given by prof. RNDr. Marie Korabečná, Ph.D., and her Ph.D. student Mgr. Alžběta Zinková, who kindly helped me with the experimental part of the study. I acknowledge the contribution of Division of Molecular Genetic Epidemiology headed by prof. dr. Kari Hemminki in German Cancer Research Center based in Heidelberg, Germany, to sample analysis and I appreciate the data they provided me. Last but not least, I would like to thank Ing. Stanislav Kormunda, who carried out the statistical analysis.

Abstract

Telomeres are non-coding nucleoprotein structures that make up the very end of each linear chromosome. They stabilize chromosome structure and thus prevent the ends from being recognized by DNA damage response machinery. Telomere shortening in the synthesis phase of the cell cycle is related to the loss of protective ability and the finite replicative potential of the cell. The environmental factors, impaired DNA repair pathways, and loss of telomeric DNA-binding proteins exert negative effects on telomere function. Telomere dysfunction instigates chromosomal rearrangements and together with telomere erosion precedes tumorigenesis. Extension of telomeric DNA is catalyzed by the enzyme telomerase, whose activity is repressed in most adult somatic cells, except for stem cells, lymphocytes, and some cancer cell types.

Colorectal cancer comprises malignant tumors of the colon and rectum. It is the second most common cancer in both sexes in the Czech Republic, with over 81,000 cases diagnosed in 2013 and 55.2% overall survival at 5 years. This study focuses on the association of telomere length to clinico-pathological features of the colorectal cancer patients and investigates also the effect of cancer treatment on telomere length. Further, it compares two methods of telomere length measurement; the quantitative polymerase chain reaction and the multiplex quantitative polymerase chain reaction. Relative telomere length was evaluated in peripheral blood lymphocytes in repeated samples from 193 patients. We have observed significant telomere shortening in time period 0 - 1 year after diagnosis ($\chi^2(2) = 17.59$, $P = 0.0002$, $N = 74$, the 1^{st} - 3^{rd} sampling). Regarding telomere length and clinico-pathological and molecular traits of colorectal cancer, the shortest telomere length was observed in patients with proximal colon cancer (mean relative telomere length ± standard deviation in the 1^{st} sampling: 0.77 ± 0.31), followed by rectal (0.92 ± 0.32) and distal colon (1.00 ± 0.40) cancer patients. In all the patients we found a consistent decreasing trend in telomere length over time irrespectively of tumor stage and location. Moderately shorter telomere length was recorded in patients with high microsatellite instability. Regarding the treatment response, poor responders had on average longer telomeres in the 1^{st} (1.15 ± 0.29) and the 2^{nd} sampling (1.01 ± 0.25) compared to good responders (1.00 ± 0.33 in the 1^{st} sampling and 0.82 ± 0.30 in the 2^{nd} sampling).

Key Words: colorectal cancer, telomeres, telomerase, peripheral blood lymphocytes

Abstrakt

Telomery jsou nekódující nukleoproteinové struktury tvořící konce všech lineárních chromozomů. Jsou nezbytné pro zachování chromozomové stability a zabránění rozpoznání jejich konců dráhami na poškození DNA. Zkracování telomer v syntetické fázi buněčného cyklu souvisí se ztrátou jejich ochranné funkce a omezenou replikační schopností buňky. Negativní vliv na funkci telomer mohou mít také faktory životního prostředí, porucha opravných drah DNA a chybějící DNA-vazebné proteiny v oblasti telomer. Poškození telomer vyvolává chromozomové přestavby a narušení fyziologické délky telomer stojí na počátku vzniku nádorových onemocnění. Syntéza telomer je katalyzována enzymem telomerázou, jejíž aktivita je u většiny somatických buněk, s výjimkou buněk kmenových, lymfocytů a některých typů rakovinných buněk, umlčena.

Kolorektální karcinom, maligní nádorové onemocnění tlustého střeva a konečníku, je druhým nejčastějším nádorovým onemocněním mužů i žen v ČR. K roku 2013 bylo v ČR diagnostikováno více než 81 000 nových případů, celkové pětileté přežívání pro obě pohlaví činilo 55,2 %. Tato práce se zaměřuje na telomerovou délku v souvislosti s klinicko-patologickými daty pacientů s kolorektálním karcinomem a zkoumá také vliv léčby na telomerovou délku. Dále porovnává měření telomerové délky metodou kvantitativní polymerázové řetězové reakce a metodou multiplexové kvantitativní polymerázové řetězové reakce. Relativní telomerová délka byla měřena v periferních lymfocytech pocházejících z opakovaných krevních odběrů 193 pacientů. Statisticky významné zkracování telomer bylo pozorováno v intervalu 0 - 1 rok od diagnózy ($\chi^2(2) = 17.59$, $P = 0.0002$, $N = 74$, 1. - 3. odběr). S přihlédnutím ke klinicko-patologickým datům a molekulárním aspektům kolorektálního karcinomu byla nejkratší telomerová délka pozorována u pacientů s nádory v proximální části střeva (průměrná relativní telomerová délka ± směrodatná odchylka u 1. odběrů: 0.77 ± 0.31), a poté u nádorů rekta (0.92 ± 0.32) a distální části střeva (1.00 ± 0.40). U všech pacientů byla v průběhu času pozorována klesající telomerová délka nezávisle na stádiu a umístění nádoru. Kratší telomerová délka byla zjištěna v případě pacientů s vysokou mírou mikrosatelitové nestability. Pacienti špatně reagující na léčbu měli průměrně delší telomery (1.15 ± 0.29, 1. odběr, a 1.01 ± 0.25, 2. odběr) než pacienti na léčbu reagující (1.00 ± 0.33, 1. odběr, a 0.82 ± 0.30, 2. odběr).

Klíčová slova: kolorektální karcinom, telomery, telomeráza, lymfocyty periferní krve

Content

List of Tables

List of Figures

Abbreviations

36B4	reference gene encoding acidic ribosomal phosphoprotein P0
ρ	Spearman's rank correlation coefficient
χ^2	variance over the mean ranks
A	adenine
ANOVA	repeated-measures analysis of variance
ALB	gene encoding human serum albumin
ALT	alternative lengthening of telomeres
alt-NHEJ	alternative non-homologous end joining
ATM	ataxia-telangiectasia mutated kinase
ATR	Rad3-related kinase
BER	base excision repair
C	cytosine
c-NHEJ	canonical non-homologous end joining
CD	clusters of differentiation
cDNA	complementary deoxyribonucleic acid

CRC	colorectal cancer
Ct	cycle threshold
CV	coefficient of variation
D-loop	displacement loop
DDR	DNA damage response
DNA	deoxyribonucleic acid
DNA-PK	DNA-dependent protein kinase
dNTP	deoxyribonucleoside triphosphate
DSB	double-strand break
dsDNA	double-stranded DNA
E	amplification efficiency
F	value of variation between sample means
flow FISH	flow cytometry and fluorescent *in-situ* hybridization
G	guanine
HR	homologous recombination
hTERT	human telomerase reverse transcriptase
KRAS	gene encoding Kirsten rat sarcoma viral oncogene homolog
MLH1	gene encoding mutL homolog 1
MMqPCR	multiplex quantitative polymerase chain reaction
MMR	mismatch repair
MRN	complex consisting of meiotic recombination 11 protein, RAD50 double-strand break repair protein and Nijmegen breakage syndrome 1 protein
mRNA	messenger ribonucleic acid
MSH2	mutS homolog 2
MSH6	mutS homolog 6
MSI	microsatellite instability
MSS	microsatellite stable
N	sample size
NER	nucleotide excision repair
NHEJ	non-homologous end joining

NK cell	natural killer cell
OD	optical density
P	probability value
PBL	peripheral blood lymphocytes
PBS	phosphate-buffered saline
PCR	polymerase chain reaction
POT1	protection of telomere 1
qPCR	quantitative polymerase chain reaction
R^2	correlation coefficient
RAP1	repressor-activator protein 1
Rn	normalized reporter
RNA	ribonucleic acid
RNase	ribonuclease enzyme
ROX	6-carboxy-X-rhodamine
RT	reverse transcription
RT-qPCR	quantitative reverse-transcription polymerase chain reaction
RTL	relative telomere length
SD	standard deviation
ssDNA	single-stranded DNA
T	thymine
T-loop	telomere loop
TIN2	TRF1-interacting protein 2
TL	telomere length
TNM	tumor-node-metastasis, characteristics used in the tumor staging system
TPP1	telomere protection protein 1
TRF1	telomere repeat binding factor 1
TRF2	telomere repeat binding factor 2
Z	standard normal distribution value

1 Introduction

1.1 Colorectal Cancer

Colorectal cancer (CRC) is a disease that originates in epithelial cells of the large intestine (colon) or the rectum. In both sexes combined, CRC is the fourth most commonly diagnosed cancer (19.7% age-standardized incidence rate per 100,000) worldwide [1]. Of all new cancer cases in the Czech Republic, CRC is the second most common among both men and women (90 cases per 100 000 population in men, and 59 cases per 100,000 population in women). Approximately 90 % of all CRC cases occur in people older than 50 years of age [2].

Most often, CRC develops sporadically, and in less than 10 % of cases is caused by an inherited high-risk mutation. Genetic syndromes, which may predispose individuals to develop CRC, can be divided into those associated with colonic polyposis, e.g. familiar adenomatous polyposis and polyposis associated with mutations in MutY deoxyribonucleic acid (DNA) glycosylase, and those not associated with colonic polyposis, e.g. Lynch syndrome, also called hereditary nonpolyposis colorectal cancer [3,4].

Most sporadic CRCs start from an adenomatous polyp (adenoma), usually benign growth which arises from a mucosal layer of the colon or the rectum. There is about a 20% chance that these polyps will turn to adenocarcinoma. However, in unlimited time all adenomas would ultimately transform to malignancy [5]. Transformation of colorectal epithelium to polyp and then to tumor can be driven by microsatellite instability (MSI) [6], which results from defects in mismatch repair (MMR) genes. Further, it can be caused by chromosomal instability [7], aberrant methylation [8], or by defects in DNA damage response (DDR), particularly in the MMR pathway [9,10].

The genomic instability, one of the main characteristic of human cancers, can result from telomere attrition, because critically short, uncapped or in another way dysfunctional telomeres are more prone to chromosome fusion. Thus, telomere attrition is suggested as an initial event in colorectal carcinogenesis [11].

1.1.1 Colorectal Cancer Screening and Treatment

The success rate of recovery from CRC strongly depends on the stage of the cancer at diagnosis. An early-stage CRC does have no or non-specific symptoms like problems with bowel movements or vague abdominal pain, which can be mistaken for benign conditions and contribute to delayed diagnosis. Hence, CRC is often diagnosed at stage II or higher, when the chances for successful treatment and good quality of life decrease. The development and implementation of more specific screening methods to predict CRC before symptoms appear is the aim of the research.

In the Czech Republic, CRC screening is offered regularly as part of an organized program. All people age 50 to 54 undergo fecal occult blood test (gastrointestinal tumors are soft and tend to bleed easily). In the event of a positive test, the source of the blood is further specified by colonoscopy. People aged 55 and older can choose from two screening tools. They can receive a fecal occult blood test every two years or colonoscopy every ten years. People with a family history of CRC should begin screening for CRC earlier [12–14].

Patients treated for colon cancer usually undergo surgical removal of the tumor, which can be followed by adjuvant chemotherapy (therapy given in addition to the primary treatment). For rectal cancer, there is also commonly used radiation therapy, which is given before (preoperative, neoadjuvant radiotherapy) and/or after the surgery alone, or in conjunction with chemotherapy (chemoradiation). Therapy before the main therapy (which means surgery, in case of CRC) is called neoadjuvant and it is often used in locally advanced rectal cancer to decrease the size of the tumor before surgery and reduce local recurrence [15,16]. A commonly used chemotherapy for CRC is based on 5-fluorouracil and oxaliplatin or their combinations; folinic acid/5-fluorouracil/irinotecan (called FOLFIRI) and folinic acid/5-fluorouracil/oxaliplatin (called FOLFOX), which can be further combined with e.g. bevacizumab, cetuximab, panitumubab and others [17,18]. Not surprisingly, anticancer therapies are supposed to have an impact on the telomere length (TL) [19]. Thus, in the future, the TL could be an additional tool to monitor patients' response to cancer treatment.

1.2 Telomeres

Telomeres are repetitive DNA regions located at the very ends of eukaryotic chromosomes. In vertebrates, telomeres consist of the short repeats with the consensus sequence 5'-TTAGGG-3' and telomeres-associated proteins [A, T, G, and C are IUPAC nucleotide codes; A stands for adenine, T for thymine, G for guanine and C (does not occur in sequence) for cytosine]. The major part of telomeres comprises about 3 to 14 kilobases of double-stranded DNA (dsDNA) [20], ending in a 3' single-stranded guanine-rich overhang which is on average 130-210 bases long [21]. Telomeric terminus is arranged into a lariat like structure termed a telomere loop (T-loop), stabilized by a smaller displacement loop (D-loop) (**figure 1**). Although T-loop configuration is proposed to protect the telomere 3' end from DNA repair signaling [22], it potentially interferes with replication fork progression during the synthesis phase [23]. Therefore, the resolution and re-establishment of the T-loop after the replication must be tightly controlled.

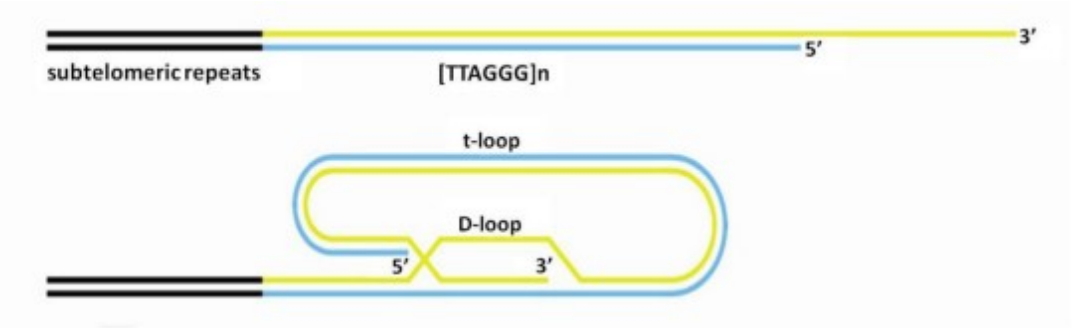

Figure 1. Telomere Structure. Guanine-rich 3' overhang loops back and invades to the dsDNA forming a T-loop, thereby simultaneously generates a triple-stranded D-loop. The loops formation is mediated by the shelterin complex (discussed below). The guanine-rich overhang can also fold into another secondary structures known as guanine quadruplexes, together with the T-loop involved in telomere end protection [24]. Figure adapted from Nanić and Rubelj [25].

1.2.1 Shelterin Protein Complex

The T-loop formation is coordinated and stabilized by a six-protein complex called shelterin or telosome. In humans, shelterin is composed of the telomere repeat binding factors 1 and 2 (TRF1 and TRF2), protection of telomere 1 (POT1), the telomere protection protein 1 (TPP1), repressor-activator protein 1 (RAP1) and the TRF1-interacting protein 2 (TIN2) (**figure 2**). Shelterin subunits TRF1 and TRF2 are preformed homodimers which bind directly to the telomeric dsDNA, while POT1 binds to the telomeric

3' single-stranded DNA (ssDNA). These DNA binding proteins are interconnected by the rest two; TPP1 and TIN2. TRF2 selectivity to dsDNA is induced by RAP1, which binds exclusively to TRF2 [26]. In general, shelterin complex is involved in maintaining the integrity of chromosomal ends, being responsible for telomerase recruitment to telomeres and inhibiting the undesired DDR, see chapter 2.3 below.

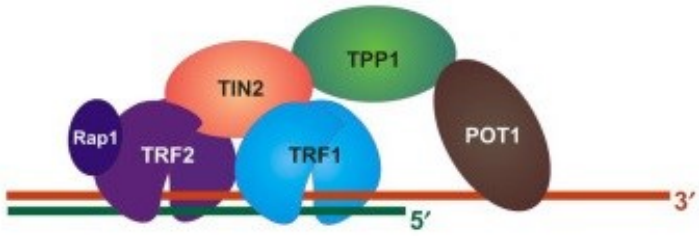

Figure 2. Shelterin subunits and their composition on telomere. TRF1 and TRF2 anchor shelterin complex to telomere and bind telomeric duplex DNA, POT1 binds to telomeric ssDNA. TIN2 and TPP1 bridge TRF1 and TRF2 to POT1 and mediate the protein complex assembly. RAP1 binds only to TRF2. Figure adapted from Ilicheva et al. [27].

TIN2 is a shelterin core hub that acts as a protein-protein interaction domain [28]. Via TPP1, TIN2 links TPP1/POT1 heterodimer to TRF1 and TRF2, complexing with RAP1 [29]. POT1/TPP1 is a processivity factor for telomerase, whose loading to ssDNA is dependent on TPP1 [30]. During the synthesis phase, TIN2-anchored POT1/TPP1 recruits telomerase to telomere through the TPP1-TERT telomerase subunit interaction [31]. Additionally, TPP1/POT1 loading on ssDNA is negatively regulated by TRF1 [32]. This suggests TRF1 involvement in telomerase-mediated telomere elongation and the information transmission between the double-stranded and single-stranded telomeric regions. Remodeling telomere into T-loop, as depicted in **figure 3**, is controlled mostly by TRF2, which facilitates guanine-rich strand tail invasion and hybridization to the telomeric dsDNA [33]. As a result of this process, dsDNA twists around and creates a larger T-loop and D-loop, which arise at its base in a region where the 3' overhang inserts back inside the dsDNA. POT1 is the only protein, which enables the shelterin complex to bind ssDNA at the 3' overhang and in the D-loop.

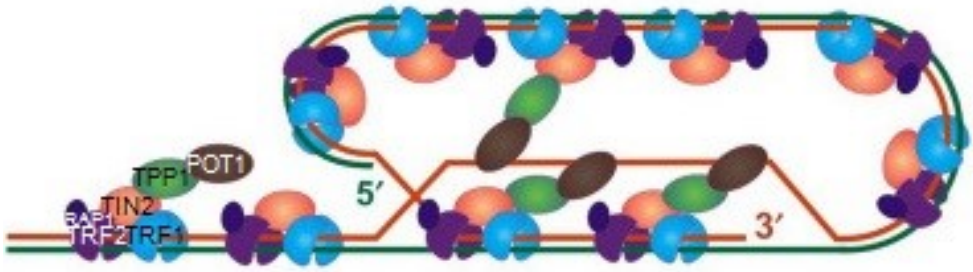

Figure 3. Shelterin subunits and their potential arrangement within the T-loop. Shelterin caps the telomere and coordinates telomere looping. Coating of telomeres by the shelterin is essential for preventing telomere dysfunction leading to the DDR, apoptosis or senescence. Figure adapted from Ilicheva et al. [27].

1.2.2 Telomere Shortening

Telomeres do not contain active genes, their role is strictly protective. Because eukaryotic chromosomes are linear, they face the so-called end replication problem, which results from the inability of DNA polymerases to completely replicate the chromosome ends. For this reason, each cell division of an average somatic cell loses 100 to 200 telomeric base pairs, a lymphocyte about 120 base pairs [34,35]. Hayflick and colleagues reported that human diploid non-malignant fibroblasts experience 50-60 divisions before entering replicative senescence [36,37]. The number of possible cell divisions a cell can undergo is now known as the Hayflick limit.

Telomere shortening (**figure 4**) explains the fact that human DNA polymerase cannot initiate DNA synthesis *de novo* and requires ribonucleic acid (RNA) primer with a free 3' hydroxyl group. After the DNA replication, primers in both leading and lagging strands are eliminated and replaced with DNA. The issue is an end gap arising on 5' termini due to the ultimate primer removal. Because DNA polymerase cannot attach the nucleotides to the 5' end, both daughter DNA strands have an incomplete 5' end with 3' guanine-rich overhang. Length of the 3' overhang depends on the distance from telomeric end to initial primer positioning, but it is always at least as long as removed RNA segment, i. e. about 10 nucleotides [38]. Telomere shortening also results from post-replication processing of 3' overhang [39,40].

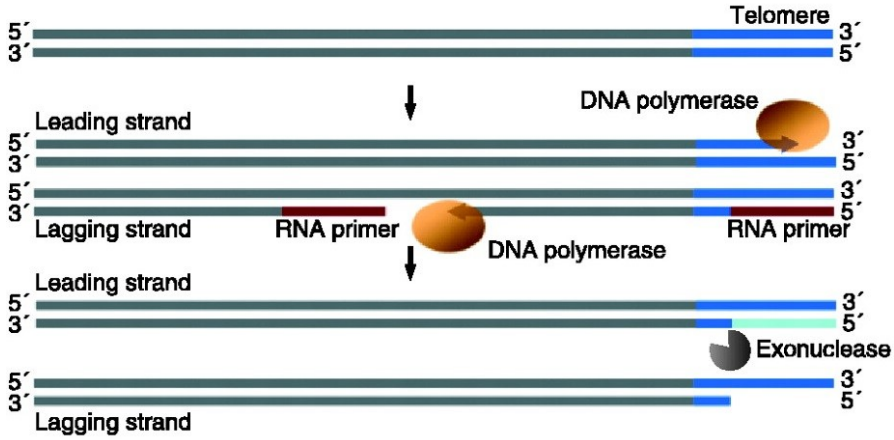

Figure 4. Telomere shortening mechanism. Because of the chromosome linearity, the lagging strand cannot by synthesized entirely and its 5' end remains incomplete. Figure adapted from Else [41].

Over time, telomeres progressively shorten and reach a critical length, and thus they cannot perform their protective function anymore. Cells with too short telomeres lose shelterin subunits and their chromosome termini become exposed and fusogenic. Rearrangements induced by DDR result in chromosome fusion, and during the mitosis can lead to genomic instability onset due to dicentric chromosome breakage followed by other breakage-fusion events.

The condition described above triggers, depending on the context in which the telomere uncapping occurs, cell cycle arrest (also called replicative senescence or mortality stage 1) and/or apoptosis. Entering the senescence is activated by cell cycle checkpoints pathways (e.g. by tumor suppressor proteins p53, retinoblastoma protein, etc.). If any of the checkpoints is crippled, cells bypass mortality stage 1 and telomeres are getting to a length of about 1.5 kilobases until a point called crisis (or mortality stage 2) [42]. This stage is characterized by widespread apoptosis, many dicentric and in other way aberrant chromosomes. Rarely, some of the cells extend their lifespan or become immortal by restoring telomerase activity and stabilizing TL. The indefinite proliferative potential is reputed to be an early step in the initiation of carcinogenesis.

1.3 Activation of the DNA Damage Response at Telomeres

Telomere biology and DDR are inseparably linked. Telomeres prevent cells from mistaking natural chromosome ends from DNA breaks and the activation of telomeric DDR. Without the repressive activity of shelterin, uncapped telomeres are recognized as double-strand breaks (DSBs) and processed primarily through non-homologous end joining (NHEJ) repair. Whereas canonical or classical non-homologous end joining (c-NHEJ) is a predominant pathway of DNA DSBs repair in subtelomeres [43], telomeric regions employ homologous recombination (HR) and alternative, also called microhomology or backup, non-homologous end joining (alt-NHEJ) mediated repair [44]. Unlike natural ends of chromosomes, internal telomeric DSBs are recognized by DNA damage sensors, such as ataxia-telangiectasia mutated kinase (ATM), deliberately. At functional telomeres, suppressing the DDR signaling thus varies according to DSB position (see **figure 5**).

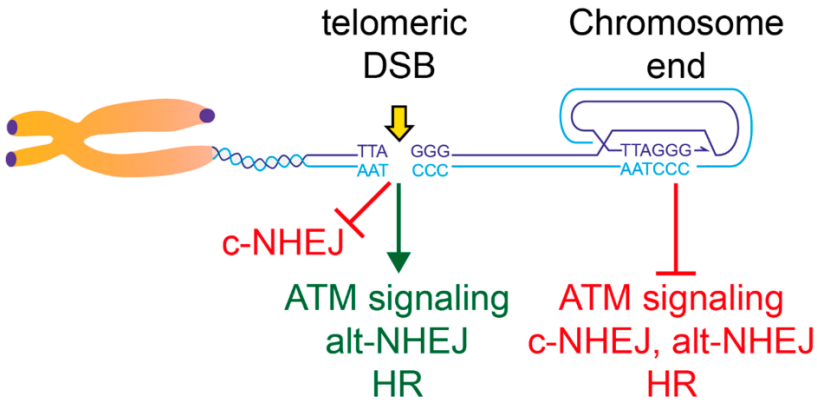

Figure 5. DSB response at telomeres. Internal DSBs are repaired by pathways, which are due to telomere end-protection on telomere termini repressed. Active pathways are highlighted in green color, inactive ones are highlighted in red color. Figure adapted from Doksani [45].

Present studies provide, however, very little information about other DNA repair pathways at telomeres. Telomeres proficiency for base excision repair (BER) correlates with their ability to fix oxidative DNA lesions, monitoring the telomeres by nucleotide excision repair (NER) and MMR is, however, disputable.

1.3.1 Non-Homologous End Joining

The NHEJ is a major DSB repair pathway that triggers the fusion of dysfunctional telomeres [46]. Although c-NHEJ directly ligates DNA ends without any sequence homology, alt-NHEJ involves 5-25 base pairs microhomologous sequences and uses the same initial DNA-end resection step as HR [47]. Engagement of c-NHEJ or alt-NHEJ relies on the type of telomere defect and also on its position. While c-NHEJ becomes employed in naturally shortened and TRF2 depleted telomeres [48,49], internal DSBs and ssDNA overhang lacking TPP1/POT1 are repaired by alt-NHEJ [44,48].

The function of NHEJ and also HR repair pathways is conditioned by three members of phosphoinositide 3-kinase-like family – ATM kinase, Rad3-related kinase (ATR), and DNA-dependent protein kinase (DNA-PK) [50,51]. ATM, ATR and DNA-PK act as DSB sensor proteins and are considered as hallmarks of dysfunctional telomeres. While ATM and ATR mediate series of protein phosphorylation events within the DNA damage checkpoints, DNA-PK is a core protein of c-NHEJ with possible involvement in the gap 2 phase of the cell cycle [52].

C-NHEJ is dependent on its core factors DNA ligase IV and Ku70/80 heterodimer, which together with DNA-PK catalytic subunit forms DNA-PK [53]. At the break, Ku encircles duplex DNA and recruits DNA-PK catalytic subunit, thereby activates its kinase function, and other downstream c-NHEJ factors [54]. Recent data suggests, that Ku heterotetramerization, the first step of c-NHEJ, is inhibited through TRF2 association with Ku70 [49]. Consistent with this assumption, *in vitro* findings showed that RAP1 depletion results in loss of TRF1 and TRF2 and manifests by c-NHEJ of telomeric termini [55].

Alt-NHEJ relies on its main components; poly(ADP-ribose) polymerase 1 and DNA ligase 3 and contributes to the repair of telomeric internal DSBs [56]. It is because initial end-resection at DSBs generates, due to TTAGGG repeating sequence, cohesive ends, and these microhomologies then become a substrate for alt-NHEJ [45]. Althougt alt-NHEJ is fully repressed at chromosome termini, its activity is unleashed at shelterin-free telomere overhangs in the absence of Ku70/80, which reflects shelterin and c-NHEJ factors inhibition effect [57,58]. These findings support the theory that at chromosome ends, alt-NHEJ can function as a backup pathway to c-NHEJ. Alt-NHEJ can be mediated via ATR signaling, which is at functional telomeres prevented e.g. by POT1/TPP1 [59]. The most presumable mechanism of ATR repression is that

POT1/TPP1 antagonizes replication protein A binding to telomeric ssDNA and prevents ATR signaling by excluding replication protein A from telomeres [60].

Alt-NHEJ-mediated telomere fusion was detected in both colorectal polyps and carcinomas [61]. What is more, non-malignant mucosal cells and polyps displayed similarly shortened TL and adenomatous polyposis coli gene mutations, which implies that telomere erosion precedes the initiation of colon adenoma formation.

1.3.2 Homologous Recombination

A DSBs within the internal telomeric regions can be processed by homology-directed repair, through alt-NHEJ (see chapter 2.3.1) and HR [44]. Both HR and alt-NHEJ share the initial nucleolytic degradation of the 5' ends in a process called end resection [62]. While HR proceed by ssDNA 3' strand invasion into the homologous sequence and its extension according to the template sequence, in alt-NHEJ-mediated repair exposed microhomologies anneal each other, overhanging bases are removed and the gaps then filled in by DNA polymerase. The initial DSB recognition and resection are promoted by MRN complex, consisting of meiotic recombination 11, RAD50 DSB repair protein, and Nijmegen breakage syndrome 1 protein, which further acts as a DNA damage marker. It seems that both HR and NHEJ factors are recruited to the site of DSB, if available, and that assembly of NHEJ factors precedes HR factors [63]. The preference of a particular DNA DSB repair pathway is probably based on the DNA end structure, location of DNA lesion and phase of the cell cycle [64,65]. However, the interplay between HR and NHEJ at telomeres is not fully comprehended.

A recombination-based telomerase independent mechanism of maintaining TL is called alternative lengthening of telomeres (ALT) and is employed in up to 10 % of human tumors, the remaining proportion utilizes telomerase. ALT phenotype is unique for cancer cells, which do not express telomerase and need to extend critically short telomeres [66]. The template for such DNA synthesis can be a sister chromatid or a telomeric DNA of the non-homologous chromosome [67,68]. Telomerase-positive cancer cells can after inhibition of telomerase activity switch to the ALT pathway [69], which makes an obstacle for telomerase-targeted cancer therapy [70]. ALT activity is assayed by telomeric cytosine-rich ssDNA circles [71]. These molecules are specific for ALT, but the underlying mechanism is unknown. Apart from the participation in ALT,

HR pathway apparently contributes to the formation of telomere protective structures, such as D-loop, at chromosome ends after replication [65].

The homology-directed repair at telomere ends is prevented through TRF2-RAP1 heterodimer. TRF2 and RAP1 cooperate to suppress telomere resection facilitated by poly(ADP-ribose) polymerase 1 and structure-specific endonuclease subunit SLX4, and their impaired interaction results in telomeric loss and sister chromatid exchanges [72]. Additionally, the TRF2-RAP1 complex suppresses HR repair in the absence of Ku70/80 [26]. TRF2 is considered to be the main repressor of DDR at telomeres also because acts as a direct inhibitor of ATM, by preventing its autophosphorylation on serine 1981 and subsequent p53 activation [73,74]. At functional before replication, T-loop by TRF2 prevents ATM signaling by blocking MRN complex from binding to telomere terminus [75].

In connection to CRC, it was found that microsatellite stable (MSS) and chromosomally unstable rectal cancers use ALT rather than telomere extension by telomerase [76]. The *in vitro* study on colon cancer cells with a defect in MMR protein mutS homolog 6 (MSH6) showed that telomerase inhibition in these cells induces ALT mechanism and that MMR insufficiency may be contributive to the engagement of the ALT pathway [77].

1.3.3 Base Excision Repair

BER pathway corrects small non-helix-distorting base lesions that arise due to oxidation, deamination, alkylation, hydrolysis, and also repairs ssDNA breaks. The BER pathway is initiated by a damage-specific DNA glycosylase that recognizes and removes altered base(s), and then further continues by short-patch repair or long-patch repair. Oxidative lesions at telomeres are together with the rest of the genomic regions maintained by BER.

Since guanine is the most readily oxidized base, telomeric guanine-rich motifs are very vulnerable to oxidative DNA damage, such as 8-oxo-7,8-dihydroguanine (8-oxoguanine) adducts and their dominant products 5-guanidinohydantoin and spiroiminodihydantoin [78,79]. Telomeres also contain other oxidatively modified DNA bases, e.g. thymine glycol [80]. BER promotion at telomeres, although less efficient upon some damaged base positions, was demonstrated on 8-oxoguanine DNA glycosylase

involved in 8-oxoguanine removal [81]. Other studies also reported recruitment of BER DNA glycosylases, such as endonuclease VIII-like 1, endonuclease VIII-like 3 and endonuclease III-like 1, recruitment of DNA polymerase β, flap endonuclease 1, etc., to the DNA damage [78,82].

As for shelterin proteins, POT1, TRF1, and TRF2 were found to allow the proteins of long-patch BER to access the damaged DNA [83]. TRF1 also interacts with endonuclease VIII-like 3, which cleaves thymine glycol bases and initiates long-patch BER [78,84]. Further, thymine glycol and misincorporation of uracil to thymine decrease recognition by POT1 [85,86].

In summary, available studies conclude that telomere loss is largely driven by oxidative damage and that BER is the important DDR pathway in the maintenance of telomere integrity [87,88].

1.3.4 Nucleotide Excision Repair

NER is responsible for removing helix-distorting DNA lesions caused by exogenous agents, such as chemicals (e.g. intercalating agents) or ultraviolet radiation. Although telomeres are liable to ultraviolet-induced dipyrimidine photoproducts, such as cyclobutane pyrimidine dimers, NER proficiency at telomeres remains unclear. Telomeres likely tolerate some unrepaired lesions. Chronically irradiated cells with high levels of telomeric cyclobutane pyrimidine dimers do not experience telomere shortening and continue to proliferate [89]. A later study conducted in cells found that xeroderma pigmentosum group A protein, a core component of NER, seems to be involved in photoproducts removal [90]. Compared to the bulk genome, purified telomeric fragments exhibited comparable amounts of ultraviolet light lesions. However, the pre-incubation of purified telomeres with TRF1 significantly reduced photoproduct formation at telomeres. The study indicates that telomeres are partially protected by shelterin against ultraviolet-induced DNA damage. The impact of bulky DNA adducts induced by chemical agents on telomere length and integrity was not investigated, yet.

1.3.5 Mismatch Repair

MMR facilitates the repair of mismatched bases generated by DNA polymerase during replication. Satellite sequences, including telomeres, are more prone to polymerase slippage during DNA replication. If unrepaired, the slipped-strand mispairing may yield a frameshift event. Impaired MMR gene function thus leads to mutations that accumulate in repetitive regions and consequent MSI. Around 15 % of sporadic and 86 % of hereditary CRC is characterized by MSI [91,92]. It is no wonder that MSI is a molecular hallmark used to identify hereditary CRC, and also both a predictive and a prognostic marker for sporadic CRC. In hereditary forms of CRC, MSI has been attributed to germline mutations in MMR, in sporadic cases, the majority of MMR deficiencies occur due to aberrant hypermethylation of 5' cytosine-phosphate-guanine island promoter of MMR gene *MLH1*, encoding mutL homolog 1 [93,94].

In numerous CRC studies, defect in a key MMR gene *MSH2*, encoding mutS homolog 2, was related to telomere shortening, end-to-end fusion and attenuation of DDR at telomeres [92,95–98]. The study of individuals from Lynch syndrome families showed that cancer-affected MMR gene mutation carriers had significantly shorter telomeres than cancer-free mutation carriers [99]. Subsequently, the same collective of authors linked longer TL to Lynch syndrome-associated cancer risk in MMR-proficient carriers [100]. Loss-of-function mutations in some MMR proteins seem to promote ALT. Bechter et al. reported that telomerase and MMR gene *MSH6* deficient colon cancer cells exhibited the ALT pathway and increased sister chromatid exchange [77]. Increased prevalence of ALT was observed in MMR-deficient patients with gastric cancer, too [101]. Telomeric repeats may be also present in non-terminal regions of chromosomes. ATPase activity of MLH1 is important to suppress the insertion of aberrant telomeric sequences, called interstitial telomeric sequences, at intrachromosomal sites [102,103].

Lastly, it can be said that defective MMR proteins have various effects on telomere recombination and attrition. Although the repetitive nature of telomeric DNA provides a hint of susceptibility to potential mismatch incorporation, presence of mismatches at telomeres, the mechanism of their recognition, and anticipated impact on shelterin binding affinity to DNA remain unanswered. In summary, maintenance of telomeric ends by proteins involved in MMR was not acknowledged.

1.4 Telomere Biology and Novel Approaches to Cancer Screening

Telomere shortening has been implicated in risk for aging-related diseases, such as Werner syndrome and cardiovascular diseases [104,105], and for developing many cancers, e.g. tumors of the urinary bladder, breast, digestive system, endometrioid, head and neck, lungs, and renal cancer [106–112]. A possible elevated risk associated with short TL show especially cancers of the head and neck, lungs and urinary bladder, and with long TL endometrial, breast and kidney cancers. Regarding CRC, the association between lymphocytes TL and CRC risk and prognosis was not definitely validated.

Studies of telomere attrition are predominantly conducted on pairs of matched tumor and adjacent healthy tissue samples, or less often on peripheral blood lymphocytes (PBL). TL in tumor tissue can be a potential marker of cancer prognosis, but it is neither a suitable tool in cancer detection nor an applicable risk assessment tool. CRC studies evaluating TL in tumor and adjacent healthy tissue reported significantly shorter telomeres in tumor tissue [113,114]. The same association was reported in the study conducted in our laboratory and, moreover, the smaller TL ratio between tumor tissue and adjacent mucosa was associated with better CRC prognosis [115]. Further, TL in tumor tissue was associated with a *KRAS* mutation, a gene encoding Kirsten rat sarcoma viral oncogene homolog [114].

Compared to tissues, blood, urine or fecal sampling is a minimally invasive procedure and thus represents an easily obtainable material for cancer screening, including CRC [116,117]. In body fluids, traces of a tumor's genetic material, such as circulating tumor DNA fragments and circulating tumor cells, can be tested by so-called liquid biopsy. This technique is a new, gentle alternative to surgical biopsies of solid tissue, and enables real-time assessment of the molecular profile of the tumor. It was estimated that from tumor reaching the size of 100 grams, corresponding to approximately 3×10^{10} neoplastic cells, 3.3 % of tumor tissue DNA is found into bloodstream each day [118]. DNA, occurring in stool through natural exfoliation, is used for the detection of tumor markers [119]. However, human DNA in stool is highly heterogenous. Its content is only 1 to 0.01 %, and tumor DNA originates from 1 % of the cells sloughed [120]. Particularly in gastrointestinal cancer, liquid biopsy has promising potential for future clinical implementation [121]. The main source of liquid biopsy in CRC is peripheral blood, less frequently stool. Interestingly, Fujii et al. found that tumor-derived cell-free DNA in urine evinced the same *KRAS* mutations as

CRC tissue [122]. Likewise, changes in TL based on cell-free urinary DNA may be suitable biological material not even for urological tract cancers.

1.5 Telomerase

It is well known that telomeres shorten with increasing cell age. Telomere shortening occurs in 85–90 % of malignant cells counteracted by enzyme telomerase, RNA-dependent DNA polymerase [123]. The rest of these cells utilize ALT [124]. Under physiological circumstances, the telomerase is active in germ, embryonic cells, and some white blood cells like B and T lymphocytes [125]. In cells that underwent terminal differentiation, telomerase becomes silenced and shortening telomeres causes their finite proliferative life span. In telomerase-positive cells, telomere shortening is arrested and telomeres are continually being built up by adding repeat sequences to the 3' end (depicted in **figure 6**) [42]. As TL is proportional to a cell replicative capacity, telomerase expression renders cells to be immortal. Interestingly, telomerase extends preferably shorter telomeres and does not act on all telomeres in each cycle [126]. Telomerase recruitment is mediated by shelterin protein TIN2 and other telomere-associated proteins [28,127].

In humans, telomerase consists of human telomerase reverse transcriptase (hTERT), a catalytic protein subunit of the enzyme, and an integral telomerase RNA component (hTERC), which specifies the sequence for telomere synthesis. Functional telomerase holoenzyme also contains H/ACA small nucleolar ribonucleoprotein with dyskerin, NOP10 and NHP2 ribonucleoproteins, and nuclear assembly factor 1 ribonucleoprotein, later replaced by GAR1 ribonucleoprotein [128]. While *hTERC* seems to be ubiquitously expressed in all somatic cells, *hTERT* is expressed only in telomerase-positive cells [129]. Therefore, transcriptional activation of *hTERT* is a rate-limiting step for telomerase activity and the activity can be reflected in the level of *hTERT* expression [130–132]. Further, it was found that *hTERT* upregulation correlates with alterations on its promoter [133]. These changes are the most frequently point mutations and aberrant promoter methylations [134–136].

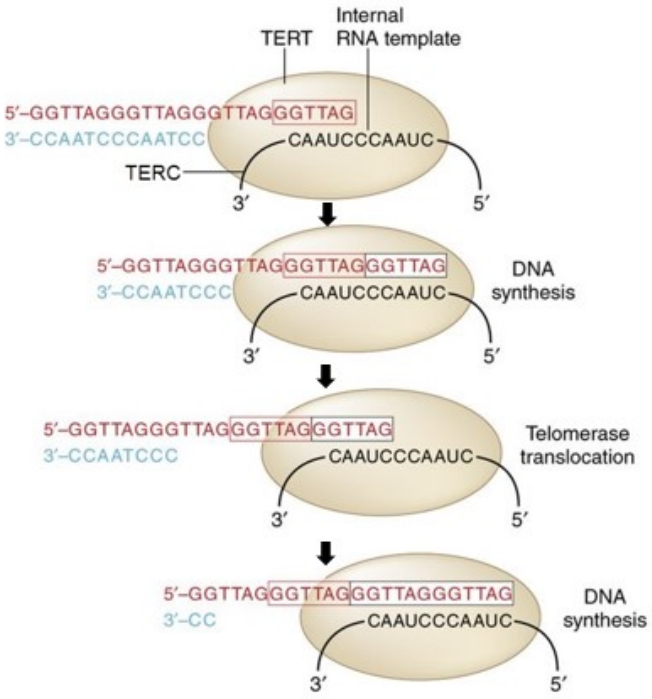

Figure 6. Telomerase mechanism of telomere synthesis. Telomerase subunit hTERC hybridizes 3' guanine-rich overhang at the end of the chromosome. Subsequently, RNA is used as a template for hTERT and telomere synthesis is accomplished to the very end of the template. The telomerase complex then relocates along with the template and synthesizes additional repeats. Once the telomere guanine-rich (leading) strand is elongated, DNA primase and DNA polymerase can finish the synthesis of the complementary cytosine-rich (lagging) strand. Figure adapted from Sarek et al. [137].

Telomerase activity is an independent marker of poor clinical outcome in cancer, including CRC [138–140]. Because most somatic cells exhibit none or weak telomerase activity, telomerase inhibitors could be very useful for selective targeting of cancer cells [141]. Recently, Jeung et al. described that telomerase activity in CRC patients is regulated by alternative splicing of hTERT pre-messenger ribonucleic acid, which implies that the hTERT expression level may not always correlate with telomerase activity [142]. Further, Ayiomamitis et al. observed different telomerase and MutL homolog 1 profiles in cancer cells from colon and rectum, in which case colon cancer cells had significantly higher telomerase level and were more frequently MutL homolog 1 proficient [143]. Moreover, p53 status was confirmed to inversely correlate with telomerase activity, which points to the impaired regulation of the cell cycle and apoptosis in these cells.

1.6 Lymphocyte Telomere Length

Peripheral blood mononuclear cells, a biological material used in this study, represent blood cells having a round nucleus, which can be categorized into monocytes and cells of lymphoid lineage; B-lymphocytes, T-lymphocytes, and natural killer cells (NK cells). As mature myeloid cells (and so monocytes as well) are differentiated and do not divide [144], lymphocytes undergo proliferation [145–147]. In humans, lymphocytes account for about 90 % of peripheral blood mononuclear cells [148]. Thus, in the following chapters of the diploma thesis we used the term PBL.

Studies confirmed that telomere attrition in both lymphoid and myeloid cell lineages is associated with age [149,150]. Telomere shortening has been also observed during naive T-lymphocytes differentiation to memory T-lymphocytes and during $CD28^+$ T-lymphocytes differentiation to $CD28^-CD8^+$ T-lymphocytes (the clusters of differentiation, abbreviated as CD, refers to antigens present on the surface of leukocytes) [151,152]. Besides that, altered PBL TL is linked to some types of blood cancer, such as acute myeloid leukemia and myelodysplastic syndromes [153], and several above-mentioned malignancies [106–112]. Present findings of Lin et al. show that TL changes in $CD4^+$, $CD8^+CD28^+$, and $CD8^+CD28^-$ T-lymphocytes and B-lymphocytes are in each individual person correlated, and thus it is likely that PBL TL is regulated systematically [154]. PBL TL can oscillate between elongation and shortening in the order of months [155]. Comparing different human tissues, the most variable TL was observed specifically in PBL, and in addition to that PBL and tissue telomeres did not demonstrate synchronous maintenance [156].

During the immunological response, the cells of adaptive immunity are induced to extensively multiply or differentiate. Although telomerase may be active in NK cells and both naive and activated T and B-lymphocytes [157,158], its level is tightly regulated and differ among particular T and B-lymphocyte subsets and also among the resting and stimulated forms [150]. Telomerase rapid increase was after the hTERT-transduced $CD8^+$ and $CD4^+$ T-lymphocytes activation observed by Hooijberg et al. and Roth et al. [159,160]. The study of T-lymphocytes conducted by Huang et al. further suggested that telomerase activity is required during long-term lymphocytes proliferation due to critical telomere loss, not for short-term proliferation even if telomerase is presented [161]. Roth et al. reported that memory T-lymphocyte *hTERT* up-regulation

decreases over time upon activation and inversely correlates with the replicative history of the cells [160]. Thus telomerase likely limits the growth of T-lymphocytes. Progressively, telomerase is not able to maintain the lymphocyte TL and owing to proliferation, the telomeres are getting shorter. Therefore, it can be assumed that maintenance of the TL protects blood cells from premature telomere erosion and prolong their involvement in the adaptive immune response.

In CRC patients it was confirmed that PBL TL dynamics is a result of regulatory mechanisms associated to the presence of a tumor [162]. In the study, high lymphocytes infiltration within the tumor correlated with the short TL in PBL. The abundance of tumor-infiltrating lymphocytes signifies a MSI phenotype of CRC tumors [163]. MSI association with improved diagnosis and high presence of tumor-infiltrating lymphocytes in nearly half of the MSI-high CRC cases provide plausible evidence that MSI CRC better prognosis is reliant on the increased immunogenicity of a tumor [164,165]. This is not applicable in the combination with MSI-high and cytosine-phosphate-guanine island methylator phenotype-positive tumors [166].

The short TL in CRC patients was significantly associated with higher PBL $CD4^+$ T-lymphocyte fraction (Chen *et al.*, 2014), which confirms that the function of adaptive immune system changes with the altered TL (see above). Adaptive immune system aging and its relation to the TL was summarized by Kaszunowska [167]. A study on 94 patients by Mzahma et al. comparing the TL in CRC tissues and corresponding PBL samples confirmed the TL correlation between these two types of samples [168], but the others did not prove this association [115]. In general, the tumor tissue showed a shorter TL than PBL.

1.6.1 Leukocyte Telomere Length Association to Colorectal Cancer Risk

Present findings describing PBL TL dynamics in relationship to CRC risk are ambiguous. Two studies, comprising 441 CRC cases and 549 healthy controls and 598 CRC cases and 2,212 healthy controls, reported an elevated CRC risk in individuals with both extreme short or extreme long PBL telomeres, suggesting a U-shape association [169,170]. In the latter study, a U-shape relationship correlated with age as well. Among younger individuals (≤ 50 years of age) with shorter telomeres, CRC risk was 2 - 6 times higher, older individuals (> 50 years of age) with shorter telomeres had the CRC risk increased 2–12 times. A possible U-shaped association with

the rectal cancer was also suggested by Pellat et al. [171]. In addition to that, their case-control study of 249 colon cancer cases and 371 controls and 276 rectal cancer cases and 372 controls found that after adjusting for age and sex, a longer TL was significantly related to reduced colon cancer risk.

Other studies indicate that the theory, assigning very short or very long telomeres to CRC risk, might be correct. The publication, including 628 Chinese patients with CRC and 1,256 healthy controls, revealed a significant association between short PBL TL and increased CRC risk [172]. Further, Chen et al. published that short PBL TL occurs in patients with advanced TNM (tumor-node-metastasis) stage (III and IV), and have a relation to worse CRC prognosis and adaptive immune response stimulated by $CD4^+$ helper T-lymphocytes [173]. Ninety patients in the training set, 96 patients in the testing set and an independent cohort of 395 patients participated in the research. In contrast, the present largest cohort study, comprising more than 26,000 participants with 776 CRC cases included, reported that longer PBL TL is linked to a higher risk for CRC, particularly in the rectum [174].

Above all the studies, which reported a null association of PBL TL with CRC, it should be noted the large case-control study involving 2,011 individuals: 384 CRC cases, 544 high and 537 low-risk adenoma patients and 546 colonoscopy-negative controls [175]. However, the above study identified significantly longer telomeres in CRC patients, comparing to colonoscopy-negative controls. Also, the prospective cohort study of 28,000 women, with 134 incident CRC cases and 357 age-matched controls, found no evidence linking PBL TL with CRC risk [176]. These findings are in concordance with the other two studies; the prospective cohort study in 14,916 men with 191 incident cases and 306 controls matching on age, smoking, and length of therapy, and the prospective case-control study in 185 cases and 406 controls [177,178]. In the retrospectively designed study, however, where authors of the latter named study reported on a data set of 2,249 CRC cases and 2161 matched-controls, after adjusting for age and gender, a significant association between the shorter TL and cancer status [178]. The authors of the former study reported that TL negatively correlates with age [177]. Despite the conflicting results, imposed by large CRC heterogeneity, relatively low numbers of patients due to the variable clinical features of the disease, the topic indeed merits further investigation.

2 Aims and Objectives of the Thesis

The general purposes of this study were to analyze the clinical manifestations of the PBL TL in CRC patients and to investigate the association of TL with the prognosis and clinico-pathological features of the patients. Further, utilization of PBL TL as a potential non-invasive blood biomarker for CRC treatment management was investigated.

The study aimed to monitor TL of patients in the course of the disease. The main objectives were:

I. To compare two quantitative polymerase chain reaction-based methods for measuring the relative telomere length (RTL) and find out if there is a correlation between the values obtained by both methods.
II. To investigate, whether and how the telomere length changes over time, and to determine the correlation between the telomere length and selected study population characteristics. A particular attention was paid to changes of TL after treatment since sequential samplings enabled this approach.

The research currently underway in our Department follows the objectives described above and focuses on telomerase activity, determined by *hTERT* gene and protein expressions. This study includes the same group of patients as in the case of monitoring the TL.

The main objectives are:

I. To elucidate the role of *hTERT* messenger ribonucleic acid (mRNA) expression as a prognostic marker in CRC.
II. To determine whether there is a correlation between the PBL TL and *hTERT* mRNA expression.

Even though the determination of telomerase activity is beyond the scope of this diploma thesis, a principle of the methods used to measure *hTERT* mRNA expression and illustrative *hTERT* mRNA expression data are stated in this diploma thesis, too.

3 Materials and Methods

3.1 Study Population

Peripheral blood samples from 172 newly diagnosed, untreated and histologically confirmed CRC patients (1st sampling) were obtained at Thomayer Hospital in Prague, Czech Republic. In the case of another group of 21 patients, the samples were missing. Blood specimens obtained from this group of patients were taken at a later date after initiation of therapy, and thus were classified as repeated. The repeated samples were collected periodically half a year (2nd sampling of 158 individuals), one year (3rd sampling of 125 individuals) and one and half year (4th sampling of 29 individuals) from the time of patient's diagnosis. Complete set of samples (comprising four different samplings) was available from 13 patients, the first three samples from 74 patients. For the rest of 142 patients, only the first two samples were drawn. In all, we collected 484 samples from 193 patients.

All participants provided a written informed consent before entering the study. Sampling of peripheral blood was carried out according to the ethical standard of the World Medical Declaration of Helsinki. Clinicopathological characteristics of all patients were collected from the medical records, personal data were acquired from lifestyle questionnaires. Only collaborating clinicians could disclose the identity of the participants, since they entered the study coded.

3.1.1 Patient's Stratification for Telomere Length Data Analysis

On the basis of the personal data, clinico-pathological and lifestyle characteristics, patients were clustered into the subgroups according to their age (using median split), gender (males vs. females), cigarette smoking habit (smokers vs. non-smokers), primary tumor site (proximal colon, distal colon and rectum), TNM stage (0 + I + II vs. III + IV), microsatellite status (MSS vs. MSI), therapy response (good responders vs. poor responders), use of the neoadjuvant therapy in rectal cancer cases (yes/no) and type 2 *diabetes mellitus* status (diabetics vs. non-diabetics). Individuals, for whom these sub-criteria were not available, were excluded from particular analyses. Baseline characteristics of the patients are outlined in table 1.

Table 1. Patients' clinical and demographic characteristics. A total number of patients N was 193. SD stands for standard deviation.

Characteristic	Frequency
Median age at diagnosis (range)	67 years (34−88)
Gender	**N (%)**
Male	123 (63.73)
Female	70 (36.27)
Tobacco use (Missing data N = 10)	
Smoker	43 (23.50
Non-smoker	140 (76.50)
Site of the primary tumor (Missing data N = 2)	
Proximal colon	35 (18.33)
Distal colon	83 (43.46)
Rectum	73 (38.21)
Type 2 *diabetes melitus*	
Diabetic	42 (21.76)
Non-diabetic	151 (78.24)
TNM stage group	
0+ I+II	13 + 59 + 55 (65.80)
III+IV	42 + 24 (34.20)
Microsatellite status (Missing data N = 34)	
Stable	136 (85.53)
Instable	23 (14.47)
Response to therapy (Missing data N = 106)	
Good	61 (70.11)
Poor	26 (29.89)
Neoadjuvant therapy (rectal cancer patients)	
Yes	46 (63.01)
No	27 (36.99)

To verify the common knowledge that telomere shortening is connected to aging, patients were divided into two groups based on their median age. The connection between gender and TL was tested between men's and women's groups. Cigarette smoking impact on TL was tested in two groups. As smokers were classified current and former smokers who had quit smoking within the past 5 years. Non-smokers were the patients who reported that they had never smoked and former smokers who had quit smoking more than 5 years before diagnosis.

Further, TL was compared between the groups of patients spanning in early (0 and I + II) and late (III + IV) stages of tumor progression. Tumor staging was done by Union for International Cancer Control TNM classification of tumors, where T describes the size of the primary tumor and its extent in nearby tissue, N refers to the number of regional lymph nodes to which cancer has spread and M describes the spread of cancer to different parts of the body. TNM classification divides patients from least (0) to most severe

(IV) TNM stages (see **table 2**). Stage 0 is carcinoma *in situ*, an early, non-invasive form of cancer. In contrast to stage 0, stage I is assigned by cancer cells growing beyond mucosa and in stage II, cancer continues to grow through the muscle or outer layer of colon or rectum. In Stage III, cancer affects the nearby lymph nodes. Stage IV is then a final stage characterized by cancer spreading to distant sites (particularly liver).

Table 2. TNM Staging Classification of Colon and Rectal Cancer. A combination of each of the T, N, and M variables correspond to stages 0–IV, where IV is the most advanced. Adapted from Nelson et al. [179].

	Characteristics
Tumor (T)	
Tis	Carcinoma *in situ*
T1	Tumor invades submucosa
T2	Tumor invades muscularis propria
T3	Tumor invades througt muscularis propria into the subserosa or nonperitonealized pericolic or perirectal tissues
T4	Tumor perforates visceral peritoneum or directly invades other organs or structures
Regional Lymph Nodes (N)	
N0	No regional lymph node metastases
N1	Metastases in 1–3 regional lymph nodes
N2	Metastases in ≥ 4 regional lymph nodes
Distatant Metastases (M)	
M0	No distant metastases
M1	Distant metastases
TNM stage	**Categories**
0	Tis, N0, M0
I	T1–2, N0, M0
II	T3–4, N0, M0
III	Any T, N1–2, M0
IV	Any T, any N, M1

The TL was also investigated in relation to a primary tumor location. Concerning the different clinical behavior of colon and rectum, patients were categorized into two groups according to Clinical Modification of the 10th revision of the International Classification of Diseases Codes. Individuals with the primary tumor(s) located in the cecum (code C18.0), ascending colon (C18.2), hepatic flexure (C18.3) or transverse colon (C18.4) were classified as proximal colon cancer group. The patients having the primary tumor within the splenic flexure (C18.5), descending colon (C18.6), sigmoid colon (18.7), rectosigmoid junction (C19.0) or those with an unspecified malignant neoplasm of the colon (18.9) were considered to have distal colon cancer. The last group comprised patients having malignant neoplasm of the rectum (C20.0). In the case of synchronous CRC, defined by more than one distinct

primary tumor, developed in colon and rectum, patients were classified in the colon cancer group. A common treatment strategy for stage II and III rectal cancer requires a neoadjuvant therapy. Patients with rectal cancer were therefore further stratified by neoadjuvant chemotherapy to those, who received it and those, who did not, and we examined its association with TL.

The relationship between TL attrition and chromosome instability was studied in two groups of patients; with MSI (MSI-high and MSI-low individuals were combined) and MSS tumors. To determine whether the TL predicts response to chemotherapy, patients were divided into good and poor responder groups, too. The stratification took account of clinical responses to neoadjuvant and adjuvant therapy and the date of death from cancer. In case that patients did not receive either therapy or their cancer therapy data were incomplete, they were excluded from the analysis. Further, the effect of *diabetes mellitus* on TL was tested by comparing patients having type 2 *diabetes mellitus* with non-diabetic patients. Last but not least, the role of TL in CRC survival was investigated. For this purpose, the group of patients, from whom the data were available at least 5 years after diagnosis, was created.

3.2 Blood Collection, Processing, and Storage

All the blood specimens were collected into blood collection tubes containing dipotassium ethylenediaminetetraacetic acid as a strong anticoagulant. After blood sampling, fresh specimens were partially processed to produce plasma and mononuclear cells, and the remainder was left unprocessed and long term stored with obtained blood fractions at -80 °C. Before use, frozen samples were thawed at a 37 °C in the thermostat. In this experiment, only whole blood, as a source of DNA, and PBMC, intended to RNA isolation, were used. Both DNA and RNA were a starting material for the quantitative polymerase chain reaction (qPCR)-based analyses. Blood processing is performed in our department continuously by all the lab members according to the regular schedule.

3.3 Peripheral Blood Lymphocytes Isolation

Living peripheral blood lymphocytes were isolated from fresh whole blood specimens. Their separation from other blood components was performed by Ficoll-Paque PLUS (GE Healthcare Life Sciences) flotation. Ficoll is a synthetic polysaccharide which together with sodium diatrizoate and calcium disodium ethylenediamintetraacetic acid makes up a density fluid widely used for gradient centrifugation. Lymphocytes, monocytes, and platelets have a lower density and after the centrifugation stay between plasma and Ficoll, while red blood cells and granulocytes are dense enough to pass through and are found at the bottom of the tube.

Two ml of anticoagulant-treated blood were diluted with an equal volume of sterile phosphate-buffered saline (PBS). One liter of 1X PBS was prepared by dissolving 9.0 g NaCl, 1.2 g $Na_2HPO_4 \cdot 12H_2O$, 0.2 g $NaH_2PO_4 \cdot 2H_2O$, 0.2 KCl in distilled water. The volume was adjusted to 1 l and pH to 7.4. The mixture of blood and PBS was carefully layered over the 3 ml of Ficoll and centrifuged at 580 x g for 15 min at 4 °C. Brake off ensures density gradient not disrupted by deceleration and mononuclear cells stay within the buffy coat, a concentrated white blood cell fraction. After the centrifugation, a white blood cell band was harvested with Pasteur pipette to get about 3–4 ml of cells. Collected suspension was then washed three times with PBS. Washing was performed to remove Ficoll, plasma, and platelets off lymphocytes and monocytes.

The sample volume was filled to 8 ml with PBS and the sample spun down at 2400 x g for 8 min at 4 °C, with brake 8. Brake should be turned on because the low-speed centrifugation allows the cells to pellet at the bottom of the tube without the platelets. The supernatant was discarded, pellet washed with 4 ml of PBS and the next centrifugation proceeded at the same settings only for 5 min. Subsequently, the supernatant was removed and the cell pellet washed with 2 ml of PBS last time. This step was followed by 5 min centrifugation at 2000 x g (6000 rpm) and supernatant fluid removal by a filtered pipette tip. Obtained PBL were resuspended in 1 ml of TRIzol Reagent (Invitrogen) and cell homogenized by vortexing. To permit a complete dissociation of nucleoprotein complexes such as ribosomes, the homogenate was allowed to sit for 5 min at room temperature. Samples were frozen at -80 °C until RNA extraction.

3.4 DNA Extraction from Blood and Concentration Measurement

There are numerous possibilities for DNA extraction. The most common isolation methods can be divided into two classes: the commercial spin column-based protocols and the solution-based protocols, such as the traditional phenol-chloroform method. The methods should be carefully chosen to optimize the yield and quality of the extracted DNA for endpoint applications. Commercial DNA extraction kits are fast, designed for small samples, and well suited for experiments requiring a high DNA purity. Since the yields may be lower than yields obtained by using the manual method, those commercial kits are ideal for polymerase chain reaction (PCR)-based techniques. Phenol-chloroform extraction is cheap and provides large amounts of high molecular weight DNA convenient for DNA hybridization or preparing the concentrated DNA stock solutions. However, its drawbacks include high sample consumption, the toxicity of phenol and chloroform, and their leftovers affecting enzyme activity in sensitive downstream applications, especially in sequencing and PCR.

Genomic DNA was extracted manually from whole blood using the DNeasy Blood and Tissue Kit (Qiagen, Valencia, CA) according to the instruction manual. An additional advantage of this kit is that it facilitates a simultaneous isolations of multiple samples. In a single run, 24 samples proved to be appropriate to process. A part of the samples was purified semi-automatically using the QIAcube (Qiagen, Valencia, CA) robotic workstation, following the same protocol with minor modifications. Processing of up to 20 samples could be performed per run. Due to the previous studies, DNA from about 300 samples was already isolated. Hence, the isolation of only about 200 samples was needed to be done.

For the manual extraction method, samples were first lysed by incubation with proteinase K. Twenty µl of proteinase K (600 mAU/ml, AU = Anson unit) were pipetted into a 1.5 ml microcentrifuge tube, then 100 ml of anticoagulated blood was added. The final sample volume was adjusted to 220 µl with PBS. In the next step, 200 µl of commercial buffer assigned as AL was added to the tube. The content was mixed thoroughly by vortexing for 5 min and incubated for 10 min at 56 °C in a thermoblock. After proteinase K digestion, 200 µl of 96% ethanol was placed in a sample. The solution was mixed by vortex for 5 min and heated again for 10 min at 56 °C. The whole mixture was applied to the spin column inserted in a 2 ml collection tube. The column was centrifuged at 6000 x g (8000 rpm) for 1 min. The eluate was discarded,

while the column was retained and placed into a new 2 ml collection tube. When DNA was loaded onto the silica matrix, the column was washed with 500 ml of the commercial buffer assigned as AW1 under the same centrifugation conditions. The eluate was discarded again and the column was washed by adding 500 ml of the commercial buffer assigned as AW2 and centrifugation at 20000 x g (14000 rpm) for 3 min. After the series of repeated washing and centrifuging steps, the column was inserted in a clean 1.5 ml microcentrifuge tube. To elute DNA, the silica membrane was incubated with 100 µl of the elution commercial buffer assigned as AE at room temperature for 1 min. Then, the sample was centrifuged at 6000 x g (8000 rpm) for 1 min. For maximum DNA yield, elution was repeated once more as described in the previous step.

As for automatic isolation with QIAcube, the extraction was performed according to the same protocol as the manual procedure described above. No change in purification chemistry was required. To improve the yield of DNA, a blood volume size was raised to 200 µl from 100 µl, thus the blood dilution step with PBS was abandoned.

The DNA concentration and its purity were determined using the Thermo Scientific NanoDrop 2000 spectophotometer, which enables nucleic acid quantification with minimal (1 µl) consumption of the sample. Evaluation of DNA integrity and thus quality was not examined. Pure DNA samples typically yield an optical density (OD) 260/280 absorbance ratio of 1.8. Purity ratios that are significantly lower than 1.8 indicate the presence of proteins, organic solvents, or other contaminants that absorb strongly at or near 280 nm. The wavelength of maximum absorption for both DNA and RNA is 260 nm. An OD 260/230 absorbance ratio serves as a secondary measure of nucleic acid purity. The generally accepted value is in the range of 2.0-2.2. Lower values may indicate contamination with salts or organic solvents which absorb at 230 nm. An OD 260/230 absorbance ratio is also dependent on the pH and ionic strength of the buffer used to dissolve the samples. Incompletely dissolved samples have the ratio < 1.7. Some chemicals such as phenol lower both the ratios, since phenol's ultraviolet spectrum consists of two absorbtion peaks at 230 nm and 270 nm.

3.5 RNA Extraction from Lymphocytes and Concentration Measurement

Compared with DNA isolation, RNA is more susceptible to degradation due to highly reactive 2' hydroxyl group, and a single-stranded structure makes it sensitive to heat. Another difficulty is the potential RNA digestion by ribonuclease enzymes (RNases). RNases are groups of enzymes which facilitate degradation of RNA, thereby control gene expression and defense organisms against RNA viruses. The presence of RNases is common in all cell types and the external environment. RNA isolation thereby requires cautious handling of samples, which should be processed in an RNase-free environment with RNase-free chemicals, plastics, and filtered pipette tips. Common methods of RNA extraction are phenol-chloroform-based, including total RNA extraction with TRIzol used in this study. An alternative to phenol-based methods are kits based on silica spin column technology. At the moment of submitting the diploma thesis, only the 1st sampling isolation has been done. When summarizing the work, I personally isolated about half of these samples, the rest was already extracted to be used in other experiments.

Starting material for RNA isolation were PBL in TRIzol (see chapter 3.3). TRIzol mainly consists of acid phenol and guanidine isothiocyanate. Guanidine salts work as a strong denaturating agent solubilizing cell components during homogenization as well as endogenous RNases. Phenol acts as a deproteinizing agent but alone retains water with dissolved RNA. For that reason, phenol is usually mixed with chloroform which prevents this retention and thus facilitates phase separation, a very first step of RNA extraction, more sharper. Likewise the phenol, chloroform helps to remove proteins from nucleic acids. Chloroform is usually sold as a premixed solution of chloroform and isoamyl alcohol, which is added to the chloroform to reduce foaming.

Describing the RNA extraction, TRIzol homogenates were defrosted and shaken vigorously by vortex with 0.2 ml of chloroform:isoamyl alcohol (24:1) for 15 seconds. These mixtures were incubated at room temperature for 3 min and centrifugated at 12 000 g for 15 min at 4 °C. After centrifugation, RNA remains in the aqueous phase, where DNA is found in the white interphase and proteins are extracted to the red-colored organic phase. To separate DNA, RNA, and proteins into different phases, an extraction has to be carried out under acidic conditions. The phosphate groups on DNA become in this pH uncharged by protonation and DNA partitions into the organic solvent. On the contrary, RNA is kept in aqueous phase because its bases are exposed and form hydrogen bonds with water, although its phosphate groups are protonated as well.

Denaturated proteins are soluble in the organic phase. The upper aqueous layer containing RNA was removed to a new tube and RNA was precipitated by adding 0.5 ml of isopropanol at room temperature. Even at low concentrations, isopropanol quickly precipitates RNA from the solution. Co-precipitation of salts can be partially avoided by using room temperature isopropanol since increasing temperature enhances salt solubility. After the addition of isopropanol, a tube was gently flipped up and down several times and incubated for 10 minutes at room temperature. Incubation was followed by 10 min centrifugation at 12 000 g at 4 °C during which RNA formed a transparent, gell-like pellet at the bottom of the tube. The supernatant was removed by pipetting and RNA resuspended in 1 ml of ice-cold 75% ethanol by vortexing. This step was crucial because RNA pellets are difficult to dissolve and, in the case of imperfect RNA washing, residual salts chelated to RNA would not be washed away. Ethanol is used as the second precipitation agent because, unlike isopropanol, evaporates easily without residues and is also more polar which makes it a better solvent for RNA and other polar compounds. Thus, ethanol forces RNA to precipitate more slowly and the salts tend to stay soluble. The resuspended samples were centrifugated at 10 000 g for 10 min at 4 °C and the supernatant discarded. At this point, RNA pellets became white and more visible. To remove the supernatant completely, the residual droplets on the tube walls were spun down again at 5 000 g for 1 min at 4 °C and carefully discarded with a pipette. After that, RNA pellets were allowed to air dry about 5 min until the last traces of ethanol was evaporated. RNA pellet should not over dry, because this will greatly decrease their solubility. The dry pellets were dissolved in 30 µl of RNase-free water and held on ice for a while to obtain fully dissolved RNA.

Just as DNA, RNA quality control was performed using Thermo Scientific NanoDrop 2000 instrument. Quantification of RNA integrity was not performed. An OD 260/280 absorbance ratio of 2.0 is generally accepted as pure for RNA, but it can vary depending on the dissolving agent. Samples measured in pure water give an OD of about 1.8. Slightly alkaline pH increases the ratio by 0.2–0.3 and on the contrary, slightly acidic pH equally decreases the ratio [180]. Partially dissolved RNA has an OD 260/280 absorbance ratio < 1.6. However, a ratio of < 1.8 usually indicates contaminants absorbing at 280 nm. These are mainly proteins (in particular, with aromatic amino acids) that stem from the interface when transferring aqueous phase of the TRIzol separation. Proteins remain in the sample also because of an incomplete

dissociation of nucleoprotein complexes. Common contamination lowering the ratio comes from organic solvents absorbing at 280 nm. An OD 260/230 absorbance ratio is the second criterion for RNA purity. A ratio of 2.0-2.2 generally means a pure RNA. A low 260/230 absorbance ratio indicates salt, e.g. guanidine isothiocyanate, or other contaminants which absorb at 230 nm. Phenol present in Trizol influences both ratios, as in the ultraviolet light it has two absorption peaks at 230 nm and 270 nm. To exclude the potential contamination with DNA, RNA samples may be treated with deoxyribonuclease. It is because both RNA and DNA have a similar absorption profile with a maximum at 260 nm, and hence their presence in the sample can be reliably distinguished only by an agarose gel electrophoresis.

3.6 Measurement of Relative Telomere Length

There are currently several approaches to measure absolute or relative telomere length in cellular DNA. A modified Southern Blot of telomere restriction fragments was the first technique to measure a mean TL [181]. Flow cytometry combined with fluorescent *in-situ* hybridization (flow FISH) quantifies average TL in specific populations of cells [182]. In contrast to the telomere restriction fragment and flow FISH analyses, PCR-based single telomere length analysis called STELA determines the length of telomere regions from individual chromosomes [183]. Relative qPCR-based techniques for TL measurement, used in this study, are described in sections below. The absolute qPCR method is based on the original relative qPCR method developed by Cawthon and uses an oligomer standard [184,185]. Apart from flow FISH, all described analytical methods start with genomic DNA.

In this study, the RTL was estimated by using two different qPCR-based methods; the qPCR and the multiplex quantitative polymerase chain reaction (MMqPCR). Both these methods were adapted from Cawthon [186]. The former method was in our laboratory newly adopted in collaboration with the research group of prof. RNDr. Marie Korabečná, Ph.D., Institue of Biology and Medical Genetics, First Faculty of Medicine, Charles University and General University Hospital in Prague. This method, described in detail in their article by Zinková et al. [187], was the main one and used for the measurement of all the samples. The second method was MMqPCR, which operates successfully in laboratories of our collaborative research group of

Molecular Genetic Epidemiology headed by prof. dr. Kari Hemminki in German Cancer Research Center based in Heidelberg, Germany, and is well described in their article by Hosen et al. [188]. Despite all our efforts, method implementation in our laboratory proved to be more problematic than in the case of the traditional qPCR method used by the team of prof. Korabečná. For this reason, a part of the samples was at least measured by our co-workers in Heidelberg and provides a good comparison with the results obtained by qPCR. In the diploma thesis, we publish the original method manual as it was used for the analysis of the samples. Using the MMqPCR analysis was for a long time preferred due to its 384 well plate format. Employing a 384 well plate makes this approach less time consuming and also cheaper because the instrument is capable of assaying more samples in parallel and the reaction is adapted to smaller overall volume. In addition to that, multiplexing provides more precise comparative analysis, because the amplification reactions are performed in the same well and thus use the exact same amounts of DNA pipetted. Even when in our research group the reaction conditions are still not optimized, we believe that the MMqPCR method will be established in the future.

One, as well as the other method of RTL measurement, was performed using a ViiA 7 Real-Time PCR System (Applied Biosystems, Foster City, CA, USA). To measure RTL, the relative quantity of telomere amplification products was normalized with reference single copy gene products. Obtained relative telomere/single-copy gene ratio, calculated from cycle threshold (Ct) values using a ΔΔCt method, was proportional to the average TL of all the cells in the sample.

3.6.1 Quantitative Polymerase Chain Reaction

The quantitative polymerase chain reaction, also referred to as real-time PCR reaction, is a technique developed for either absolute or relative DNA quantification. Using the fluorescent dyes, the quantity of DNA generated in the exponential phase of the amplification is proportional to the amount of fluorescence measured. Compared to qPCR, a conventional PCR detects amplified product at the endpoint of the PCR reaction and serves for analyzing the DNA presence or simple DNA amplification.

The qPCR reaction ran in a 96 well format, MicroAmp Fast Optical 96-Well Reaction Plate (Life Technologies, Carlsbad, CA, USA) and it was designed to measure a total of 14 samples per run. Samples originating from the same patients were measured

within one plate. Each reaction plate included samples, negative controls, and interplate/intraplate calibrator. All reaction wells consisted of 24 µl of the reaction mixture, containing a DNA polymerase, primers, deoxyribonucleoside triphosphates (dNTPs), $MgCl_2$, buffer, passive reference dye, and reporter dye, and 1 µl of DNA sample diluted with double-distilled water to a concentration of 5 ng/µl. Targets – reference *36B4* gene, encoding acidic ribosomal phosphoprotein P0, and telomere sequences – were amplified separately in triplicates, one sample thus accounted for six wells. A five-point standard curve, indicating the efficiency of the primers, was created through a 2-fold serial dilution of the standard stock sample with three replicates at each point. Wells intended to standard curve measurement were set up using 24 µl of a reaction mixture and 1 µl of a standard. The DNA amount ranged between 17 ng to 1.0625 ng per well. The negative control, showing if contamination of PCR experiment or primer-dimer artifacts occurred, was set up identically to the PCR reaction, but instead of the template DNA, 1 µl of sterile water was added. The negative control was analyzed in one well for telomere and one well for single-copy gene. To assess the interplate and intraplate variability of threshold cycle values, 17 ng input of standard DNA was used and measured in triplicates in each qPCR run. Prepared reaction plate was sealed with adhesive PCR plate seal. Before the PCR reaction, the plate was briefly centrifuged at 200 rpm for a few seconds and directly processed.

The qPCR reaction was performed by using PowerUp SYBR Green Master Mix (Life Technologies, Carlsbad, CA, USA). It is universal, for the fast cycling formulated solution of all reagents required for PCR, except for the primers and the DNA template. The master mix contains Dual-Lock Taq DNA Polymerase, SYBR Green dye, ROX (6-carboxy-X-rhodamine) passive reference dye, dNTPs with deoxyuridine triphosphate/deoxythymidine triphosphate blend, heat-labile uracil-DNA glycosylase and buffer components including magnesium ions. The reaction mixture for one 96 well format was assembled as follows: the telomere reaction mixture contained 336 µl of double-distilled water, 600 µl of the master mix, 108 µl of 10 µM primer Tel1 1b and 108 µl of 10 µM primer Tel1 2b. The *36BD* reaction mixture contained 480 µl of double-distilled water, 600 µl of the master mix, 36 µl of 10 µM primer 36B4u and 36 µl of 10 µM primer 36B4d. The components of the reaction mixture are, one after the other, described in the following paragraphs.

Using the hot start Dual-Lock Taq DNA Polymerase allowed reaction set up at room temperature and preparing PCR plate up to 72 hours before cycling. The polymerase is completely inactive until the initial heat activation step at 95 °C for 2 min. Besides common dNTPs, the polymerase can also incorporate and read through non-standard nucleosides such as deoxyuridine and deoxyinosine.

Heat-labile uracil-DNA glycosylase is a recombinant enzyme preventing the reamplification of carryover PCR products in a new PCR reaction. The enzyme is activated at 50 °C and starts to cleave the uracil bases, which were incorporated into DNA in previous PCR reaction instead of thymidine bases (by substituting deoxyuridine triphosphate for deoxythymidine triphosphate in the master mix), misincorporated by DNA polymerase or arisen due to deamination of cytosine. DNA with such apyrimidinic sites is very labile and undergoes spontaneous hydrolysis, while the DNA template containing thymidine bases remains intact and can be used for subsequent PCR amplification. Uracil-DNA glycosylase inactivation is typically mediated by the consecutive heating at 95 °C for 10 min. The enzyme does not show activity on RNA.

The qPCR product was visualized by SYBR Green, an intercalating cyanine dye commonly used in qPCR. It attaches the minor groove of dsDNA and after the denaturation step again releases. When bound to dsDNA, SYBR Green fluorescences with an emission maximum of 521 nm. Single-stranded DNA is stained with about 11-fold lower performance [189]. Another dye used in the experiment was ROX, a passive reference dye designed to normalize fluorescence intensity of reporter dye (in this case SYBR Green) in qPCR. It provides a constant fluorescence signal during the amplification and helps to balance well-to-well differences caused by artifacts. The presence of ROX does not impact the PCR reaction results. The emission intensity of the reporter dye divided by the emission intensity of the passive reference dye is the normalized reporter (Rn) ratio. This value indicates the magnitude of the fluorescent signal generated continuously during the PCR. Plot ΔRn, which is the difference between the background fluorescence (i.e. baseline) Rn^- and the reaction signal Rn^+, against the cycle number is called an amplification plot and correlates with the synthesized DNA amount.

Deoxyribonucleoside triphosphates are building blocks of newly synthesized DNA. According to the template, DNA polymerase integrates the complementary dNTPs (deoxyguanosine triphosphate, deoxycytidine triphosphate, deoxythymidine triphosphate, and deoxyadenosine triphosphate) and in certain cases also the base analogs.

Each of them is made up of a nitrogenous base, deoxyribose sugar, and phosphate group. For the PCR reaction, the dNTPs are typically supplied in equimolar concentrations. Their excess may result in Mg ions chelation, thus interfering with polymerase activity and decreasing primer annealing. As for lower amounts, they usually decrease PCR yield, however with possible enhancement of the product specificity. A deoxyuridine triphosphate/deoxythymidine triphosphate blend, present in PowerUp SYBR Green Master Mix, enables deoxyuridine triphosphate incorporation into PCR amplicons and also uracil-DNA glycosylase activity.

Magnesium ions function as cofactors at the polymerase active site, which implies that they directly affect its processivity and fidelity. During polymerase synthesis, one Mg ion coordinates the 3' hydroxyl group of the terminal dNTP, allowing a nucleophilic attack of 3' oxygen on αP of incoming nucleotide. In the transition state, other Mg ion ensures the stability of this state and neutralizes the negative charge on the pyrophosphate leaving group. This event leads to the subsequent phosphodiesther bond formation and the pyrophosphate release. Additionally, the Mg ions shield the negatively charged phosphodiester backbone, thereby decrease the electrostatic repulsion between DNA strands. This enables the formation of the complex between DNA templates and primers, which will not otherwise be stable. For that reason, an optimal concentration of $MgCl_2$ is crucial to the PCR reaction progress, because the high concentration favors an increased PCR yield at the expense of specificity.

To detect a single copy gene *36B4* and telomere sequences, two sets of primers (both from Sigma-Aldrich, St. Louis, MO, USA) having a similar annealinng temperature were used. Primers for *36BD* amplification were chosen according to Cawthon and Boulay et al., primers for telomere amplification were chosen according to Gil and Coetzer [186,190,191]. Primer sequences are:

Forward *36B4* primer 36B4u 5'-CAGCAAGTGGGAAGGTGTAATCC-3'

Reverse *36B4* primer 36B4d 5'-CCCATTCTATCATCAACGGGTACAA-3'

Forward telomere primer Tel 1 1b 5'-CGGTTTGTTTGGGTTTGGGTTTGGGTTTGGGTTTGGGTT-3′

Reverse telomere primer Tel 1 2b 5'-GGCTTGCCTTACCCTTACCCTTACCCTTACCCTTACCCT-3'

All primers were diluted to obtain 10 μM working solutions. The final concentrations of primers used in the reaction were 300 nM for the *36B4* gene and 900 nM for telomeres. Available literature does not specify the design of primers closer. For *36B4* amplification is known only that primers binding the *36B4*

sequence produce a 74 base pairs product. As for telomere amplification, telomere primers are made up of repeating patterns exhibiting mismatch in every sixth base. This design likely allows DNA polymerase to add bases from the 3' end of the primer only when it is hybridized to genomic DNA, not to another primers. Both primers can anneal to any partially complementary telomeric repeat, but the last 6 bases on their 5' ends and the telomere sequences do not pair. The complement sequences of these non-pairing bases are subsequently generated at the 3' ends of all qPCR products and, therefore, those 3' ends are blocked from initiating DNA synthesis in the middle of telomere amplicons.

The standard curve and the interplate calibration were established using a reference DNA sample. This standard consists of DNA pooled from 30 individuals, 15 females and 15 males hospital volunteers. The target group enrolled healthy, middle-aged adults spanning from 41 to 55 years of age. People who had experienced cancer in the past were not included in the study. Recruitment of participants and collection of blood samples took place at Faculty Hospital Kralovské Vinohrady, Prague in 2013. DNA of selected people was isolated from the whole blood using the same DNA extraction and the DNA concentration measurement methods as described in chapter 3.4. Isolated DNA was diluted to 20-25 ng/µl, pooled together and adjusted to a final concentration of 17 ng/µl.

The reaction conditions were identical for both targets, a qPCR instrument ran in fast mode. The initial denaturation step (also called hold stage) of template DNA was performed at 50 °C for 2 min and 95 °C for 2 min. This stage is also necessary for Dual-Lock Taq DNA Polymerase and uracil-DNA glycosylase activation. DNA amplification occurred by repeated denaturation, annealing and extension steps ran through 40 cycles of qPCR at 95 °C for 30 sec and 54 °C for 1 min. Specificity of the qPCR products was, after the qPCR cycling, assessed by melting curve (also called dissociation curve) analysis. Using the default settings, the assay began at 95 °C for 15 sec and decreased to 60 °C for 1 min. With the continuous signal acquisition, the temperature was rising at a rate of 0.05 °C/sec to 95 °C, where remained for 15 sec. For all other qPCR steps, a ramp rate of 1.6 °C/sec was used.

The calculation of amplification efficiency (E) was based on the slope of the standard curves (depicted in **figure 7**), using the equation: $E = -1 + 10^{(-1/slope)}$, and evaluated by Viia7 software. The high efficiency, which was 97 % for telomeres and 101 % for *36B4*, means that the Ct values are proportional to the corresponding product concentrations (as the target sequence double during each replication cycle). It verifies that the PCR data are accurate and common mistakes as pipetting errors, the presence of contaminants, the secondary structures formation, incorrect primer design, etc., can be excluded.

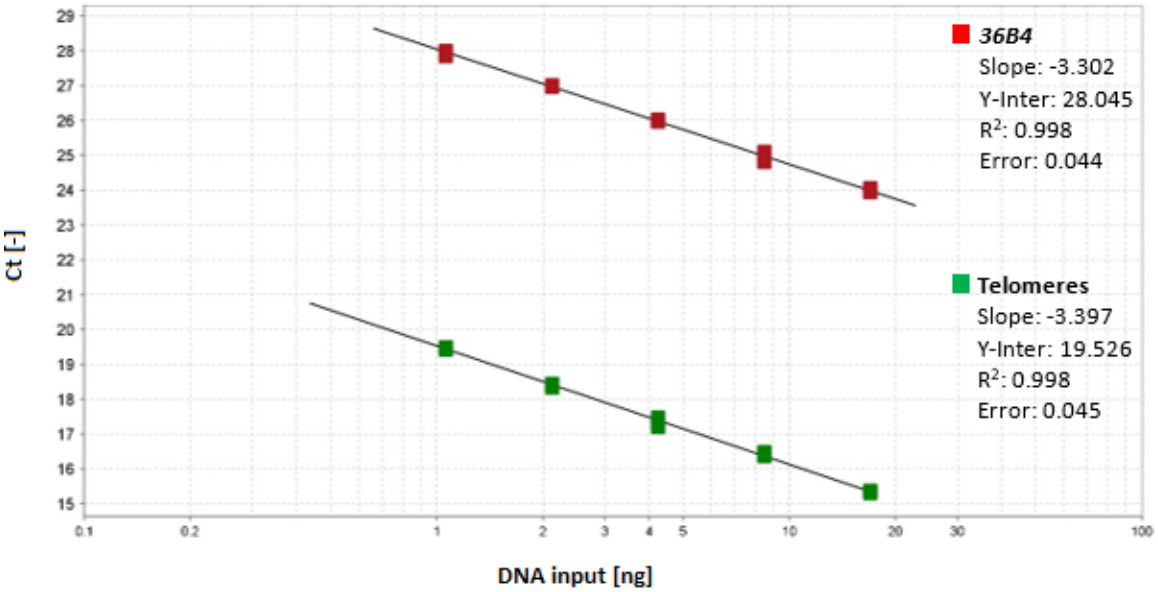

Figure 7. Representative standard curves of telomeres and *36B4* gene. Standard curves were generated from average Ct values of different standard concentrations, and are displayed using a linear regression model. The linearity of the standard curve is indicated by the correlation coefficient (R^2), which is a measure of linear association around a line. In particular assays, $R^2 \geq 0.990$ was required. The slope of the regression line, representing the rate of change in *y* as *x* change, close to -3.320 is considered optimal, indicating that the PCR reaction has 100% efficiency. The error is the standard error of the regression and refers to the average distance that the observed values scatter around the fitted regression line. A regression line has an equation of the form $Ct = m\ [\log (Qty)] + b$, where m is the slope, *Qty* is the standard quantity and *b* is the y-intercept (the value of y where the regression line crosses the y-axis).

The inter-assay coefficient of variation (CV) was calculated from the 17 ng standard sample measured on each plate in triplicate, intra-assay CV was calculated from each sample within the plate. The coefficient of variation is dimensionless quantity defined as the ratio of the standard deviation of a set of measurements to the mean of the set. The interplate CV, describing the data consistency between the plates, was 1.03 % for single-copy gene and 1.92 % for telomeres. Variability of results within the single PCR run, examined as the intraplate CV, was for the single copy-gene and telomeres 0.35 % and 0.24 %, respectively. Within the triplicates, samples with the SD of the average Ct > 0.3 were omitted from the analysis and the measurement was performed again in an independent run. In case that two replicates were nearly identical and one distant with suspected dilution error, the outlier was excluded from the calculations. Melting curves, generated after completion of the amplification reaction, determined that homogenous amplicons with a single melting temperature were produced. Representative melt curves are shown in **figure 8**.

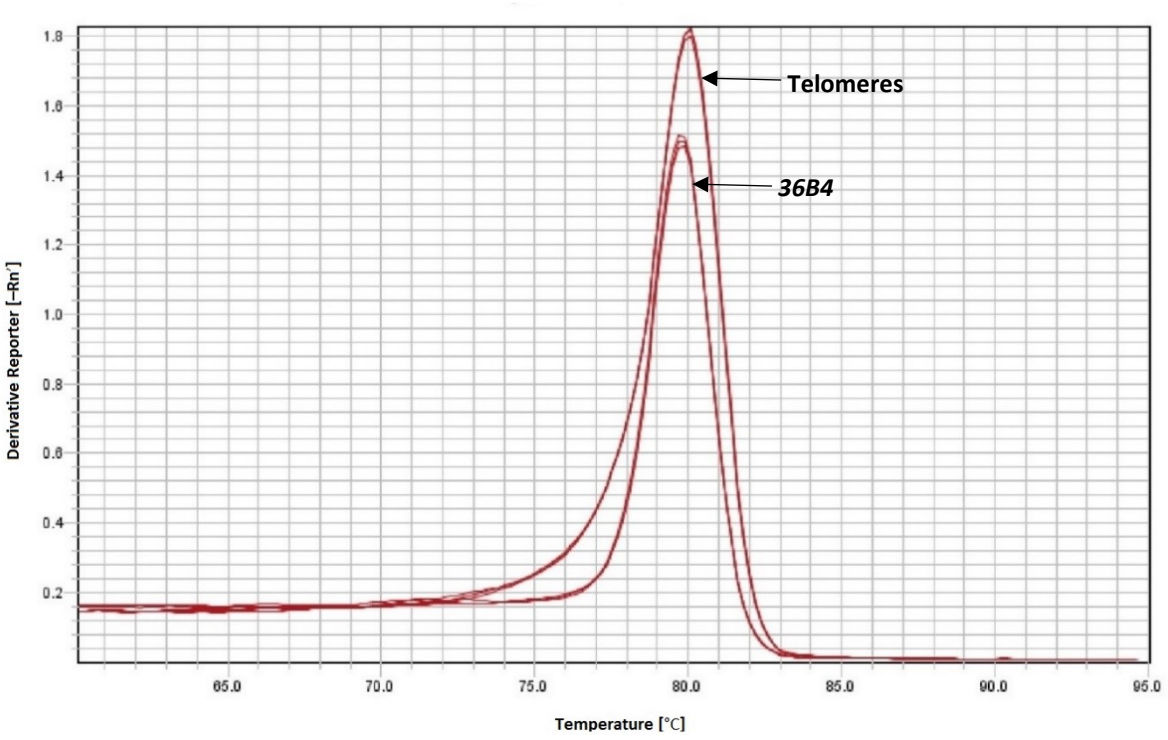

Figure 8. Melting curve analysis of qPCR amplicons. The figure displays the negative first derivative of the change in fluorescence plotted against the temperature. Both amplicons for telomeres and *36B4* revealed single peaks (the same melting temperature) indicating specific amplification, whereas the presence of multiple peaks would indicate off-target amplicons, contamination or presence of primer-dimers.

3.6.2 Monochrome Multiplex Quantitative Polymerase Chain Reaction

In contrast to conventional singleplex PCR described in chapter 3.6.1, MMqPCR allows the simultaneous amplification of several DNA sequences in the same reaction wells. The reaction is time-saving, cost-effective and does require a minimum of starting material. For a reason that each target is amplified with a different set of primers, which have to be distinguishable one from another, MMqPCR is, however, inherently more complicated in its design.

Regarding the sample preparation procedure, all DNA samples were first normalized to a concentration of 5 ng/µl and then (to get less concentrated samples) loaded with stepper in a MicroAmp Optical 96-Well Reaction Plate (Life Technologies, Carlsbad, CA, USA), which served as a dilution plate. Plate wells consisted of 12 µl of double-distilled water and 3 µl of a sample, thus the final DNA concentration was approximately 1 ng/µl. Before using, the dilution plate was sealed and shortly spun down at < 200 rpm.

The MMqPCR reaction was carried out in a 384 well format, MicroAmp Optical 384-Well Reaction Plate (Life Technologies, Carlsbad, CA, USA). Each reaction plate included samples, 8 point standard curve, and negative controls. The reaction set-up enabled to measure up to 96 samples in parallel. Samples taken from the same patient were measured within one plate. Each reaction well contained 8 µl of the reaction mixture, consisting of DNA polymerase, primers, dNTPs, $MgCl_2$, buffer, passive reference dye and reporter dye, and 1.75 µl of a sample (1.75 ng of DNA). The prepared reaction mixture was dispensed to wells using a stepper pipette, samples were added in triplicates afterward. Standard curve estimating PCR efficiency and interplate/intraplate variability was constructed using eight known concentrations of DNA. These were produced by a two-fold serial dilution of standard, conducted in 8 wells strip. Then, 1.75 µl of dilution series was transferred with 8 channel automatic pipette in two triplicates to 8 µl of the reaction mixture. The amount of DNA was in a range from 30 ng to 0.23 ng per well. To exclude contamination of PCR reagents and primer-dimer formation, a negative control consisting of 8 µl of reaction mixture without a template, and 1.75 µl of water, was pipetted in 9 wells. The prepared reaction plate was sealed and spun down at 200 rpm for a few seconds to get all liquid to the bottom of the wells and to remove air bubbles. After that, the plate was immediately measured.

Master mix used in this experiment was 5X HOT FIREPol Probe qPCR Mix Plus with ROX (Solis BioDyne, Tartu, Estonia). It is a ready-to-use solution containing all components that are not sample-specific: a thermostable HOT FIREPol DNA Polymerase (5 U/µl), commercial 5X Probe qPCR buffer, 15 mM $MgCl_2$, dNTPs and ROX dye. Only template, primers, and SYTO 9 reporter dye need to be added. The reaction mixture for one 384 well format was prepared by adding following regents: 2262 µl of double-distilled water, 740 µl of master mix, 7.4 µl of 100 µM primer Telg, 14.8 µl of 100 µM primer Telc, 7.4 µl of 100 µM primer Albugcr2, 14.8 µl of 100 µM primer Albdgcr2 and 5.5 µl of 1.5 µM SYTO 9. The components of the reaction mixture (those which were not already described in the qPCR method, chapter 3.6.1) are described in the following paragraph.

Hot-start qPCR is a type of PCR specially devised to avoid non-specific amplification of DNA. It takes advantage of hot start polymerases, that are chemically or antibody modified to be unreactive at ambient temperatures. In this experiment, HOT FIREPol DNA Polymerase was activated by a 15 min incubation step at 95 °C, which allows convenient room-temperature reaction setup. Fluoresce signal reflecting DNA amplification was detected by SYTO9 Green Fluorescent Nucleic Acid Stain (Life Technologies, Carlsbad, CA, USA). This intercalating reporter dye is an alternative to SYBR Green but distinguishes by lower inhibition effect to PCR and high melting curve reproducibility [192]. Its excitation/emission spectra are 485/498 nm for DNA. Both ROX, used in the experiment as a passive reference dye, and Syto 9 share the same fluorescent channel within the qPCR instrument. To identify an optimal dye concentration, several 2-fold dilutions of 5mM SYTO 9 [5 mM stock solution in $(CH_3)_2SO$] were tested. Some solvents may interfere with the fluorescent signal, thus for the dilution a master mix which is compatible with this stain was used. Each concentration of dilution series was pipetted in two 10 µl octuplicates. Then, 384 well plate was sealed, vortexed for 5 sec and shortly spun down at < 200 rpm. Determination of the optimal concentration was done within 5 cycles. The starting temperature ramped up from 25 °C to 60 °C with a 2 min hold and ramp rate 1.6 °C per sec. The ideal fluorescence signal was detected at 1.5 µM concentration. Using the 1.5 µM concentration, every well of 384 well plate was filled with 15 µl of solution. Before loading into the instrument, the plate was processed the same way as described above. The temperature setting for custom dye calibration was 60 °C, as it should reflect the temperature at which the PCR data collection will

be performed. When the dye calibration passed, the obtained results were saved in the system.

Two pairs of primers targeting telomeres and human serum albumin gene *ALB* (both from Sigma-Aldrich, St. Louis, MO, USA), which was selected as single-copy reference gene, were used in this study. Their sequences were set according to Cawthon et al. [186] as follow:

Forward telomere primer Telg 5'-ACACTAAGGTTTGGGTTTGGGTTTGGGTTTGGGTTAGTGT-3'
Reverse telomere primer Telc 5'-TGTTAGGTATCCCTATCCCTATCCCTATCCCTATCCCTAACA-3'
Forward *ALB* primer Albugcr2 5'-CGGCGGCGGGCGGCGCGGGCTGGGCGGCCA-TGCTTTTCAGCTCTGCAAGTC-3'
Reverse *ALB* primer Albdgcr2 5'-GCCCGGCCCGCCGCGCCCGTCCCGCCGAGCATTAAGCTCTTTGGCAACGTAGGTTTC-3'

All primers were diluted to obtain their 100 μM working solutions. The final concentration of primers Telg and Albugcr was 200 nM, for Telc and Albdgcr 400 nM final concentration was used. Because the amplification of both *ALB* and telomeres takes place in the same well, it was desirable to separate it in two diverse PCR programs. Primer pairs were manufactured to anneal at different temperatures, and also to produce short amplicons with diverse melt temperature (primers for *ALB* generated amplicons with the higher melting temperature than the telomere amplicons). The melting temperature increment was facilitated by 5'GC-clamps (non-templated sequences) attached to both 5' ends of albumin primers. These guanine/cytosine-rich regions were in each primer set mutually different, which reduced the risk of hairpin loop formation impeding the polymerase that moves along the template. Since the melting curve for *ALB* and telomere PCR products varied, the instrument could detect the fluorescent signal only for one of the targets.

Describing telomere amplification, telomere repeats at all chromosome ends were amplified using forward primer, whereas reverse primer was capable to prime only PCR fragments. Priming the native DNA strands was not allowed owing to the mismatch base at its 3' terminus. On top of that, reverse primer was designed to prime the forward primer extension product at one certain position, other configurations result in a 3' terminal base mismatch. This situation was very important, guaranteeing that amplicons of defined length (three bases shorter than the sum of the length of both primers) will be generated. Primer-dimer formation, highly suspected on the grounds of their repetitive nature, was prevented due to introduced mismatches. Primers can share only 3 base pairs overlap and this construct is not stable enough to be extended.

Standard curves, necessary for evaluation of amplification efficiency and intraplate/interplate variability, were generated using a reference sample, a DNA pool of 30 healthy controls. These individuals with age ranging from 40 to 55 years and with no specific sex ratio had no personal history of cancer. All participants have been recruited in the ongoing Colorectal Cancer Study of Austria. Preparation of the standard DNA was identical to the standard preparation procedure described in qPCR method. DNA was isolated from the whole blood, diluted to 20–25 ng/µl, pooled together and finally diluted to a concentration of 17 ng/µl.

Telomere sequences and *ALB* were amplified separately, using two consecutive qPCR programs. The thermal cycle conditions for telomere amplification were defined as follows: initial denaturation of DNA sample and activation of DNA polymerase was accomplished in a holding stage at 95 °C for 15 min. QPCR cycling began with 2 cycles at 95 °C for 20 sec and 49 °C for 1 min needed to telomere primers annealing and extension. To amplify the telomere DNA, the reaction then proceeds with 25 cycles of repeated denaturation, annealing and extension steps. These cycles were performed at 85 °C for 20 sec with signal acquisition at 59 °C for 30 sec. For *ALB* amplification, a total of 35 qPCR cycles were performed. These cycles comprised a denaturation temperature of 95 °C for 15 sec and an annealing/extension temperature of 85 °C for 30 sec with signal acquisition at 84 °C for 30 sec. During the denaturation step, the telomere amplicon melts, DNA polymerase releases the early-amplified telomere product and is free to copy the albumin gene. DNA synthesis at 85 °C is allowed due to DNA polymerase thermostability and ability of *ALB* primers to anneal at such high temperatures. Signal acquisition at 84 °C was chosen because at this temperature the telomere product is melted, therefore does not interfere with a fluorescence signal from *ALB* amplicon. To assess the specificity of MMqPCR products and visualize possible primer-dimers, qPCR cycling was followed by the melting curve (also called a dissociation curve) analysis. Performed with the same default settings as in the qPCR method, the thermal profile consists of 95 °C for 15 sec, followed by of 1 min at 60 °C. From this point, the fluorescence was measured continuously. The temperature was elevated to 95 °C with a ramp rate of 0.05 °C/sec and under these conditions, the plate was heated for 15 sec.

The amplification efficiency of MMqPCR and was calculated alike in the case of qPCR from the slope of the regression line in the standard curve, using the equation $E = -1 + 10^{(-1/slope)}$. The amplification efficiency of particular assays varied from 95 to 102 % and its values were generated automatically by Viia7 software. Monitoring of inter-assay CV was allowed by measuring triplicates of standard curve dilutions twice in each qPCR run, intra-assay CV was determined from all samples within the plate. Interplate variation, an expression of consistency across the plates, was 3.37 % for *ALB* and 3.50 % for telomeres. Intraplate variation, representing a variation of results obtained from a single run, was 0.28 % for single-copy gene and 0.42 % for telomeres. Triplicate samples with the SD of the average Ct > 0.5 were omitted from the study and the sample was measured again in an independent run.

3.7 Relative Telomere Length Calculation

RTL was expressed as the ratio of telomere repeat copy number to single gene copy number and calculated from Ct values using the ΔΔCt method. Ct reflects the cycle number at which an amplification curve (representative amplification plot is depicted in **figure 9**) crosses a threshold line. In other words, it states for a point at which a signal in the early exponential stage of the reaction is detected. Ct absolute value is affected by many factors (e.g. amplification efficiency, master mix components), but in particular by baseline.

During the initial PCR cycles, there is almost no PCR product. At this point, the amplification signal is very low and occurs below a fluorescence background. The background shows up as a fluctuating signal arising from autofluorescence, instrument, etc., and it is used to determine the mean background fluorescence (i.e. baseline) across the plate. Baseline correction to zero ΔRn (its subtraction from the reaction signal) is necessary for proper interpretation of relative quantities of samples. Accurately established baseline has a linear course and in itself stands for the detection limit of the instrument. To obtain reliable Ct values, the baseline should be set from the 3rd cycle to approximately two cycles before the amplification of the most abundant target. Ct value is then automatically placed by software at 10 standard deviations above the baseline fluorescence in the linear phase of amplification.

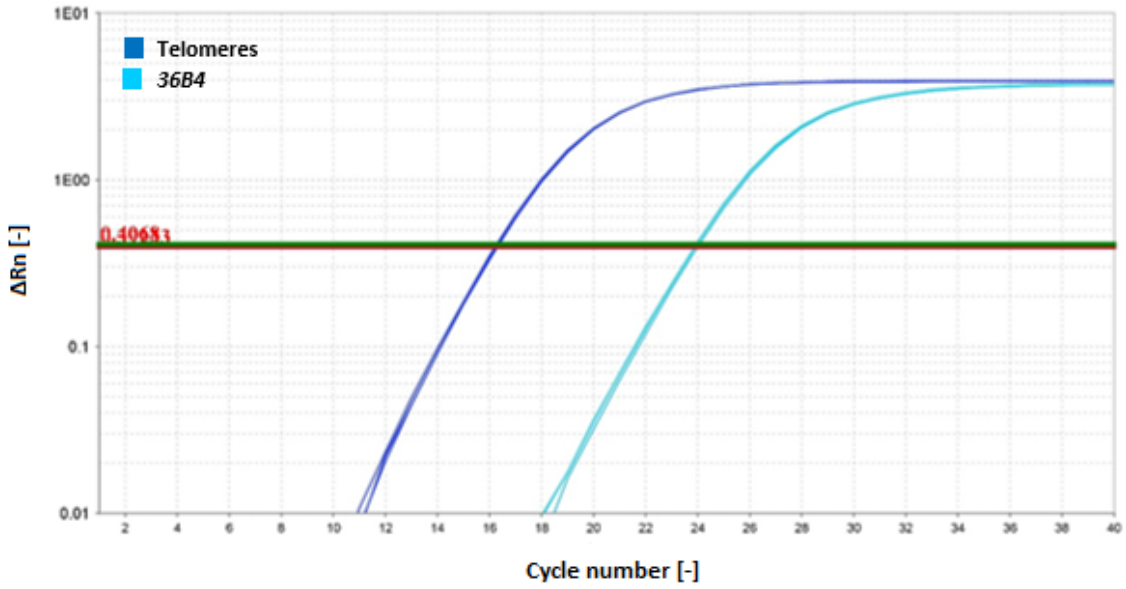

Figure 9. Amplification plots in triplicate of telomeres and *36B4* by qPCR. Telomere amplification plots are shown in dark blue, *36B4* amplification plots are shown in light blue. ΔRn, which corresponds to the normalized fluorescence signal of the reporter dye, is plotted against a number of PCR cycle. Zero ΔRn is called baseline and corresponds to the fluorescence intensity of the background. The intersection of the amplification plots with the threshold line, set automatically within the linear portion of the curves, gives Ct values, used for RTL calculation.

Three Ct results (three for telomeres and three for single-copy gene amplification) were obtained for each DNA sample. For RTL calculation, mean Ct of telomeres was initially subtracted from mean Ct of single-copy gene and such calculated ΔCt of each sample and ΔCt of standard (derived from ΔCts of standard replicates within the calibration curve) were then substituted into the formula $2^{-(\Delta Ct(sample)-\Delta Ct(standard)}$, giving the final relative telomeres/single-copy gene ratio. A ratio above 1 means that the patient has longer telomeres than the reference DNA sample, a ratio bellow 1 means that the patient has shorter telomeres than the reference DNA sample.

Standard deviation (SD) was calculated using the formula $SD = \sqrt{\frac{\sum(x-\bar{x})^2}{n-1}}$, where x means each value in data set, $\bar{x}$ means the mean of the set and n means a number of data points. Assay CVs were calculated for both targets using the formula $CV = \frac{SD}{\bar{x}} \times 100\ \%$. Intraplate variability was the mean CV derived from the CVs among individual wells, and interplate variability was the CV calculated from the replicate measurements of standard sample serving as interplate calibrator.

3.8 Measurement of *hTERT* mRNA Expression

Levels of *hTERT* mRNA expression were measured by the quantitative reverse-transcription polymerase chain reaction (RT-qPCR). Due to limited available time, the measurement was performed only in few samples yet, the study is still ongoing. For this reason, the diploma thesis contains only illustrative amplification data from a single experiment.

RNA molecules cannot be amplified directly by qPCR. Therefore, RNA was first converted to a complementary deoxyribonucleic acid (cDNA) by reverse transcription (RT). Like DNA, an aliquot of the RT reaction was then used as a template for qPCR amplification of specific targets (*hTERT* and two endogenous controls), whose quantities correspond to the gene expression, and thus protein levels. The RT-qPCR described above is termed as two-step, whereas in one-step reaction, both RT and qPCR take place in the same tube. Relative *hTERT* mRNA levels were normalized to reference genes and then, its expression was calculated using the ΔΔCt method, as in the case of the TL measurement. As for reference genes, their expression should be stable, identical across different cell types and independent on different cell treatments. For accurate normalization, RT-qPCR is always conducted by employing more than one reference gene, and their usage is considered with respect to the expression stability values.

3.8.1 Reverse Transcription Polymerase Chain Reaction

Each sample intended for RT consisted of 7.5 µl of the reaction mixture (1.5 µl of a buffer, 0.75 µl of reverse transcriptase, 0.6 µl of dNTPs and 1.5 µl of random primers and 3.15 µl of RNase-free water) and an equal volume of RNA with a concentration of 20 ng/µl. All the components were combined on ice, using RNase-free reagents and plastics. Some kits are also supplied with an RNase inhibitor, which binds to and neutralizes the activity of RNase superfamily members. In this RT reaction, the RNase inhibitor was not applied.

A two-fold concentrated reaction mixture was prepared by using the High Capacity cDNA Reverse Transcription Kit (Life Technologies, Carlsbad, CA, USA) comprising 10X RT Buffer, MultiScribe Reverse Transcriptase (50 U/µL), 100 mM 25X dNTPs, 10X Random Primers, and RNase-free water. Total RNA intended for RT was diluted with RNase-free water and reaction mixture to final concentration of

10 ng/µl in 15 µl reaction volume. MultiScribe Reverse Transcriptase is a recombinant Moloney murine leukemia virus RNA-dependent DNA polymerase. Random sequences of the primers enable them to anneal throughout the entire RNA template. Since RT is initiated from non-specific positions, MultiScribe Reverse Transcriptase generates single-stranded cDNA molecules of various lengths (7 kilobases or less) produced from any species of RNA. Ten-fold concentrated RT Buffer is a commercial buffer maintaining a favorable pH environment. It may also contain additives for increasing RT efficiency, e.g. ions acting as cofactors.

Prepared samples were gently mixed, briefly spun down at 2000 x g and loaded into the Bio-Rad PTC-200 Thermal Cycler. RT reaction started with 10 min of incubation of samples at 25 °C. This temperature was chosen because random primers have typically lower melting temperature (~10–15 °C) due to their shorter length. After the primer annealing, samples were heated to 37 °C and DNA synthesis then proceeded within 1 cycle for 2 h, followed by the subsequent enzyme inactivation at 85 °C for 5 min and cooling at 4 °C holding temperature. Generated single-stranded cDNA was used directly as a template in the qPCR step.

The qPCR reaction was carried out in a 96 well format, using MicroAmp Optical 96-Well Reaction Plate (Life Technologies, Carlsbad, CA, USA), allowing measurement of up to 9 samples and 1 healthy control without a personal cancer history in parallel. For all assembled 20 µl qPCR reactions was included 18 µl of reaction mix consisting of AmpliTaq Gold DNA Polymerase, dNTPs (with deoxyuridine triphosphate), ROX dye, uracil-DNA glycosylase, buffer, particular TaqMan Assay, RNase-free water, and 2 µl of 2-fold diluted cDNA obtained by reverse transcription (cDNA from 10 ng total RNA) to each well. Measurement of transcript levels of test and reference genes has been performed separately in triplicates, which implies that one sample was pipetted into 9 wells.

The reaction mixtures for all monitored genes were blended identically and differed only in the type of the Taqman assay used. For 96-well plate, each of them was composed of 300 µl of TaqMan Universal Master Mix II, with UNG (Life Technologies, Carlsbad, CA, USA) consisting of AmpliTaq Gold DNA Polymerase, dNTPs (with deoxyuridine triphosphate), ROX dye, uracil-DNA glycosylase and optimized buffer components, 210 µl of RNase-free water and 30 µl of TaqMan assay matches the gene of interest.

Except for TaqMan assays and AmpliTaq Gold DNA Polymerase, master mix components were already described in chapter 3.6.1.

TaqMan assays (Applied Biosystems, Carlsbad, CA, USA) comprise of unlabeled pair of primer and probe with a reporter label on the 5' end, a quencher on the 3' end placed 10–30 bases apart and conjugated minor groove binder. The assay is based on the 5' to 3' nuclease activity of Taq DNA Polymerase. While carrying out a TaqMan qPCR reaction, the probe and primers, designed to have melting temperature about 10 °C lower, bind to the target-specific sequence. This feature enables the probe to bind ahead of time downstream of the one of the primer and when the Taq polymerase reaches it, the probe is hydrolyzed via its 5' exonuclease activity. As a consequence, the reporter dye is separated from the quencher. This event results in an increase in fluorescence which is proportional to the amount of the PCR product. In this study, *hTERT* mRNA expression was analyzed by using a human TERT TaqMan Assay (Hs00972650_m1). Human ACTB TaqMan Assay (Hs01060665_g1) and human GAPDH TaqMan Assay (Hs02786624_g1) were used for the endogenous normalizers. Amplification of cDNA was carried out by AmpliTaq Gold DNA Polymerase, which is a chemically modified form of AmpliTaq DNA Polymerase provided in a complex with a thermolabile, neutralizing antibody, which blocks its polymerase activity until the pre-PCR 95 °C heat activation step. The 5' to 3' nuclease activity of the polymerase also enables cleavage of the TaqMan probe during the PCR.

The reactions were performed on the Applied Biosystems 7500 Real-Time PCR System. Thermocyclicling conditions consisted of initial uracil-DNA glycosylase activation at 50 °C for 2 min, followed by DNA polymerase activation and coincident uracil-DNA glycosylase within 2 cycles at 95 °C for 10 min. The polymerization reaction was repeated in 40 cycles of denaturation at 95 °C for 15 sec, annealing at 60 °C for 1 min and extension steps. Fluorescence was measured in each cycle at the end of the 60 °C segment.

The intraplate variation was 0.37 % for *hTERT*, 0.64 % for *GAPDH* and 0.43 % for *ACTB*. Because the thesis contains only the data from one qPCR reaction, interplate variation was not calculated yet. Technical replicates with the SD of the average Ct > 0.5 were omitted from the study.

3.9 Relative *hTERT* mRNA Expression Calculation

The relative quantity of amplified *hTERT* cDNA was calculated from Ct values using the ΔΔCt method. Because the relative mRNA gene expression was calculated the same way as RTL (for detailed description proceed to chapter 3.7), the following text only briefly summarizes the ΔΔCt method. The calculation procedures of SD and CVs are given in chapter 3.7, too.

In short, relative gene expression calculation was based on expression levels of a target gene (*hTERT*) versus two reference genes (*GAPDH*, *ACTB*). Ct means obtained for each of these genes were used to calculate the relative difference between the target gene and the reference genes using the formula ΔCt = Ct mean (*hTERT*) - Ct mean (reference genes). ΔCt of samples and ΔCt of the control were substituted into the formula $2^{-(\Delta Ct(sample)-\Delta Ct(control)}$ to calculate a relative *hTERT* gene expression. Relative gene expression > 1 means that the gene is upregulated compared to control, relative gene expression < 1 means that the gene is downregulated compared to control.

3.10 Statistical Methods

Statistical analyses were performed using Statistical Analysis System software (SAS Institute Inc., Cary, NC, USA). The whole data set and study groups were evaluated using primary statistical parameters such as mean, standard deviation, variance, median, interquartile range, minimum and maximum.

Differences between independent groups on one continuous dependent variable were established by using a two-samples Wilcoxon test, which uses the standard normal distribution (Z) value to test of significance. The strength and direction of the association between two variables were tested by the Spearman's rank-order correlation method and linear regression. The measure of linear relationship between two variables was evaluated using Spearman's rank correlation coefficients (ρ). To test for differences between the factor level means within study groups was used repeated-measures analysis of variance (ANOVA). A non-parametric alternative to repeated measures ANOVA is Friedman's test used to examine the differences between groups when the dependent variable is ordinal. The F value, used in ANOVA, refers to variation between sample means. Friedman statistic χ^2 indicates a variance

over the mean ranks. The overall survival rate was estimated using Kaplan-Meier analysis. The effect of TL on overall survival was analyzed using the log-rank test and the Gehan-Wilcoxon test. The cut-off point, determined by the log-rank test, with the most significant splint met the condition of the maximum Cox score criterion. The scores were generated from the Cox-hazard regression model. In all statistical analyses, the level of significance α was set at 0.05. Probability value (P) determines statistical significance and represents the chance the results occurred at random. In this thesis, we refer to statistically significant as $P < 0.05$. N values refer to sample size.

4 Results

4.1 Comparison of qPCR and MMqPCR Methods for Telomere Length Measurement in Patients Suffering from Colorectal Cancer

The Spearman's rank-order correlation method was used to analyze the correlation between the TL measured by qPCR and MMqPCR (**table 3**) in patients with CRC. In each analysis, only those patients that have RTL measured by both methods were included. In all the following statistical analyses, only the RTL data determined by the qPCR method were used.

Table 3. Correlation of qPCR and MMqPCR methods between the samplings. The 1st samplings were drawn at the moment of cancer diagnosis. The 2nd, 3rd and 4th samplings were drawn at 6-month intervals during a course of the treatment (see chapter 3.1).

Sampling	Correlation coefficient ρ	Probability value P	Number of patients N
1st	0.533	<0.001	131
2nd	0.352	<0.001	124
3rd	0.418	0.001	58
4th	0.929	0.003	7

Spearman correlation coefficient ρ in the 1st sampling equaled to 0.533 ($P < 0.001$, $N = 131$) indicates that there is a positive relationship between the used assays. In the 2nd sampling ($\rho = 0.352$, $P < 0.001$, $N = 124$) and the 3rd sampling ($\rho = 0.418$, $P = 0.001$, $N = 58$), a positive relationship between the assays used for RTL measurement was retained. A highly positive relationship was found in the 4th sampling ($\rho = 0.929$, $P = 0.003$, $N = 7$), but it was estimated only for a small data set. The correlation between the calculated TL from qPCR and MMqPCR was also tested by linear regression analysis. This correlation was strong ($R^2 = 0.901$, $P < 0.001$) in the 1st sampling, **figure 10**.

All p-values were < 0.05 and thus considered significant. As a result, the both methods used mutually correlate.

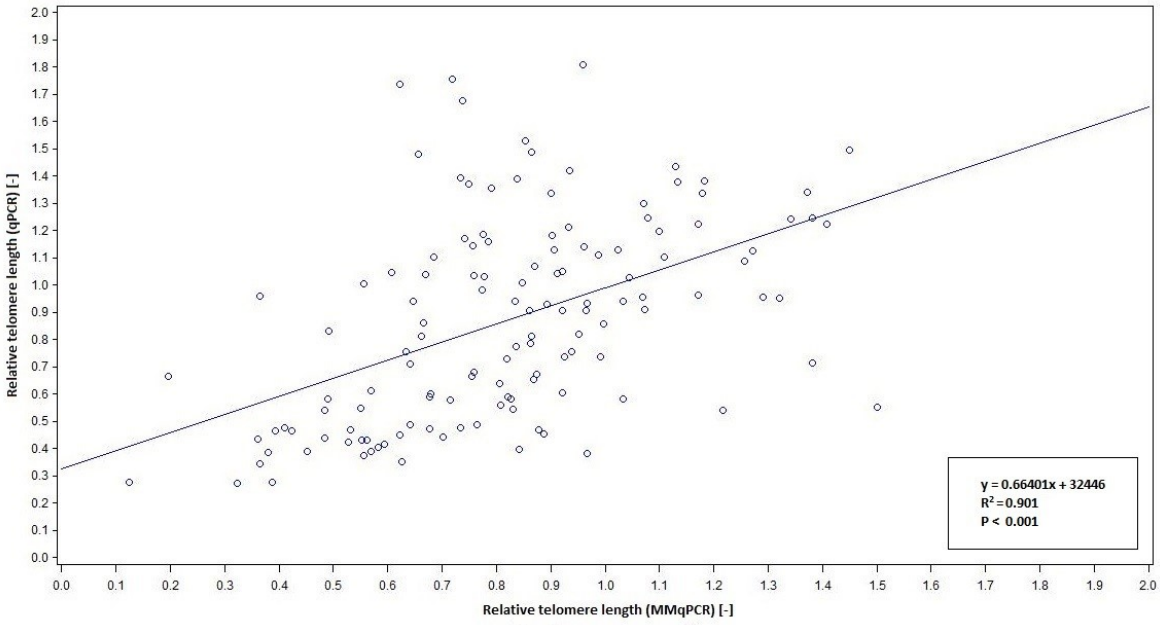

Figure 10. Correlation between qPCR and MMqPCR assays in the 1st sampling by linear regression analysis. The linear regression analysis showed a strong linear relationship between the RTL values from qPCR and MMqPCR (N = 131). The equation corresponding to the linear regression, correlation coefficient R^2, and probability value P are presented in the box.

4.2 Associations between Telomere Length and Age of Colorectal Cancer Patients

The mean age (± SD) at which the patients were diagnosed was 66.40 ± 10.68. The relationship between TL and age was estimated using the Spearman's rank-order correlation method. The results obtained by correlating age with the RTL measured in the 1st sampling, i.e. before cancer treatment (ρ = 0.721, P = 0.027, N = 172) show significant positive relationship. It appears that longer telomeres were associated with a moderately increasing age. Further, the correlation between the TL and age was tested by linear regression analysis, but no linear relationship between these variables was found (R^2 = 0.171, P < 0.001 in the 1st sampling, **figure 11**). These results may suggest that in colorectal cancer-affected individuals, the TL does not correlate with age.

There was also no statitically significant difference in the TL between the groups (</> 66 years) formed by splitting the data set according to the median age (Z = 0.20, P = 0.844, N(< 66 years) = 77, N(> 66 years) = 95 in the 1st sampling). The results suggest that younger individuals diagnosed with CRC have no statistically

significant difference in TLs compared to older individuals. The groups were compared by using two-samples Wilcoxon test.

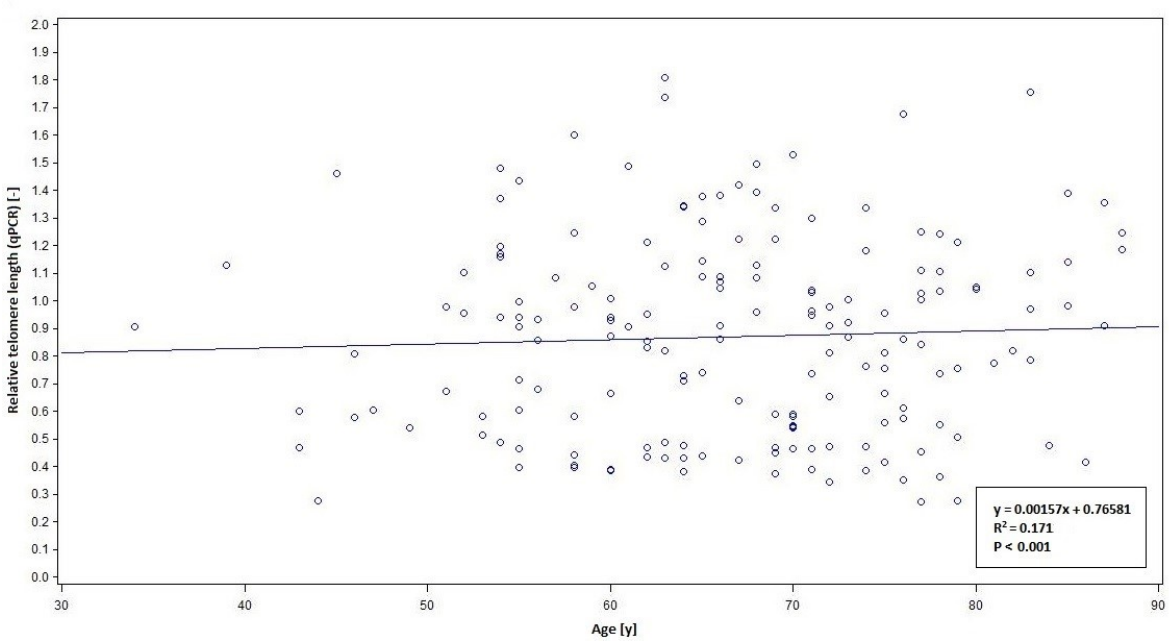

Figure 11. Correlation between RTL and age in the 1st sampling by linear regression. The linear regression analysis showed no linear association between the RTL and age (N = 172). The linear regression equation, correlation coefficient R^2 and probability value P are presented in the box.

4.3 Sex-Specific Associations with Telomere Length in Colorectal Cancer Patients

A comparison of the RTL of male (mean ± SD: 0.89 ± 0.37, N = 109 in the 1st sampling, and 0.83 ± 0.36, N = 102 in 2nd sampling) and female CRC patients (mean ± SD: 0.84 ± 0.34, N = 63 in the 1st sampling, and 0.89 ± 0.35, N = 56 in the 2nd sampling) showed that between them there was no significant difference. Shorter TL was in the 1st sampling (i.e. before cancer treatment) a bit more pronounced in women, while in the 2nd sampling (during cancer treatment) in men. However, the differences were not statistically significant (Z = -0.61, P = 0.546 in the 1st sampling, and Z = 0.95, P = 0.348 in the 2nd sampling; two-samples Wilcoxon test). It follow that in CRC patients, there is probably no sex difference in TL.

4.4 The Effect of Smoking on Telomere Length in Colorectal Cancer Patients

The RTL of patients who were classified as smokers (mean ± SD: 0.85 ± 0.36, N = 35 in the 1st sampling, i.e. before cancer treatment, and 0.83 ± 0.29, N = 37 in the 2nd sampling, i.e. during cancer treatment) was moderately shorter than that of non-smokers (mean ± SD: 0.90 ± 0.35, N = 127 in the 1st sampling, and 0.88 ± 0.37, N = 115 in the 2nd sampling), but there was no statistically significant difference between the groups (Z = -0.73, P = 0.469 in the 1st sampling, and Z = -0.44, P = 0.661 in the 2nd sampling; two-samples Wilcoxon test). A statistically significant difference between the TL of smokers and non-smokers was not found.

4.5 Telomere Length and Its Association to Tumor Location in Colorectal Cancer Patients

The peripheral blood lymphocyte TL of the CRC patients was also investigated in the relation to the primary tumor origin; i.e. in the proximal colon (N = 13), distal colon (N = 31) or rectum (N = 29) (**figure 12**). The difference between the groups (F = 2.35, P = 0.103), as well as the groups/time course interaction (F = 1.09, P = 0.366), was not significant, although the TL showed a tendency to shortening over time. These associations were tested using repeated-measures ANOVA. The shortest PBL RTL (mean ± SD: 0.77 ± 0.31 in the 1st sampling, i.e. before cancer treatment) was observed in the patients with proximal colon cancer relative to the distal colon (mean ± SD: 1.00 ± 0.40 in the 1st sampling) and rectal (0.92 ± 0.32 in the 1st sampling) cancer patients. The highest PBL RTL was found in patients with distal colon cancer.

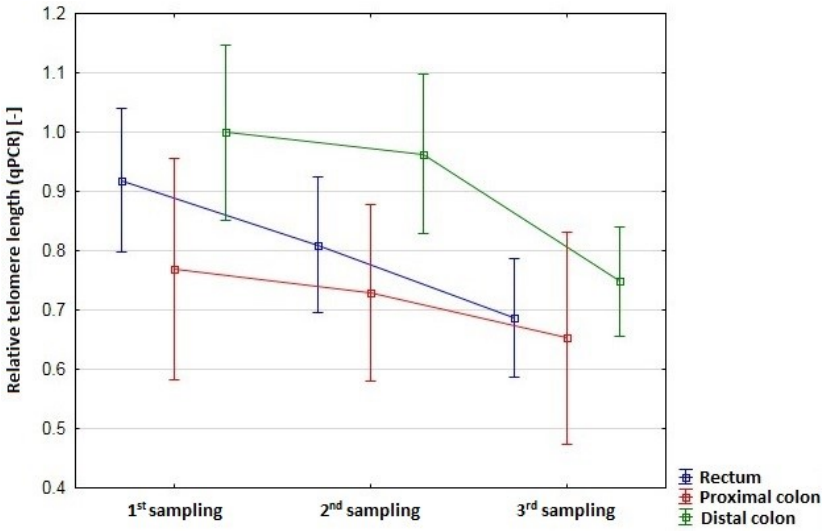

Figure 12. Changes in RTL between the samplings according to the site of the primary tumor origin. Plots represent mean RTL values, vertical bars denote 0.95 confidence intervals. The 1st samplings originate from the time of cancer diagnosis. The 2nd and 3rd samplings were drawn at 6-month intervals during cancer treatment

4.6 Association of Telomere Length with Type 2 *Diabetes Mellitus* in Colorectal Cancer Patients

The TL was compared in diabetic and non-diabetic patients using a two-samples Wilcoxon test. There was no significant difference in TL in diabetics (mean ± SD: 0.89 ± 0.33, N = 36 in the 1st sampling, i.e. before cancer treatment) and non-diabetics (mean ± SD: 0.86 ± 0.36, N = 136 in the 1st sampling; Z = 0.59, P = 0.553).

4.7 Telomere Length at Different TNM Stages of Colorectal Cancer

When analyzing TNM stages in relation to TL by the Wilcoxon two-samples test, there was no statistically significant difference noted between the early (stage 0 + I + II, N = 47) and advanced (stage III + IV, N = 27) TNM groups (Z = 0.09, P = 0.280 in the 1st sampling, i.e. before cancer treatment, Z = 0.28, P = 0.780 in the 2nd sampling, i.e. 6 months after diagnosis, and Z = 0.22, P = 0.823 in the 3rd sampling, i.e. 1 year after diagnosis) of CRC patients. However, the patients were found to have a consistent decreasing trend in TL over time (**figure 13**). Due to a low number of participants, the 4th sampling (collected 2 years after diagnosis) was excluded from the analysis.

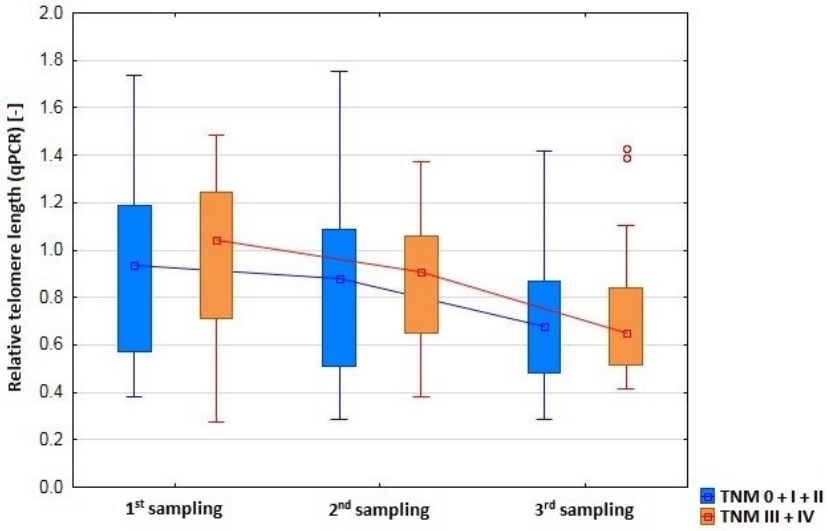

Figure 13. RTL changes of patients with early and advanced TNM stages over time. The 1st samplings were drawn from newly diagnosed patients before the start of treatment. The 2nd and 3rd were collected at 6-month intervals during treatment. Box and whisker plot displays the median, 25th–75th percentiles (box limits) and maximum and minimum RTL values (whiskers). Open circles represent outliers.

4.8 Telomere Length and Microsatellite Stability Status in Colorectal Cancer Patients

The association of TL with microsatellite instability was tested as well. The mean TL value in MSS patients was 0.88 ± 0.35 in the 1st sampling, i.e. before cancer treatment (N = 120), and 0.87 ± 0.34 in the 2nd sampling, i.e. during cancer treatment (N = 115). In MSI patients, the mean TL value was 0.81 ± 0.29 in the 1st sampling (N = 23), and 0.71 ± 0.26 in the 2nd sampling (N = 16) patients. The two-samples Wilcoxon test showed no significant difference between the groups (Z = 0.27, P = 0.547 in the 1st sampling, and Z = 0.04, P = 0.084 in the 2nd sampling). However, in the 2nd sampling, the difference was more pronounced. The results suggest that the TL in MSS and MSI CRC patients may differ. A larger sample size should hypothetically lead to more accurate results.

4.9 Role of Telomere Length in Predicting the Response to Therapy Among Patients with Colorectal Cancer

Repeated measures ANOVA test did not revealed any significant difference between the TL of good (N = 29) and poor (N = 8) CRC therapy responders (F = 0.49, P = 0.489), together with no significant interaction between the time and the groups (F = 1.32, P = 0.274, see **figure 14**). However, poor responders of patients with CRC had on average longer PBL RTL in the 1st sampling (1.15 ± 0.29) and the 2nd sampling (1.01 ± 0.25) compared to good responders (mean ± SD: 1.00 ± 0.33 in the 1st sampling and 0.82 ± 0.30 in the 2nd sampling, respectively). To sum up, it appears that the TL in poor therapy responder does not differ significantly from good therapy responders. However, in both analyzed groups, it was observed a decreasing trend in the TL over time

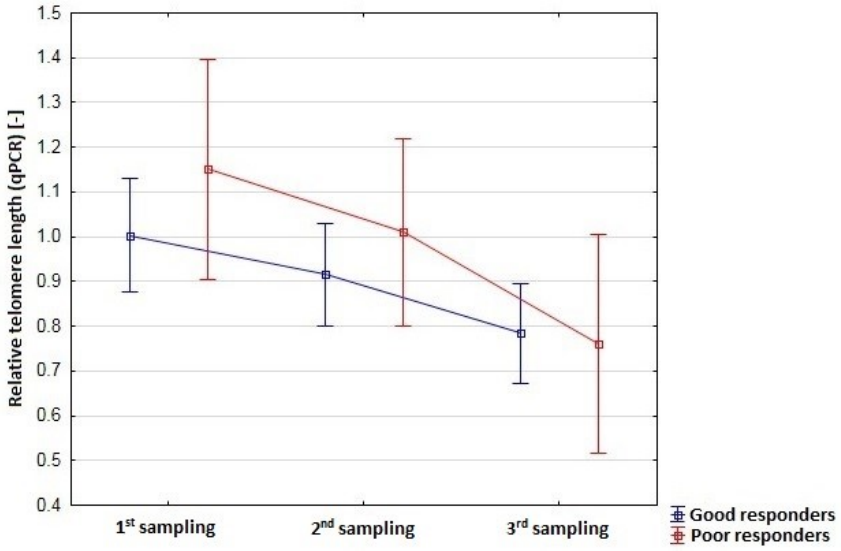

Figure 14. RTL changes in samples from good a poor therapy responders over time. The graph shows a plot of mean RTL values taken versus particular samplings. The 1st samplings were drawn from the patients before initiation of treatment. The 2nd and 3rd samplings were drawn every 6 months during the treatment. Error bars indicate a 0.95 confidence interval.

4.10 Effect of Neoadjuvant Therapy on Telomere Length in Rectal Cancer Patients

The effect of cancer treatment on TL was investigated in rectal cancer patients who received or did not receive neoadjuvant therapy. Two-samples Wilcoxon test confirmed that after starting neoadjuvant therapy, the patients' (N = 39) RTL did not significantly differ from those without neoadjuvant therapy (N = 24; Z = 0.06, P = 0.949 in the 2nd sampling). The RTL of patients did not differ substantially before (mean ± SD: 0.86 ± 0.32, N = 33 in the 1st sampling) and after (mean ± SD: 0.82 ± 0.32, N = 39 in the 2nd sampling) the neoadjuvant therapy.

4.11 Longitudinal Changes in Telomere Length in Colorectal Cancer Patients

The TL was also investigated to record its change within the same individuals over time. A comparison of the repeated measures (the 1st, 2nd and 3rd sampling) was performed using the Friedman's test showing a significant, time-dependent effect on telomere shortening ($\chi^2(2) = 17.59$, P = 0.0002, N = 74), the 4th sampling was excluded from the analysis. **Figure 15** illustrates the effect of time on the TL attrition. The results indicate the presence of decreasing trend in the TL observed from the date of CRC diagnosis (the 1st sampling) to 1 year after this event (the 3rd sampling).

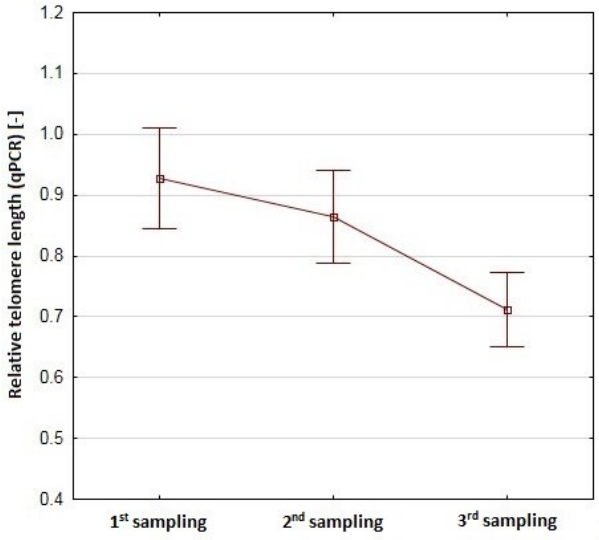

Figure 15. The effect of time on telomere shortening. The plot shows the means and 0.95 confidence interval bars of RTL in the 1st, 2nd and 3rd sampling (0 – 1 year after diagnosis).

4.12 The Overall Survival Rate of Colorectal Cancer Patients

The 5-year survival probability calculated on the basis of TLs measured in the 1st sampling, i.e. before treatment (N = 119, patients diagnosed < 31. 12. 2013) was 0.756 ± 0.049. Quartile distribution showed that the patients in the 1st quartile (N = 28), having the shortest RTL (< 0.82), had the highest 5-year survival rate (79%) followed by the patients in the 2nd (76%, N = 25) 3rd (71%, N = 27) and the 4th (71%, N = 27) quartile (see **table 4**, and Kaplan-Meier survival curve depicted in **figure 16**). However, a significant difference in 5-year survival distribution between these groups was not revealed either by log-rank ($\chi^2(3) = 0.094$, P = 0.993) or by Wilcoxon test ($\chi^2(3) = 0.43$, P = 0.935). A cut-off RTL value, the point with the most significant split, was set at 1.40. Both log-rank ($\chi^2(1) = 0.45$, P = 0.504) and Wilcoxon test ($\chi^2(1) = 0.55$, P = 0.457) did not shown a significant difference between the two groups (RTL < 1.40, N = 96 and RTL > 1.40, N = 11). The results suggest that any phenotypic variation in the TL does not significantly impact the 5-year survival of CRC patients.

Table 4. Overall 5-year survival of patients according to quartiles of RTL. Twelve observations with invalid time, censoring, or strata values were deleted. SE is the standard error of the estimated survival.

Number of quartile	Number of patients	RTL [-]	5-year survival ± SE
1st	28	< 0.82	0.791 ± 0.084
2nd	25	0.82-1.00	0.758 ± 0.112
3rd	27	1.00-1.24	0.711 ± 0.113
4th	27	> 1.24	0.710 ± 0.136

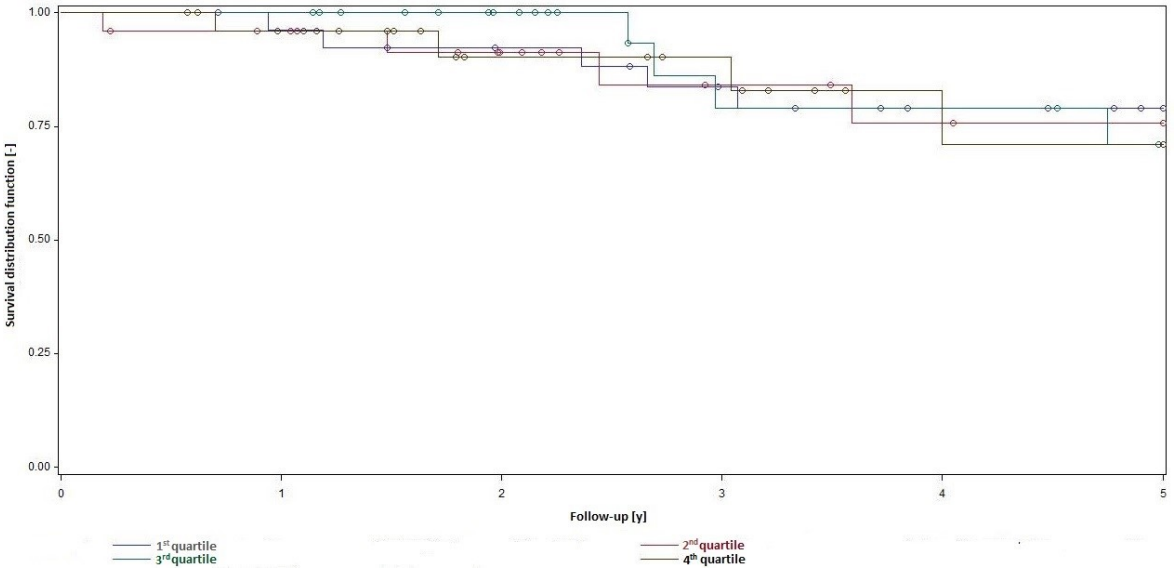

Figure 16. The 5-year survival curves by RTL quartiles of RTL measured in the 1st sampling. The first quartile has the lowest RTL. Circles represent the time when the patients was censored.

4.13 Expression of *hTERT* mRNA in Colorectal Cancer Patients

The analysis of *hTERT* mRNA expression in CRC patients has been performed only in a limited number of PBL samples and the results are incomplete at present. Hence, the following graph shows the results obtained only from one qPCR assay. The samples are from the 1st sampling (the time before treatment) and were chosen at random.

When speaking about this particular assay, *hTERT* mRNA was detected in all PBL samples, control included (**figure 17**), and *hTERT* mRNA expression levels were approximately 1.5–5.6 fold lower in colon cancer cases (two patients with proximal colon cancer and five patients with distal colon cancer) than in a healthy control with no history of a previous malignancy. However, the result from measuring the repeated samples drawn during the cancer treatment are not available, yet. It can be assumed that changes in the *hTERT* mRNA expression and possible telomerase upregulation during the treatment could be affected by cancer therapy.

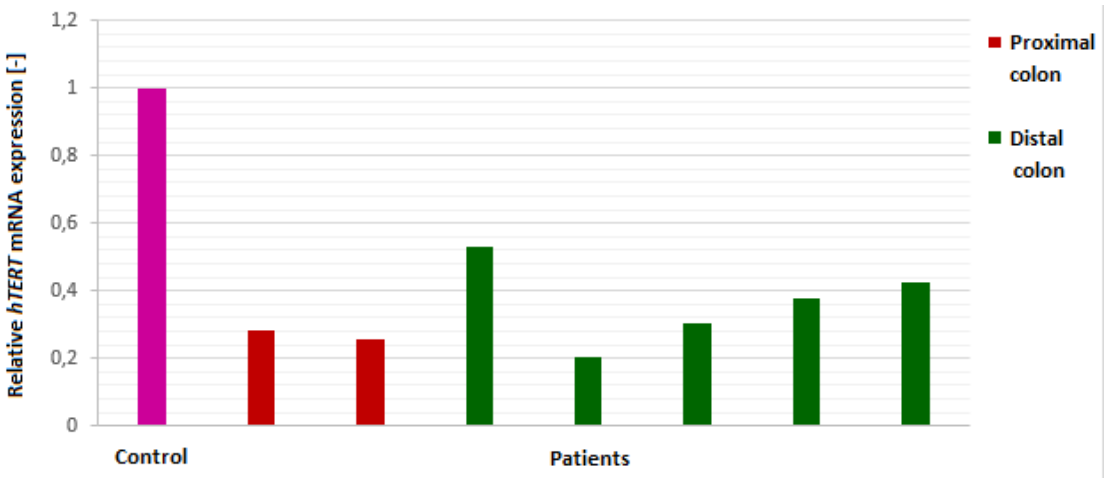

Figure 17. Expression of *hTERT* mRNA gene in patients from the 1st sampling. The *hTERT* mRNA was reversely transcribed, quantified by qPCR, and its levels were normalized to the control sample. Relative hTERT mRNA expression bars of patients with proximal colon cancer are indicated in red, of patients with distal colon cancer are indicated in green. The healthy control bar is indicated in violet.

5 Discussion

Considering the high prevalence of CRC, a relatively poor survival rate and the impact on a person's quality of life, there is a strong demand to find novel clinical biomarkers. In several studies, PBL TL was proposed as a potential biomarker for CRC risk, diagnosis, and prognosis. However, most of these studies bring inconsistent outcomes in general, which suggest that the relationship between TL and CRC is complex and can be potentially affected by a particular molecular phenotype, cancer site, histology, and other factors. Ultimately, the employment of different methods of RTL measurement or different pre-analytical conditions may lead to a distortion of RTL results [193]. The RTL can be affected by blood and the DNA storage methods, DNA treatment, and different experimental methods for DNA extraction [194–197]. Moreover, the study conducted by Dlouha et al. reported that even a slight DNA degradation leads to false RTL results [156].

Apart from the fact that available studies are often based on a small number of incident CRC patients, which limits an ability to detect minute effects on the TL, the results originate from ethnically different populations and thus may not be applicable across all races and ethnicities [198]. Beyond that, the studies often include samples only from one-time point. This study, though it comprises 193 Czech patients, was very beneficial especially because it investigated the association of the TL with disease progression. Changes in the TL were examined across the multiple time points with six-month intervals (from the date of the diagnosis through treatment and follow-up care). The TL was examined in relationship to the following features – age, sex, tobacco use, site of the primary tumor, type 2 *diabetes mellitus*, TNM stage, microsatellite status, therapy response, and neoadjuvant therapy.

To clarify the influence of using two different RTL measurement methods, correlation analysis between the RTL values was performed. The absolute values differed, the results cannot be therefore compared directly. The RTL values showed, however, the same trend and the results were correlating quite decently (ρ of 0.352–0.929). The dissimilar RTL values can be attributed to methodological differences such as using a different standard, primers, reference genes, thermal cycling profiles, etc. The effect of the pre-analytical conditions was ruled out because for both methods the same samples of DNA were used. To improve agreement between laboratories, a potential solution could be to develop and use one optimized protocol plus establish a set of pooled TL standards,

which allow for race, ethnicity, sex and age comparisons and would be uniformly used [193].

The majority of studies reported an inverse relationship between age and PBL TL in healthy individuals [150,199]. This study confirmed that PBL RTL correlates with age on the level of statistical significance, but against expectations, the mean TL was mildly increased in elderly patients. This effect may be related to the telomere lengthening induced by the disease. It has also to be taken into account a selection bias: the study comprises of patients with a constrained age range (interquartile range 60–74 years), and therefore the representation of younger age patients is almost missing. At present, the largest case-control study of PBL TL (including 2,011 CRC patients) reported a TL inverse association with age [175], as studies based on healthy individuals.

Regarding gender, it is assumed that healthy women tend to have on average longer telomeres than men [200]. It might by attributed to slower PBL telomere attrition, presumably because of the telomerase stimulation mediated by estrogen [201]. In this study, the mean TL of men and women did not significantly differ. This finding might be influenced by the disease phenotype and also an unequal gender distribution (only 70 females vs. 123 males) can lead to misrepresenting results. The study by Zöchmeister et al. mentioned in the above paragraph, showed that the longer TL was more pronounced in females, but they had at the same time also faster telomere attrition [175]. Thus, in older age, the mean TL of both males and females converged.

Regarding lifestyle habits such as smoking, cigarette smoke exposure was confirmed to enhance telomere shortening [202]. Even though the difference of TL between smokers and non-smokers was not statistically significant, the effect of smoking on TLs was demonstrated in this study, too. Interestingly, tobacco use seems to exert only a transient telomere shortening effect. According to Huzen et al., in individuals, who quitted smoking, the telomere attrition rate proceeds slowlier and it is comparable to the rate of those who never smoked [203]. Besides, Getliffe et al. associated smoking with decreased *hTERT* mRNA expression and thus with lower telomerase activity leading to impaired TL maintenance [204].

CRC comprises tumors with distinct phenotypes and genotypes. The heterogeneity of this disease is also mediated by the facts that proximal colon, distal colon, and rectum have distinct embryonic origins, functions and show different sensitivity to cancer therapy and telomerase profiles [143,205,206]. In this study, the mean PBL TL was in

the 1st sampling (i.e. in the moment of CRC diagnosis, before undergoing cancer treatment) shortest in proximal colon cases, and almost identical in distal colon cases and rectal cases, which might be due to the prevalence of rectosigmoideal cancer in a distal colon cancer group. The same trend (the shortest TL in the proximal colon, medium TL in rectal and the longest TL in distal colon cases) was showed in the 2nd and 3rd sampling (i.e. six months and one year after the diagnosis, during cancer treatment). Due to the limited size of the study, the results did not achieve statistical significance. However, in our recent study on CRC patients, we observed both in tumor tissue and adjacent mucosa pronounced gradient from the shortest telomeres in the proximal colon to the longest in the rectum [115].

Microsatellite instable colorectal cancers are often characterized by an increased lymphocytic infiltrate, which suggests a robust immune response against the tumor [207]. While in tumor cells the MSI with a frequency of telomere shortening correlates [208], in PBL of patients having MSI tumors, the association was not investigated in detail, yet. In this study, patients with MSS tumor had in both the 1st and the 2nd sampling longer PBL TL than those with MSI tumors, but the difference between them was not statistically significant. The results indicate that possible association of microsatellite status to the TL status would be interesting to test again in a larger group of patients (as we did in the study published by Kroupa et al. [115].

The mean TL differences over time could be an effect of the disease progression or reflect cancer treatment. Both radiotherapy and chemotherapy can cause DNA damage, but it is unclear yet to what extent is their effect in lymphocytes manifested and persistent [209,210]. Transient PBL telomere shortening (around 2 years) driven by chemotherapy was described in sporadic breast cancer cases [211]. Telomere shortening in T-lymphocytes *in vitro* as a consequence of radiotherapy was reported by Su et al. [212]. Although the study by Maeda et al. did not reveal any change of the mean TL upon radiation, radiation therapy was found to have an effect in fraction of PBL with short telomeres [213]. Besides that, neoadjuvant therapy was reported to change the lymphocyte composition in tumor-draining lymph nodes [214]. In this study, no statistically significant association between the neoadjuvant therapy and TL was found. However, it is not out of the question that the possible relationship to TL can be found in a larger group of patients, after its stratification according to the type of neoadjuvant therapy.

Neoadjuvant therapy-derived toxicity and the way how it translates into TL likely varies depending on the class of chemotherapeutic agents and radiation doses [19].

Correlation among the TL in colorectal cancer tumor cells and TNM stage or International Union Against Cancer (UICC) stage was reported [114,115], however not for TLs in PBL. In this study, the mean PBL TL did not vary between the different TNM stages, but it was decreasing in both 0 + I + II and III + IV groups over time. The same tendency was also observed when studying the change of TLs in good and poor responders, change of TLs in relationship to tumor location and longitudinal changes in TL in general. Friedman's test showed that during the 1st year after the diagnosis (the period between the 1st and 3rd sampling) the telomere shortening is time-dependent and that this association is statistically significant. The TL shortening in PBL can be associated with T-lymphocyte hyper-stimulation [215]. On a wider scale, telomere attrition can reflect the reduced adaptive immune response of patients, because the proliferative capacity of $CD8^+$ T-lymphocytes and antibody production of B-lymphocytes with long telomeres is higher than those with short telomeres [216].

Diabetes mellitus is linked to telomere shortening for a relatively long time. The association of the type 1 *diabetes mellitus* and shortened PBL TL was for the first time reported in the study by Jeanclos et al., but a significant association with type 2 *diabetes mellitus* was not observed back then [217]. A major part of the following studies this association between shorter TLs and type 2 *diabetes* nevertheless confirmed and pronounced that telomere shortening in diabetics could be attributed to the oxidative stress [218,219]. Further, the type 2 *diabetes mellitus* seems to predispose patients to have shorter monocyte TL [220]. Regarding the own results, the statistically significant difference between patients having the type 2 *diabetes* and non-diabetic patients was not found. It can be concluded that the tentative effect needs to be examined in a larger population.

It was found an inverse relationship between 5-year survival and TL. Patients with the shortest TL were associated with the best 5-year survival rate, and then this rate was gradually decreasing among the TL quartiles. Conversely, a meta-analysis based on data from a total of 956 patients by Jia and Wang associated the short TL in PBL with poorer overall survival, and the association was, unlike our results, statistically significant [221]. On the other hand, our study was focused on 5-year survival and, additionally, it was calculated from RTL measured before the initiation of the treatment, which both can explain the difference. On the whole, the TL is suggested to be an indicator of

the magnitude of immune response and the shorter TL may point out the degree of lymphocytes employment against tumor cells, the reaction to cancer treatment, etc. Whether the PBL TL is predictive of CRC survival is still not clear, however.

In this follow-up study, we will further evaluate the interplay between TL and telomerase activity. At the time the diploma thesis was handled in, the assay was only just beginning. Because of this fact, here we discuss only the results measured on randomly chosen samples. It may be noted that *hTERT* mRNA expression was detectable in all measured samples and healthy control, but it was lower in cases than in control. Again, this finding can be explained by the fact that these results originate from the blood samples of CRC patients taken by the time the patients were diagnosed (the 1st sampling), and therefore the samples are not affected by CRC treatment, which is related to up-regulation of hTERT expression (Guo *et al.*, 2009). We can expect the *hTERT* may become temporarily higher during the follow-up. Nevertheless, the number of samples is too low. Further evaluation of completed data (e.g. association of *hTERT* mRNA expression with RTL, or clinicopathological data of patients) could produce more informative results, with a potential use in the treatment prediction.

6 Conclusions

The peripheral blood leukocyte telomere length fluctuates during the CRC treatment and follow-up care. Those changes are likely, besides other factors, caused by the presence of the tumor and therapeutic regimens. None of the investigated clinico-pathological features – age, sex, tobacco use, primary tumor location, type 2 *diabetes mellitus*, TNM stage, MSI, therapy response, and neoadjuvant therapy – was statistically significant associated to the shorter or longer TL.

The main contribution of this study lies in the evaluation of the relationship between PBL TLs and clinico-pathological informations. The study is unique for the availability of repeated samples, which allowed to measure TL changes over time. Moreover, this work led to the establishment of the qPCR RTL measurement method and the method for analyzing hTERT mRNA expression levels in our laboratory. Comparing the two techniques for RTL measurement, qPCR and MMqPCR, showed moderate to the high correlation between the data. Quantitative polymerase chain reaction-based methods for RTL analysis are not methodologically standardized, which results in a lower reproducibility between the laboratories. Steps towards the protocol unification, such as using the same set of TL standards, are desirable.

Despite the relatively low number of patients analyzed, our study suggests that the PBL TL is not an independent prognostic marker of CRC. Nevertheless, deeper undestanding of telomere biochemistry in CRC patients could lead to more personalized care for these patients. Therefore, further large-scale studies are needed to assess the PBL TL diagnostic value and its potential clinical utility.

7 Funding

The research was supported by grants GACR 19-10543S, GACR 18-09709S, and AZV NV18/03/00199.

References

[1] F. Bray, J. Ferlay, I. Soerjomataram, R.L. Siegel, L.A. Torre, A. Jemal, Global cancer statistics 2018: GLOBOCAN estimates of incidence and mortality worldwide for 36 cancers in 185 countries, CA. Cancer J. Clin., 68 (2018) 394–424.

[2] R. Siegel, A. Jemal, Colorectal cancer facts & figures 2011-2013, American Cancer Society, Atlanta, 2011.

[3] W.M. Grady, S.D. Markowitz, The molecular pathogenesis of colorectal cancer and its potential application to colorectal cancer screening, Dig. Dis. Sci., 60 (2015) 762–772.

[4] J.M. Carethers, B.H. Jung, Genetics and genetic biomarkers in sporadic colorectal cancer, Gastroenterology, 149 (2015) 1177-1190.

[5] A.R. Williams, B.A. Balasooriya, D.W. Day, Polyps and cancer of the large bowel: a necropsy study in Liverpool, Gut, 23 (1982) 835–842.

[6] C.R. Boland, A. Goel, Microsatellite instability in colorectal cancer, Gastroenterology, 138 (2010) 2073-2087.

[7] B. Orsetti, J. Selves, C. Bascoul-Mollevi, L. Lasorsa, K. Gordien, F. Bibeau, B. Massemin, F. Paraf, I. Soubeyran, I. Hostein, V. Dapremont, R. Guimbaud, C. Cazaux, M. Longy, C. Theillet, Impact of chromosomal instability on colorectal cancer progression and outcome, BMC Cancer, 14 (2014) e121.

[8] C. Lengauer, K.W. Kinzler, B. Vogelstein, Genetic instability in colorectal cancers, Nature, 386 (1997) 623–627.

[9] J.M. Wheeler, W.F. Bodmer, N.J. Mortensen, DNA mismatch repair genes and colorectal cancer, Gut, 47 (2000) 148–153.

[10] M. Mirza-Aghazadeh-Attari, S.G. Darband, M. Kaviani, A. Mihanfar, J. Aghazadeh Attari, B. Yousefi, M. Majidinia, DNA damage response and repair in colorectal cancer: Defects, regulation and therapeutic implications, DNA Repair, 69 (2018) 34–52.

[11] E. Rampazzo, R. Bertorelle, L. Serra, L. Terrin, C. Candiotto, S. Pucciarelli, P. Del Bianco, D. Nitti, A. De Rossi, Relationship between telomere shortening, genetic instability, and site of tumour origin in colorectal cancers, Br. J. Cancer, 102 (2010) 1300–1305.

[12] N. Khakimov, G. Khasanova, K. Ershova, L. Gibadullina, T. Vetkina, G. Lobisheva, A. Chumakova, Screening for colon cancer: a test for occult blood, Int. J. Risk Saf. Med., 27 (2015) 110-111.

[13] J.K. Triantafillidis, C. Vagianos, G. Malgarinos, Colonoscopy in Colorectal Cancer Screening: Current Aspects, Indian J. Surg. Oncol., 6 (2015) 237–250.

[14] M. Zavoral, G. Vojtěchová, O. Májek, O. Ngo, T. Grega, B. Seifert, L. Dušek, Š. Suchánek, Population colorectal cancer screening in the Czech Republic, Cas. Lek. Cesk., 155 (2016) 7–12.

[15] A. Kalyan, S. Rozelle, A. Benson, Neoadjuvant treatment of rectal cancer: where are we now?, Gastroenterol. Rep., 4 (2016) 206–209.

[16] T. Matsuda, K. Yamashita, H. Hasegawa, T. Oshikiri, M. Hosono, N. Higashino, M. Yamamoto, Y. Matsuda, S. Kanaji, T. Nakamura, S. Suzuki, Y. Sumi, Y. Kakeji, Recent updates in the surgical treatment of colorectal cancer, Ann. Gastroenterol. Surg., 2 (2018) 129–136.

[17] M.E. Royce, D. Medgyesy, T.H. Zukowski, S. Dwivedy, P.M. Hoff, R. Pazdur, Colorectal cancer: chemotherapy treatment overview, Oncology (Williston Park, N.Y.), 14 (2000) 40–46.

[18] J. Aparicio, C. Fernandez-Martos, J.M. Vincent, I. Maestu, C. Llorca, I. Busquier, J.M. Campos, D. Perez-Enguix, M. Balcells, FOLFOX alternated with FOLFIRI as first-line chemotherapy for metastatic colorectal cancer, Clin. Colorectal Cancer, 5 (2005) 263–267.

[19] L. Gallicchio, S.M. Gadalla, J.D. Murphy, N.I. Simonds, The effect of cancer treatments on telomere length: a systematic review of the literature, J. Natl. Cancer Inst., 110 (2018) 1048–1058.

[20] T. de Lange, L. Shiue, R.M. Myers, D.R. Cox, S.L. Naylor, A.M. Killery, H.E. Varmus, Structure and variability of human chromosome ends, Mol. Cell. Biol., 10 (1990) 518–527.
[21] V.L. Makarov, Y. Hirose, J.P. Langmore, Long G tails at both ends of human chromosomes suggest a C strand degradation mechanism for telomere shortening, Cell, 88 (1997) 657–666.
[22] J.D. Griffith, L. Comeau, S. Rosenfield, R.M. Stansel, A. Bianchi, H. Moss, T. de Lange, Mammalian telomeres end in a large duplex loop, Cell, 97 (1999) 503–514.
[23] S. Luke-Glaser, H. Poschke, B. Luke, Getting in (and out of) the loop: regulating higher order telomere structures, Front. Oncol., 2 (2012) e180.
[24] Q. Wang, J. Liu, Z. Chen, K. Zheng, C. Chen, Y.-H. Hao, Z. Tan, G-quadruplex formation at the 3' end of telomere DNA inhibits its extension by telomerase, polymerase and unwinding by helicase, Nucleic Acids Res., 39 (2011) 6229–6237.
[25] L. Nanić, S. Ravlić, I. Rubelj, Extrachromosomal DNA in genome (in)stability – role of telomeres, Croat. Chem. Acta, 89 (2016) 175–181.
[26] E. Janoušková, I. Nečasová, J. Pavloušková, M. Zimmermann, M. Hluchý, V. Marini, M. Nováková, C. Hofr, Human Rap1 modulates TRF2 attraction to telomeric DNA, Nucleic Acids Res., 43 (2015) 2691–2700.
[27] N.V. Ilicheva, O.I. Podgornaya, A.P. Voronin, Telomere repeat-binding factor 2 is responsible for the telomere attachment to the nuclear membrane, Adv. Protein Chem. Struct. Biol., 101 (2015) 67–96.
[28] A.K. Frank, D.C. Tran, R.W. Qu, B.A. Stohr, D.J. Segal, L. Xu, The shelterin TIN2 subunit mediates recruitment of telomerase to telomeres, PLoS Genet., 11 (2015) e1005410.
[29] S. Kim, C. Beausejour, A.R. Davalos, P. Kaminker, S.-J. Heo, J. Campisi, TIN2 mediates functions of TRF2 at human telomeres, J. Biol. Chem., 279 (2004) 43799–43804.
[30] D. Hockemeyer, W. Palm, T. Else, J.-P. Daniels, K.K. Takai, J.Z.-S. Ye, C.E. Keegan, T. de Lange, G.D. Hammer, Telomere protection by mammalian Pot1 requires interaction with Tpp1, Nat. Struct. Mol. Biol., 14 (2007) 754–761.
[31] J. Nandakumar, C.F. Bell, I. Weidenfeld, A.J. Zaug, L.A. Leinwand, T.R. Cech, The TEL patch of telomere protein TPP1 mediates telomerase recruitment and processivity, Nature, 492 (2012) 285–289.
[32] D. Loayza, T. De Lange, POT1 as a terminal transducer of TRF1 telomere length control, Nature, 423 (2003) 1013–1018.
[33] R.M. Stansel, T. de Lange, J.D. Griffith, T-loop assembly in vitro involves binding of TRF2 near the 3' telomeric overhang, EMBO J., 20 (2001) 5532–5540.
[34] M.Z. Levy, R.C. Allsopp, A.B. Futcher, C.W. Greider, C.B. Harley, Telomere end-replication problem and cell aging, J. Mol. Biol., 225 (1992) 951–960.
[35] H. Vaziri, F. Schächter, I. Uchida, L. Wei, X. Zhu, R. Effros, D. Cohen, C.B. Harley, Loss of telomeric DNA during aging of normal and trisomy 21 human lymphocytes, Am. J. Hum. Genet., 52 (1993) 661–667.
[36] L. Hayflick, P.S. Moorhead, The serial cultivation of human diploid cell strains, Exp. Cell Res., 25 (1961) 585–621.
[37] L. Hayflick, The limited in vitro lifetime of human diploid cell strains, Exp. Cell Res., 37 (1965) 614–636.
[38] S. Waga, B. Stillman, The DNA replication fork in eukaryotic cells, Annu. Rev. Biochem., 67 (1998) 721–751.
[39] K. Muraki, K. Nyhan, L. Han, J.P. Murnane, Mechanisms of telomere loss and their consequences for chromosome instability, Front. Oncol., 2 (2012) e135.
[40] P. Wu, H. Takai, T. de Lange, Telomeric 3' overhangs derive from resection by Exo1 and Apollo and fill-in by POT1b-associated CST, Cell, 150 (2012) 39–52.
[41] T. Else, Telomeres and telomerase in adrenocortical tissue maintenance, carcinogenesis, and aging, J. Mol. Endocrinol., 43 (2009) 131–141.
[42] C.M. Counter, A.A. Avilion, C.E. LeFeuvre, N.G. Stewart, C.W. Greider, C.B. Harley, S. Bacchetti, Telomere shortening associated with chromosome instability is arrested in immortal cells which express telomerase activity, EMBO J., 11 (1992) 1921–1929.

[43] P. Mao, J. Liu, Z. Zhang, H. Zhang, H. Liu, S. Gao, Y.S. Rong, Y. Zhao, Homologous recombination-dependent repair of telomeric DSBs in proliferating human cells, Nat. Commun., 7 (2016) e12154.
[44] Y. Doksani, T. de Lange, Telomere-internal double-strand breaks are repaired by homologous recombination and PARP1/Lig3-dependent end-joining, Cell Rep., 17 (2016) 1646–1656.
[45] Y. Doksani, The response to DNA damage at telomeric repeats and its consequences for telomere function, Genes (Basel), 10 (2019) e318.
[46] S. Espejel, M. Martín, P. Klatt, J. Martín-Caballero, J.M. Flores, M.A. Blasco, Shorter telomeres, accelerated ageing and increased lymphoma in DNA-PKcs-deficient mice, EMBO Rep., 5 (2004) 503–509.
[47] M. McVey, S.E. Lee, MMEJ repair of double-strand breaks (director's cut): deleted sequences and alternative endings, Trends Genet., 24 (2008) 529–538.
[48] R. Rai, H. Zheng, H. He, Y. Luo, A. Multani, P.B. Carpenter, S. Chang, The function of classical and alternative non-homologous end-joining pathways in the fusion of dysfunctional telomeres, EMBO J., 29 (2010) 2598–2610.
[49] A. Ribes-Zamora, S.M. Indiviglio, I. Mihalek, C.L. Williams, A.A. Bertuch, TRF2 interaction with Ku heterotetramerization interface gives insight into c-NHEJ prevention at human telomeres, Cell Rep., 5 (2013) 194–206.
[50] C. Allen, A. Kurimasa, M.A. Brenneman, D.J. Chen, J.A. Nickoloff, DNA-dependent protein kinase suppresses double-strand break-induced and spontaneous homologous recombination, Proc. Natl. Acad. Sci. U. S. A., 99 (2002) 3758–3763.
[51] M.A. Serrano, Z. Li, M. Dangeti, P.R. Musich, S. Patrick, M. Roginskaya, B. Cartwright, Y. Zou, DNA-PK, ATM and ATR collaboratively regulate p53-RPA interaction to facilitate homologous recombination DNA repair, Oncogene, 32 (2013) 2452–2462.
[52] S.J.H. Arlander, B.T. Greene, C.L. Innes, R.S. Paules, DNA protein kinase-dependent G2 checkpoint revealed following knockdown of ataxia-telangiectasia mutated in human mammary epithelial cells, Cancer Res., 68 (2008) 89–97.
[53] H.L. Hsu, D. Gilley, E.H. Blackburn, D.J. Chen, Ku is associated with the telomere in mammals, Proc. Natl. Acad. Sci. U. S. A., 96 (1999) 12454–12458.
[54] J.R. Walker, R.A. Corpina, J. Goldberg, Structure of the Ku heterodimer bound to DNA and its implications for double-strand break repair, Nature, 412 (2001) 607–614.
[55] N.S. Bae, P. Baumann, A RAP1/TRF2 complex inhibits nonhomologous end-joining at human telomeric DNA ends, Mol. Cell, 26 (2007) 323–334.
[56] H. Pashaiefar, M. Yaghmaie, J. Tavakkoly-Bazzaz, S. Hamidollah Ghaffari, K. Alimoghaddam, P. Izadi, A. Ghavamzadeh, The association between PARP1 and LIG3 expression levels and chromosomal translocations in acute myeloid leukemia patients, Cell J., 20 (2018) 204–210.
[57] M. Wang, W. Wu, W. Wu, B. Rosidi, L. Zhang, H. Wang, G. Iliakis, PARP-1 and Ku compete for repair of DNA double strand breaks by distinct NHEJ pathways, Nucleic Acids Res., 34 (2006) 6170–6182.
[58] A. Sfeir, T. de Lange, Removal of shelterin reveals the telomere end-protection problem, Science, 336 (2012) 593–597.
[59] K.K. Takai, T. Kibe, J.R. Donigian, D. Frescas, T. de Lange, Telomere protection by TPP1/POT1 requires tethering to TIN2, Mol. Cell, 44 (2011) 647–659.
[60] Y. Gong, T. de Lange, A Shld1-controlled POT1a provides support for repression of ATR signaling at telomeres through RPA exclusion, Mol. Cell, 40 (2010) 377–387.
[61] L. Roger, R.E. Jones, N.H. Heppel, G.T. Williams, J.R. Sampson, D.M. Baird, Extensive telomere erosion in the initiation of colorectal adenomas and its association with chromosomal instability, J. Natl. Cancer Inst., 105 (2013) 1202–1211.
[62] L.N. Truong, Y. Li, L.Z. Shi, P.Y.-H. Hwang, J. He, H. Wang, N. Razavian, M.W. Berns, X. Wu, Microhomology-mediated end joining and homologous recombination share the initial end resection step to repair DNA double-strand breaks in mammalian cells, Proc. Natl. Acad. Sci. U. S. A., 110 (2013) 7720–7725.

[63] J.-S. Kim, T.B. Krasieva, H. Kurumizaka, D.J. Chen, A.M.R. Taylor, K. Yokomori, Independent and sequential recruitment of NHEJ and HR factors to DNA damage sites in mammalian cells, J. Cell Biol., 170 (2005) 341–347.
[64] M. Frank-Vaillant, S. Marcand, Transient stability of DNA ends allows nonhomologous end joining to precede homologous recombination, Mol. Cell, 10 (2002) 1189–1199.
[65] R.E. Verdun, J. Karlseder, The DNA damage machinery and homologous recombination pathway act consecutively to protect human telomeres, Cell, 127 (2006) 709–720.
[66] K. Perrem, L.M. Colgin, A.A. Neumann, T.R. Yeager, R.R. Reddel, Coexistence of alternative lengthening of telomeres and telomerase in hTERT-transfected GM847 cells, Mol. Cell. Biol., 21 (2001) 3862–3875.
[67] M.A. Dunham, A.A. Neumann, C.L. Fasching, R.R. Reddel, Telomere maintenance by recombination in human cells, Nat. Genet., 26 (2000) 447–450.
[68] A. Muntoni, A.A. Neumann, M. Hills, R.R. Reddel, Telomere elongation involves intra-molecular DNA replication in cells utilizing alternative lengthening of telomeres, Hum. Mol. Genet., 18 (2009) 1017–1027.
[69] Y. Hu, G. Shi, L. Zhang, F. Li, Y. Jiang, S. Jiang, W. Ma, Y. Zhao, Z. Songyang, J. Huang, Switch telomerase to ALT mechanism by inducing telomeric DNA damages and dysfunction of ATRX and DAXX, Sci. Rep., 6 (2016) e32280.
[70] Z. Crees, J. Girard, Z. Rios, G.M. Botting, K. Harrington, C. Shearrow, L. Wojdyla, A.L. Stone, S.B. Uppada, J.T. Devito, N. Puri, Oligonucleotides and G-quadruplex stabilizers: targeting telomeres and telomerase in cancer therapy, Curr. Pharm. Des., 20 (2014) 6422–6437.
[71] J.D. Henson, Y. Cao, L.I. Huschtscha, A.C. Chang, A.Y.M. Au, H.A. Pickett, R.R. Reddel, DNA C-circles are specific and quantifiable markers of alternative-lengthening-of-telomeres activity, Nat. Biotechnol., 27 (2009) 1181–1185.
[72] R. Rai, Y. Chen, M. Lei, S. Chang, TRF2-RAP1 is required to protect telomeres from engaging in homologous recombination-mediated deletions and fusions, Nat. Commun., 7 (2016) e10881.
[73] K.K. Khanna, K.E. Keating, S. Kozlov, S. Scott, M. Gatei, K. Hobson, Y. Taya, B. Gabrielli, D. Chan, S.P. Lees-Miller, M.F. Lavin, ATM associates with and phosphorylates p53: mapping the region of interaction, Nat. Genet., 20 (1998) 398–400.
[74] J. Karlseder, K. Hoke, O.K. Mirzoeva, C. Bakkenist, M.B. Kastan, J.H.J. Petrini, T. de Lange, The telomeric protein TRF2 binds the ATM kinase and can inhibit the ATM-dependent DNA damage response, PLoS Biol., 2 (2004) e240.
[75] N. Dimitrova, T. de Lange, Cell cycle-dependent role of MRN at dysfunctional telomeres: ATM signaling-dependent induction of nonhomologous end joining (NHEJ) in G1 and resection-mediated inhibition of NHEJ in G2, Mol. Cell. Biol., 29 (2009) 5552–5563.
[76] L.A. Boardman, R.A. Johnson, K.B. Viker, K.A. Hafner, R.B. Jenkins, D.L. Riegert-Johnson, T.C. Smyrk, K. Litzelman, S. Seo, R.E. Gangnon, C.D. Engelman, D.N. Rider, R.J. Vanderboom, S.N. Thibodeau, G.M. Petersen, H.G. Skinner, Correlation of chromosomal instability, telomere length and telomere maintenance in microsatellite stable rectal cancer: a molecular subclass of rectal cancer, PloS ONE, 8 (2013) e80015.
[77] O.E. Bechter, Y. Zou, W. Walker, W.E. Wright, J.W. Shay, Telomeric recombination in mismatch repair deficient human colon cancer cells after telomerase inhibition, Cancer Res., 64 (2004) 3444–3451.
[78] J. Zhou, M. Liu, A.M. Fleming, C.J. Burrows, S.S. Wallace, Neil3 and NEIL1 DNA glycosylases remove oxidative damages from quadruplex DNA and exhibit preferences for lesions in the telomeric sequence context, J. Biol. Chem., 288 (2013) 27263–27272.
[79] M. Morikawa, K. Kino, T. Oyoshi, M. Suzuki, T. Kobayashi, H. Miyazawa, Analysis of guanine oxidation products in double-stranded DNA and proposed guanine oxidation pathways in single-stranded, double-stranded or quadruplex DNA, Biomolecules, 4 (2014) 140–159.

[80] H. Vallabhaneni, N. O'Callaghan, J. Sidorova, Y. Liu, Defective repair of oxidative base lesions by the DNA glycosylase Nth1 associates with multiple telomere defects, PLoS Genet., 9 (2013) e1003639.
[81] D.B. Rhee, A. Ghosh, J. Lu, V.A. Bohr, Y. Liu, Factors that influence telomeric oxidative base damage and repair by DNA glycosylase OGG1, DNA Repair, 10 (2011) 34–44.
[82] L. Sun, R. Tan, J. Xu, J. LaFace, Y. Gao, Y. Xiao, M. Attar, C. Neumann, G.-M. Li, B. Su, Y. Liu, S. Nakajima, A.S. Levine, L. Lan, Targeted DNA damage at individual telomeres disrupts their integrity and triggers cell death, Nucleic Acids Res., 43 (2015) 6334–6347.
[83] A.S. Miller, L. Balakrishnan, N.A. Buncher, P.L. Opresko, R.A. Bambara, Telomere proteins POT1, TRF1 and TRF2 augment long-patch base excision repair in vitro, Cell Cycle, 11 (2012) 998–1007.
[84] J. Zhou, J. Chan, M. Lambelé, T. Yusufzai, J. Stumpff, P.L. Opresko, M. Thali, S.S. Wallace, NEIL3 repairs telomere damage during S phase to secure chromosome segregation at mitosis, Cell Rep., 20 (2017) 2044–2056.
[85] H. Vallabhaneni, F. Zhou, R.W. Maul, J. Sarkar, J. Yin, M. Lei, L. Harrington, P.J. Gearhart, Y. Liu, Defective repair of uracil causes telomere defects in mouse hematopoietic cells, J. Biol. Chem., 290 (2015) 5502–5511.
[86] H.-T. Lee, A. Bose, C.-Y. Lee, P.L. Opresko, S. Myong, Molecular mechanisms by which oxidative DNA damage promotes telomerase activity, Nucleic Acids Res., 45 (2017) 11752–11765.
[87] T. von Zglinicki, Oxidative stress shortens telomeres, Trends Biochem. Sci., 27 (2002) 339–344.
[88] S. Kawanishi, S. Oikawa, Mechanism of telomere shortening by oxidative stress, Ann. N. Y. Acad. Sci., 1019 (2004) 278–284.
[89] P.J. Rochette, D.E. Brash, Human telomeres are hypersensitive to UV-induced DNA damage and refractory to repair, PLoS Genet., 6 (2010) e1000926.
[90] D. Parikh, E. Fouquerel, C.T. Murphy, H. Wang, P.L. Opresko, Telomeres are partly shielded from ultraviolet-induced damage and proficient for nucleotide excision repair of photoproducts, Nat. Commun., 6 (2015) 8214.
[91] L.A. Aaltonen, P. Peltomäki, F.S. Leach, P. Sistonen, L. Pylkkänen, J.P. Mecklin, H. Järvinen, S.M. Powell, J. Jen, S.R. Hamilton, Clues to the pathogenesis of familial colorectal cancer, Science, 260 (1993) 812–816.
[92] L.A. Aaltonen, P. Peltomäki, J.P. Mecklin, H. Järvinen, J.R. Jass, J.S. Green, H.T. Lynch, P. Watson, G. Tallqvist, M. Juhola, Replication errors in benign and malignant tumors from hereditary nonpolyposis colorectal cancer patients, Cancer Res., 54 (1994) 1645–1648.
[93] J.G. Herman, A. Umar, K. Polyak, J.R. Graff, N. Ahuja, J.P. Issa, S. Markowitz, J.K. Willson, S.R. Hamilton, K.W. Kinzler, M.F. Kane, R.D. Kolodner, B. Vogelstein, T.A. Kunkel, S.B. Baylin, Incidence and functional consequences of hMLH1 promoter hypermethylation in colorectal carcinoma, Proc. Natl. Acad. Sci. U. S. A., 95 (1998) 6870–6875.
[94] J.J.P. Gille, F.B.L. Hogervorst, G. Pals, J.T. Wijnen, R.J. van Schooten, C.J. Dommering, G.A. Meijer, M.E. Craanen, P.M. Nederlof, D. de Jong, C.J. McElgunn, J.P. Schouten, F.H. Menko, Genomic deletions of MSH2 and MLH1 in colorectal cancer families detected by a novel mutation detection approach, Br. J. Cancer, 87 (2002) 892–897.
[95] H.A. Pickett, D.M. Baird, P. Hoff-Olsen, G.I. Meling, T.O. Rognum, J. Shaw, K.P. West, N.J. Royle, Telomere instability detected in sporadic colon cancers, some showing mutations in a mismatch repair gene, Oncogene, 23 (2004) 3434–3443.
[96] M.R. Campbell, Y. Wang, S.E. Andrew, Y. Liu, Msh2 deficiency leads to chromosomal abnormalities, centrosome amplification, and telomere capping defect, Oncogene, 25 (2006) 2531–2536.
[97] P. Martinez, I. Siegl-Cachedenier, J.M. Flores, M.A. Blasco, MSH2 deficiency abolishes the anticancer and pro-aging activity of short telomeres, Aging Cell, 8 (2009) 2–17.
[98] A. Mendez-Bermudez, N.J. Royle, Deficiency in DNA mismatch repair increases the rate of telomere shortening in normal human cells, Hum. Mutat., 32 (2011) 939–946.

[99] N. Seguí, M. Pineda, E. Guinó, E. Borràs, M. Navarro, F. Bellido, V. Moreno, C. Lázaro, I. Blanco, G. Capellá, L. Valle, Telomere length and genetic anticipation in Lynch syndrome, PloS ONE, 8 (2013) e61286.
[100] N. Seguí, E. Guinó, M. Pineda, M. Navarro, F. Bellido, C. Lázaro, I. Blanco, V. Moreno, G. Capellá, L. Valle, Longer telomeres are associated with cancer risk in MMR-proficient hereditary non-polyposis colorectal cancer, PloS ONE, 9 (2014) e86063.
[101] Y. Omori, F. Nakayama, D. Li, K. Kanemitsu, S. Semba, A. Ito, H. Yokozaki, Alternative lengthening of telomeres frequently occurs in mismatch repair system-deficient gastric carcinoma, Cancer Sci., 100 (2009) 413–418.
[102] P. Jia, M. Chastain, Y. Zou, C. Her, W. Chai, Human MLH1 suppresses the insertion of telomeric sequences at intra-chromosomal sites in telomerase-expressing cells, Nucleic Acids Res., 45 (2017) 1219–1232.
[103] P. Jia, W. Chai, The MLH1 ATPase domain is needed for suppressing aberrant formation of interstitial telomeric sequences, DNA Repair, 65 (2018) 20–25.
[104] L. Crabbe, A. Jauch, C.M. Naeger, H. Holtgreve-Grez, J. Karlseder, Telomere dysfunction as a cause of genomic instability in Werner syndrome, Proc. Natl. Acad. Sci. U. S. A., 104 (2007) 2205–2210.
[105] P.C. Haycock, E.E. Heydon, S. Kaptoge, A.S. Butterworth, A. Thompson, P. Willeit, Leucocyte telomere length and risk of cardiovascular disease: systematic review and meta-analysis, BMJ, 349 (2014) e4227.
[106] M. McGrath, J.Y.Y. Wong, D. Michaud, D.J. Hunter, I. De Vivo, Telomere length, cigarette smoking, and bladder cancer risk in men and women, Cancer Epidemiol. Biomarkers Prev., 16 (2007) 815–819.
[107] S. Qu, W. Wen, X.-O. Shu, W.-H. Chow, Y.-B. Xiang, J. Wu, B.-T. Ji, N. Rothman, G. Yang, Q. Cai, Y.-T. Gao, W. Zheng, Association of leukocyte telomere length with breast cancer risk: nested case-control findings from the Shanghai Women's Health Study, Am. J. Epidemiol., 177 (2013) 617–624.
[108] N. Basu, H.G. Skinner, K. Litzelman, R. Vanderboom, E. Baichoo, L.A. Boardman, Telomeres and telomere dynamics: relevance to cancers of the GI tract, Expert Rev. Gastroenterol. Hepatol., 7 (2013) 733–748.
[109] Y. Sun, L. Zhang, L. Zhao, X. Wu, J. Gu, Association of leukocyte telomere length in peripheral blood leukocytes with endometrial cancer risk in Caucasian Americans, Carcinogenesis, 36 (2015) 1327–1332.
[110] Y. Gu, C. Yu, L. Miao, L. Wang, C. Xu, W. Xue, J. Du, H. Yuan, J. Dai, G. Jin, Z. Hu, H. Ma, H. Shen, Telomere length, genetic variants and risk of squamous cell carcinoma of the head and neck in Southeast Chinese, Sci. Rep., 6 (2016) e20675.
[111] B. Karimi, M. Yunesian, R. Nabizadeh, P. Mehdipour, A. Aghaie, Is leukocyte telomere length related with lung cancer risk?: a meta-analysis, Iran. Biomed. J., 21 (2017) 142–153.
[112] M.J. Machiela, J.N. Hofmann, R. Carreras-Torres, K.M. Brown, M. Johansson, Z. Wang, M. Foll, P. Li, N. Rothman, S.A. Savage, V. Gaborieau, J.D. McKay, Y. Ye, M. Henrion, F. Bruinsma, S. Jordan, G. Severi, K. Hveem, L.J. Vatten, T. Fletcher, K. Koppova, S.C. Larsson, A. Wolk, R.E. Banks, P.J. Selby, D.F. Easton, P. Pharoah, G. Adreotti, L.E.B. Freeman, S. Koutros, D. Albanes, S. Mannisto, S. Weinstein, P.E. Clark, T.E. Edwards, L. Lipworth, S.M. Gapstur, V.L. Stevens, H. Carol, M.L. Freedman, M.M. Pomerantz, E. Cho, P. Kraft, M.A. Preston, K.M. Wilson, J.M. Gaziano, H.S. Sesso, A. Black, N.D. Freedman, W.Y. Huang, J.G. Anema, R.J. Kahnoski, B.R. Lane, S.L. Noyes, D. Petillo, L.M. Coli, J.N. Sampson, C. Besse, H. Blanche, A. Boland, L. Burdette, E. Prokhortchouk, K.G. Skryabin, M. Yeager, M. Mijuskovic, M. Ognjanovic, L. Foretova, I. Holcatova, V. Janout, D. Mates, A. Mukeriya, S. Rascu, D. Zaridze, V. Bencko, C. Cybulski, E. Fabianova, V. Jinga, J. Lissowska, J. Lubinski, M. Navratilova, P. Rudnai, N. Szeszenia-Dabrowska, S. Benhamou, G. Cancel-Tassin, O. Cussenot, H.B. Bueno-de-Mesquita, F. Canzian, E.J. Duell, B. Ljungberg, R.T. Sitaram, U. Peters, E. White, G.L. Anderson, L. Johnson, J. Lou, J. Buring, I. M. Lee, W.H. Chow, L.E. Moore,

C. Wood, T. Eisen, J. Larkin, T.K. Choueiri, G.M. Lathrop, B.T. Teh, J.F. Deleuze, X, Wu, R.S. Houlston, P. Brennan, S.J. Chanock, G. Scelo, M.P. Purdue, Genetic variants related to longer telomere length are associated with increased risk of renal cell carcinoma, Eur. Urol., 72 (2017) 747–754.

[113] F. Maxwell, L.M. McGlynn, H.C. Muir, D. Talwar, M. Benzeval, T. Robertson, C.S. Roxburgh, D.C. McMillan, P.G. Horgan, P.G. Shiels, Telomere attrition and decreased fetuin-A levels indicate accelerated biological aging and are implicated in the pathogenesis of colorectal cancer, Clin. Cancer Res., 17 (2011) 5573–5581.

[114] E.L. Balc'h, N. Grandin, M.-V. Demattei, S. Guyétant, A. Tallet, J.-C. Pagès, M. Ouaissi, T. Lecomte, M. Charbonneau, Measurement of telomere length in colorectal cancers for improved molecular diagnosis, Int. J. Mol. Sci., 18 (2017) e1871.

[115] M. Kroupa, S.K. Rachakonda, V. Liska, N. Srinivas, M. Urbanova, K. Jiraskova, M. Schneiderova, O. Vycital, V. Vymetalkova, L. Vodickova, R. Kumar, P. Vodicka, Relationship of telomere length in colorectal cancer patients with cancer phenotype and patient prognosis, Br. J. Cancer, (2019). *In press*.

[116] G. De Maio, C. Rengucci, W. Zoli, D. Calistri, Circulating and stool nucleic acid analysis for colorectal cancer diagnosis, World J. Gastroenterol., 20 (2014) 957–967.

[117] V. Vymetalkova, K. Cervena, L. Bartu, P. Vodicka, Circulating cell-free DNA and colorectal cancer: a systematic review, Int. J. Mol. Sci., 19 (2018) e3356.

[118] F. Diehl, M. Li, D. Dressman, Y. He, D. Shen, S. Szabo, L.A. Diaz, S.N. Goodman, K.A. David, H. Juhl, K.W. Kinzler, B. Vogelstein, Detection and quantification of mutations in the plasma of patients with colorectal tumors, Proc. Natl. Acad. Sci. U. S. A., 102 (2005) 16368–16373.

[119] D. Sidransky, T. Tokino, S.R. Hamilton, K.W. Kinzler, B. Levin, P. Frost, B. Vogelstein, Identification of ras oncogene mutations in the stool of patients with curable colorectal tumors, Science, 256 (1992) 102–105.

[120] D. Whitney, J. Skoletsky, K. Moore, K. Boynton, L. Kann, R. Brand, S. Syngal, M. Lawson, A. Shuber, Enhanced retrieval of DNA from human fecal samples results in improved performance of colorectal cancer screening test, J. Mol. Diagn., 6 (2004) 386–395.

[121] A. Saini, Y. Pershad, H. Albadawi, M. Kuo, S. Alzubaidi, S. Naidu, M.-G. Knuttinen, R. Oklu, Liquid biopsy in gastrointestinal cancers, Diagnostics (Basel), 8 (2018) e75.

[122] T. Fujii, A. Barzi, A. Sartore-Bianchi, A. Cassingena, G. Siravegna, D.D. Karp, S.A. Piha-Paul, V. Subbiah, A.M. Tsimberidou, H.J. Huang, S. Veronese, F. Di Nicolantonio, S. Pingle, C.R.T. Vibat, S. Hancock, D. Berz, V.O. Melnikova, M.G. Erlander, R. Luthra, E.S. Kopetz, F. Meritz-Bernstam, S. Siena, H.J. Lenz, A. Bardelli, F. Janku, Mutation-enrichment next-generation sequencing for quantitative detection of KRAS mutations in urine cell-free DNA from patients with advanced cancers, Clin. Cancer Res., 23 (2017) 3657–3666.

[123] N.W. Kim, M.A. Piatyszek, K.R. Prowse, C.B. Harley, M.D. West, P.L. Ho, G.M. Coviello, W.E. Wright, S.L. Weinrich, J.W. Shay, Specific association of human telomerase activity with immortal cells and cancer, Science, 266 (1994) 2011–2015.

[124] A.J. Cesare, R.R. Reddel, Alternative lengthening of telomeres: models, mechanisms and implications, Nat. Rev. Genet., 11 (2010) 319–330.

[125] K. Liu, M.M. Schoonmaker, B.L. Levine, C.H. June, R.J. Hodes, N.P. Weng, Constitutive and regulated expression of telomerase reverse transcriptase (hTERT) in human lymphocytes, Proc. Natl. Acad. Sci. U. S. A., 96 (1999) 5147–5152.

[126] M.T. Teixeira, M. Arneric, P. Sperisen, J. Lingner, Telomere length homeostasis is achieved via a switch between telomerase-extendible and -nonextendible states, Cell, 117 (2004) 323–335.

[127] D. Hockemeyer, K. Collins, Control of telomerase action at human telomeres, Nat. Struct. Mol. Biol., 22 (2015) 848–852.

[128] J.M. Vogan, K. Collins, Dynamics of human telomerase holoenzyme assembly and subunit exchange across the cell cycle, J. Biol. Chem., 290 (2015) 21320–21335.

[129] A.A. Avilion, M.A. Piatyszek, J. Gupta, J.W. Shay, S. Bacchetti, C.W. Greider, Human telomerase RNA and telomerase activity in immortal cell lines and tumor tissues, Cancer Res., 56 (1996) 645–650.
[130] C.M. Counter, M. Meyerson, E.N. Eaton, L.W. Ellisen, S.D. Caddle, D.A. Haber, R.A. Weinberg, Telomerase activity is restored in human cells by ectopic expression of hTERT (hEST2), the catalytic subunit of telomerase, Oncogene, 16 (1998) 1217–1222.
[131] I. Guilleret, P. Yan, F. Grange, R. Braunschweig, F.T. Bosman, J. Benhattar, Hypermethylation of the human telomerase catalytic subunit (hTERT) gene correlates with telomerase activity, Int. J. Cancer, 101 (2002) 335–341.
[132] L. Boldrini, S. Pistolesi, S. Gisfredi, S. Ursino, G. Lupi, M. Caniglia, R. Pingitore, F. Basolo, G. Parenti, G. Fontanini, Telomerase in intracranial meningiomas, Int. J. Mol. Med., 12 (2003) 943–947.
[133] S. Borah, L. Xi, A.J. Zaug, N.M. Powell, G.M. Dancik, S.B. Cohen, J.C. Costello, D. Theodorescu, T.R. Cech, Cancer TERT promoter mutations and telomerase reactivation in urothelial cancer, Science, 347 (2015) 1006–1010.
[134] S. Horn, A. Figl, P.S. Rachakonda, C. Fischer, A. Sucker, A. Gast, S. Kadel, I. Moll, E. Nagore, K. Hemminki, D. Schadendorf, R. Kumar, TERT promoter mutations in familial and sporadic melanoma, Science, 339 (2013) 959–961.
[135] Y. Miyake, J.-I. Adachi, T. Suzuki, K. Mishima, R. Araki, R. Mizuno, R. Nishikawa, TERT promoter methylation is significantly associated with TERT upregulation and disease progression in pituitary adenomas, J. Neurooncol., 141 (2019) 131–138.
[136] D.D. Lee, R. Leão, M. Komosa, M. Gallo, C.H. Zhang, T. Lipman, M. Remke, A. Heidari, N.M. Nunes, J.D. Apolónio, A.J. Price, R.A. De Mello, J.S. Dias, D. Huntsman, T. Hermanns, P.J. Wild, R. Vanner, G. Zadeh, J. Karamchandani, S. Das, M.D. Taylor, C.E. Hawkins, J.D. Wasserman, A. Figueiredo, R.J. Hamilton, M.D. Minden, K. Wani, B. Diplas, H. Yan, K. Aldape, M.R. Akbari, A. Danesh, T.J. Pugh, P.B. Dirks, P. Castelo-Branco, U. Tabori, DNA hypermethylation within TERT promoter upregulates TERT expression in cancer, J. Clin. Invest., 129 (2019) 223–229.
[137] G. Sarek, P. Marzec, P. Margalef, S.J. Boulton, Molecular basis of telomere dysfunction in human genetic diseases, Nat. Struct. Mol. Biol., 22 (2015) 867–874.
[138] N. Tatsumoto, E. Hiyama, Y. Murakami, Y. Imamura, J.W. Shay, Y. Matsuura, T. Yokoyama, High telomerase activity is an independent prognostic indicator of poor outcome in colorectal cancer, Clin. Cancer Res., 6 (2000) 2696–2701.
[139] R. Bertorelle, E. Rampazzo, S. Pucciarelli, D. Nitti, A. De Rossi, Telomeres, telomerase and colorectal cancer, World J. Gastroenterol., 20 (2014) 1940–1950.
[140] T. Fernández-Marcelo, A. Sánchez-Pernaute, I. Pascua, C. De Juan, J. Head, A.-J. Torres-García, P. Iniesta, Clinical relevance of telomere status and telomerase activity in colorectal cancer, PloS ONE, 11 (2016) e0149626.
[141] S.S. Chung, B. Oliva, S. Dwabe, J.V. Vadgama, Combination treatment with flavonoid morin and telomerase inhibitor MST-312 reduces cancer stem cell traits by targeting STAT3 and telomerase, Int. J. Oncol., 49 (2016) 487–498.
[142] H.C. Jeung, S.Y. Rha, S.J. Shin, J.B. Ahn, K.H. Park, T.S. Kim, J.J. Kim, J.K. Roh, H.C. Chung, Changes in telomerase activity due to alternative splicing of human telomerase reverse transcriptase in colorectal cancer, Oncol. Lett., 14 (2017) 2385–2392.
[143] G.D. Ayiomamitis, G. Notas, A. Zaravinos, A. Zizi-Sermpetzoglou, M. Georgiadou, O. Sfakianaki, E. Kouroumallis, Differences in telomerase activity between colon and rectal cancer, Can. J. Surg., 57 (2014) 199–208.
[144] H. Kawamoto, N. Minato, Myeloid cells, Int. J. Biochem. Cell Biol., 36 (2004) 1374–1379.
[145] H.-W. Lee, S.-J. Park, B.K. Choi, H.H. Kim, K.-O. Nam, B.S. Kwon, 4-1BB promotes the survival of CD8+ T lymphocytes by increasing expression of Bcl-xL and Bfl-1, J. Immunol., 169 (2002) 4882–4888.
[146] S. Herzog, M. Reth, H. Jumaa, Regulation of B-cell proliferation and differentiation by pre-B-cell receptor signalling, Nat. Rev. Immunol., 9 (2009) 195–205.

[147] Y. Sun, Y. Sun, G. Lin, R. Zhang, K. Zhang, J. Xie, L. Wang, J. Li, Multicolor flow cytometry analysis of the proliferations of T-lymphocyte subsets in vitro by EdU incorporation, Cytometry A, 81 (2012) 901–909.
[148] C.R. Kleiveland, Peripheral blood mononuclear cells, in: K. Verhoeckx, P. Cotter, I. López-Expósito, C. Kleiveland, T. Lea, A. Mackie, T. Requena, D. Swiatecka, H. Wichers (Eds.), Impact Food Bioact. Health Vitro Ex Vivo Models, Springer, Cham, 2015, pp. 161–167.
[149] N. Rufer, T.H. Brümmendorf, S. Kolvraa, C. Bischoff, K. Christensen, L. Wadsworth, M. Schulzer, P.M. Lansdorp, Telomere fluorescence measurements in granulocytes and T lymphocyte subsets point to a high turnover of hematopoietic stem cells and memory T cells in early childhood, J. Exp. Med., 190 (1999) 157–167.
[150] N.H. Son, S. Murray, J. Yanovski, R.J. Hodes, N. Weng, Lineage-specific telomere shortening and unaltered capacity for telomerase expression in human T and B lymphocytes with age, J. Immunol., 165 (2000) 1191–1196.
[151] N.P. Weng, B.L. Levine, C.H. June, R.J. Hodes, Human naive and memory T lymphocytes differ in telomeric length and replicative potential, Proc. Natl. Acad. Sci. U. S. A., 92 (1995) 11091–11094.
[152] J. Monteiro, F. Batliwalla, H. Ostrer, P.K. Gregersen, Shortened telomeres in clonally expanded CD28-CD8+ T cells imply a replicative history that is distinct from their CD28+CD8+ counterparts, J. Immunol., 156 (1996) 3587–3590.
[153] C.M. Counter, J. Gupta, C.B. Harley, B. Leber, S. Bacchetti, Telomerase activity in normal leukocytes and in hematologic malignancies, Blood, 85 (1995) 2315–2320.
[154] J. Lin, J. Cheon, R. Brown, M. Coccia, E. Puterman, K. Aschbacher, E. Sinclair, E. Epel, E.H. Blackburn, Systematic and cell type-specific telomere length changes in subsets of lymphocytes, J. Immunol. Res., 2016 (2016) e5371050.
[155] U. Svenson, K. Nordfjäll, D. Baird, L. Roger, P. Osterman, M.-L. Hellenius, G. Roos, Blood cell telomere length is a dynamic feature, PloS ONE, 6 (2011) e21485.
[156] D. Dlouha, J. Maluskova, I. Kralova Lesna, V. Lanska, J.A. Hubacek, Comparison of the relative telomere length measured in leukocytes and eleven different human tissues, Physiol. Res., 63 (2014) 343–350.
[157] N.P. Weng, K.S. Hathcock, R.J. Hodes, Regulation of telomere length and telomerase in T and B cells: a mechanism for maintaining replicative potential, Immunity, 9 (1998) 151–157.
[158] E. Mariani, A. Meneghetti, I. Formentini, S. Neri, L. Cattini, G. Ravaglia, P. Forti, A. Facchini, Telomere length and telomerase activity: effect of ageing on human NK cells, Mech. Ageing Dev., 124 (2003) 403–408.
[159] E. Hooijberg, J.J. Ruizendaal, P.J. Snijders, E.W. Kueter, J.M. Walboomers, H. Spits, Immortalization of human CD8+ T cell clones by ectopic expression of telomerase reverse transcriptase, J. Immunol., 165 (2000) 4239–4245.
[160] A. Roth, H. Yssel, J. Pene, E.A. Chavez, M. Schertzer, P.M. Lansdorp, H. Spits, R.M. Luiten, Telomerase levels control the lifespan of human T lymphocytes, Blood, 102 (2003) 849–857.
[161] E.E. Huang, E. Tedone, R. O'Hara, C. Cornelius, T.-P. Lai, A. Ludlow, W.E. Wright, J.W. Shay, The maintenance of telomere length in CD28+ T cells during T lymphocyte stimulation, Sci. Rep., 7 (2017) e6785.
[162] U. Svenson, Å. Öberg, R. Stenling, R. Palmqvist, G. Roos, Telomere length in peripheral leukocytes is associated with immune cell tumor infiltration and prognosis in colorectal cancer patients, Tumour Biol., 37 (2016) 10877–10882.
[163] T.C. Smyrk, P. Watson, K. Kaul, H.T. Lynch, Tumor-infiltrating lymphocytes are a marker for microsatellite instability in colorectal carcinoma, Cancer, 91 (2001) 2417–2422.
[164] N. Takemoto, F. Konishi, K. Yamashita, M. Kojima, T. Furukawa, Y. Miyakura, K. Shitoh, H. Nagai, The correlation of microsatellite instability and tumor-infiltrating lymphocytes in hereditary non-polyposis colorectal cancer (HNPCC) and sporadic colorectal cancers:

the significance of different types of lymphocyte infiltration, Jpn. J. Clin. Oncol., 34 (2004) 90–98.
[165] S.M. Phillips, A. Banerjea, R. Feakins, S.R. Li, S.A. Bustin, S. Dorudi, Tumour-infiltrating lymphocytes in colorectal cancer with microsatellite instability are activated and cytotoxic, Br. J. Surg., 91 (2004) 469–475.
[166] G.H. Kang, Four molecular subtypes of colorectal cancer and their precursor lesions, Arch. Pathol. Lab. Med., 135 (2011) 698–703.
[167] L. Kaszubowska, Telomere shortening and ageing of the immune system, J. Physiol. Pharmacol., 59 (2008) 169–186.
[168] R. Mzahma, M. Kharrat, F. Fetiriche, Bouasker, M. Ben Moussa, Z. Ben Safta, C. Dziri, A. Zaouche, H. Chaabouni-Bouhamed, The relationship between telomere length and clinicopathologic characteristics in colorectal cancers among Tunisian patients, Tumour Biol., 36 (2015) 8703–8713.
[169] Y. Cui, Q. Cai, S. Qu, W.-H. Chow, W. Wen, Y.-B. Xiang, J. Wu, N. Rothman, G. Yang, X.-O. Shu, Y.-T. Gao, W. Zheng, Association of leukocyte telomere length with colorectal cancer risk: nested case-control findings from the Shanghai Women's Health Study, Cancer Epidemiol. Biomarkers Prev., 21 (2012) 1807–1813.
[170] L.A. Boardman, K. Litzelman, S. Seo, R.A. Johnson, R.J. Vanderboom, G.W. Kimmel, J.M. Cunningham, R.E. Gangnon, C.D. Engelman, D.L. Riegert-Johnson, J. Potter, R. Haile, D. Buchanan, M.A. Jenkins, D.N. Rider, S.N. Thibodeau, G.M. Petersen, H.G. Skinner, The association of telomere length with colorectal cancer differs by the age of cancer onset, Clin. Transl. Gastroenterol., 5 (2014) e52.
[171] A.J. Pellatt, R.K. Wolff, A. Lundgreen, R. Cawthon, M.L. Slattery, Genetic and lifestyle influence on telomere length and subsequent risk of colon cancer in a case control study, Int. J. Mol. Epidemiol. Genet., 3 (2012) 184–194.
[172] Q. Qin, J. Sun, J. Yin, L. Liu, J. Chen, Y. Zhang, T. Li, Y. Shi, S. Wei, S. Nie, Telomere length in peripheral blood leukocytes is associated with risk of colorectal cancer in Chinese population, PloS ONE, 9 (2014) e88135.
[173] Y. Chen, F. Qu, X. He, G. Bao, X. Liu, S. Wan, J. Xing, Short leukocyte telomere length predicts poor prognosis and indicates altered immune functions in colorectal cancer patients, Ann. Oncol., 25 (2014) 869–876.
[174] H.N. Luu, M. Qi, R. Wang, J. Adams-Haduch, I. Miljkovic, P.L. Opresko, A. Jin, W.-P. Koh, J.-M. Yuan, Association between leukocyte telomere length and colorectal cancer risk in the Singapore Chinese health study, Clin. Transl. Gastroenterol., 10 (2019) 1–9.
[175] C. Zöchmeister, S. Brezina, P. Hofer, A. Baierl, M.M. Bergmann, T. Bachleitner-Hofmann, J. Karner-Hanusch, A. Stift, A. Gerger, G. Leeb, K. Mach, S. Rachakonda, R. Kumar, A. Gsur, Leukocyte telomere length throughout the continuum of colorectal carcinogenesis, Oncotarget, 9 (2018) 13582–13592.
[176] I.-M. Lee, J. Lin, A.J. Castonguay, N.S. Barton, J.E. Buring, R.Y.L. Zee, Mean leukocyte telomere length and risk of incident colorectal carcinoma in women: a prospective, nested case-control study, Clin. Chem. Lab. Med., 48 (2010) 259–262.
[177] R.Y.L. Zee, A.J. Castonguay, N.S. Barton, J.E. Buring, Mean telomere length and risk of incident colorectal carcinoma: a prospective, nested case-control approach, Cancer Epidemiol. Biomarkers Prev., 18 (2009) 2280–2282.
[178] K.A. Pooley, M.S. Sandhu, J. Tyrer, M. Shah, K.E. Driver, R.N. Luben, S.A. Bingham, B.A.J. Ponder, P.D.P. Pharoah, K.-T. Khaw, D.F. Easton, A.M. Dunning, Telomere length in prospective and retrospective cancer case-control studies, Cancer Res., 70 (2010) 3170–3176.
[179] H. Nelson, N. Petrelli, A. Carlin, J. Couture, J. Fleshman, J. Guillem, B. Miedema, D. Ota, D. Sargent, Guidelines 2000 for colon and rectal cancer surgery, J. Natl. Cancer Inst., 93 (2001) 583–596.
[180] P. Desjardins, D. Conklin, NanoDrop microvolume quantitation of nucleic acids, J. Vis. Exp., 45 (2010) e2565.

[181] I. Mender, J.W. Shay, Telomere Restriction Fragment (TRF) Analysis, Bio. Protoc., 5 (2015) e1658.
[182] G.M. Baerlocher, I. Vulto, G. de Jong, P.M. Lansdorp, Flow cytometry and FISH to measure the average length of telomeres (flow FISH), Nat. Protoc., 1 (2006) 2365–2376.
[183] D.M. Baird, J. Rowson, D. Wynford-Thomas, D. Kipling, Extensive allelic variation and ultrashort telomeres in senescent human cells, Nat. Genet., 33 (2003) 203–207.
[184] R.M. Cawthon, Telomere measurement by quantitative PCR, Nucleic Acids Res., 30 (2002) e47.
[185] N. O'Callaghan, V. Dhillon, P. Thomas, M. Fenech, A quantitative real-time PCR method for absolute telomere length, BioTechniques, 44 (2008) 807–809.
[186] R.M. Cawthon, Telomere length measurement by a novel monochrome multiplex quantitative PCR method, Nucleic Acids Res., 37 (2009) e21.
[187] A. Zinkova, I. Brynychova, A. Svacina, M. Jirkovska, M. Korabecna, Cell-free DNA from human plasma and serum differs in content of telomeric sequences and its ability to promote immune response, Sci. Rep., 7 (2017) e2591.
[188] I. Hosen, P.S. Rachakonda, B. Heidenreich, P.J. de Verdier, C. Ryk, G. Steineck, K.Hemminki, R. Kumar, Mutations in TERT promoter and FGFR3 and telomere length in bladder cancer, Int. J. Cancer, 137 (2015) 1621–1629.
[189] H. Zipper, H. Brunner, J. Bernhagen, F. Vitzthum, Investigations on DNA intercalation and surface binding by SYBR Green I, its structure determination and methodological implications, Nucleic Acids Res., 32 (2004) e103.
[190] J.L. Boulay, J. Reuter, R. Ritschard, L. Terracciano, R. Herrmann, C. Rochlitz, Gene dosage by quantitative real-time PCR, BioTechniques, 27 (1999) 228–230, 232.
[191] M.E. Gil, T.L. Coetzer, Real-time quantitative PCR of telomere length, Mol. Biotechnol., 27 (2004) 169–172.
[192] P.T. Monis, S. Giglio, C.P. Saint, Comparison of SYTO9 and SYBR Green I for real-time polymerase chain reaction and investigation of the effect of dye concentration on amplification and DNA melting curve analysis, Anal. Biochem., 340 (2005) 24–34.
[193] C.M. Martin-Ruiz, D. Baird, L. Roger, P. Boukamp, D. Krunic, R. Cawthon, M.M. Dokter, P. van der Harst, S. Bekaert, T. de Meyer, G. Roos, U. Svenson, V. Codd, N.J. Samani, L. McGlynn, P.G. Shiels, K.A. Pooley, A.M. Dunning, R. Cooper, A. Wong, A. Kingston, T. von Zglinicki, Reproducibility of telomere length assessment: an international collaborative study, Int. J. Epidemiol., 44 (2015) 1673–1683.
[194] J.M. Cunningham, R.A. Johnson, K. Litzelman, H.G. Skinner, S. Seo, C.D. Engelman, R.J. Vanderboom, G.W. Kimmel, R.E. Gangnon, D.L. Riegert-Johnson, J.A. Baron, J.D. Potter, R. Haile, D.D. Buchanan, M.A. Jenkins, D.N. Rider, S.N. Thibodeau, G.M. Petersen, L.A. Boardman, Telomere length varies by DNA extraction method: implications for epidemiologic research, Cancer Epidemiol. Biomarkers Prev., 22 (2013) 2047–2054.
[195] J. Raschenberger, C. Lamina, M. Haun, B. Kollerits, S. Coassin, E. Boes, L. Kedenko, A. Köttgen, F. Kronenberg, Influence of DNA extraction methods on relative telomere length measurements and its impact on epidemiological studies, Sci. Rep., 6 (2016) 25398.
[196] S. Reichert, H. Froy, W. Boner, T.M. Burg, F. Daunt, R. Gillespie, K. Griffiths, S. Lewis, R.A. Phillips, D.H. Nussey, P. Monaghan, Telomere length measurement by qPCR in birds is affected by storage method of blood samples, Oecologia, 184 (2017) 341–350.
[197] C.L. Dagnall, B. Hicks, K. Teshome, A.A. Hutchinson, S.M. Gadalla, P.P. Khincha, M. Yeager, S.A. Savage, Effect of pre-analytic variables on the reproducibility of qPCR relative telomere length measurement, PloS ONE, 12 (2017) e0184098.
[198] L. Brown, B. Needham, J. Ailshire, Telomere length among older US adults: differences by race/ethnicity, gender, and age, J. Aging Health, 29 (2017) 1350–1366.
[199] J. O'Sullivan, R.A. Risques, M.T. Mandelson, L. Chen, T.A. Brentnall, M.P. Bronner, M.P. Macmillan, Z. Feng, J.R. Siebert, J.D. Potter, P.S. Rabinovitch, Telomere length in the colon declines with age: a relation to colorectal cancer?, Cancer Epidemiol. Biomarkers Prev., 15 (2006) 573–577.

[200] M. Gardner, D. Bann, L. Wiley, R. Cooper, R. Hardy, D. Nitsch, C. Martin-Ruiz, P. Shiels, A.A. Sayer, M. Barbieri, S. Bekaert, C. Bischoff, A. Brooks-Wilson, W. Chen, C. Cooper, K. Christensen, T. De Meyer, I. Deary, G. Der, A. Diez Roux, A. Fitzpatrick, A. Hajat, J. Halaschek-Wiener, S. Harris, S.C. Hunt, C. Jagger, H.S. Jeon, R. Kaplan, M. Kimura, P. Lansdorp, C. Li, T. Maeda, M. Mangino, T.S.Nawrot, P. Nilsson, K. Nordfjall, G. Paolisso, F. Ren, K. Riabowol, T. Robertson, G. Roos, J.A. Staessen, T. Spector, N. Tang, B. Unryn, P. van der Harst, J. Woo, C. Xing, M.E. Yadegarfar, J.Y. Park, N. Young, D. Kuh, T. von Zglinicki, Y. Ben-Shlomo, Gender and telomere length: systematic review and meta-analysis, Exp. Gerontol., 51 (2014) 15–27.
[201] C. Dalgård, A. Benetos, S. Verhulst, C. Labat, J.D. Kark, K. Christensen, M. Kimura, K.O. Kyvik, A. Aviv, Leukocyte telomere length dynamics in women and men: menopause vs age effects, Int. J. Epidemiol., 44 (2015) 1688–1695.
[202] Y. Astuti, A. Wardhana, J. Watkins, W. Wulaningsih, Cigarette smoking and telomere length: a systematic review of 84 studies and meta-analysis, Environ. Res., 158 (2017) 480–489.
[203] J. Huzen, L.S.M. Wong, D.J. van Veldhuisen, N.J. Samani, A.H. Zwinderman, V. Codd, R.M. Cawthon, G.F.J.D. Benus, I.C.C. van der Horst, G. Navis, S.J.L. Bakker, R.T. Gansevoort, P.E. de Jong, H.L. Hillege, W.H. van Gilst, R.A. de Boer, P. van der Harst, Telomere length loss due to smoking and metabolic traits, J. Intern. Med., 275 (2014) 155–163.
[204] K.M. Getliffe, D. Al Dulaimi, C. Martin-Ruiz, R.L. Holder, T. von Zglinicki, A. Morris, C.U. Nwokolo, Lymphocyte telomere dynamics and telomerase activity in inflammatory bowel disease: effect of drugs and smoking, Aliment. Pharmacol. Ther., 21 (2005) 121–131.
[205] B. Iacopetta, Are there two sides to colorectal cancer?, Int. J. Cancer, 101 (2002) 403–408.
[206] P. Minoo, I. Zlobec, M. Peterson, L. Terracciano, A. Lugli, Characterization of rectal, proximal and distal colon cancers based on clinicopathological, molecular and protein profiles, Int. J. Oncol., 37 (2010) 707–718.
[207] J.M. Michael-Robinson, A. Biemer-Hüttmann, D.M. Purdie, M.D. Walsh, L.A. Simms, K.G. Biden, J.P. Young, B.A. Leggett, J.R. Jass, G.L. Radford-Smith, Tumour infiltrating lymphocytes and apoptosis are independent features in colorectal cancer stratified according to microsatellite instability status, Gut, 48 (2001) 360–366.
[208] S. Takagi, Y. Kinouchi, N. Hiwatashi, F. Nagashima, M. Chida, S. Takahashi, K. Negoro, T. Shimosegawa, T. Toyota, Relationship between microsatellite instability and telomere shortening in colorectal cancer, Dis. Colon Rectum, 43 (2000) 12-17.
[209] M. Gamulin, V. Garaj-Vrhovac, N. Kopjar, Evaluation of DNA damage in radiotherapy-treated cancer patients using the alkaline comet assay, Coll. Antropol., 31 (2007) 837–845.
[210] P. Sánchez-Suárez, P. Ostrosky-Wegman, F. Gallegos-Hernández, R. Peñarroja-Flores, J. Toledo-García, J.L. Bravo, E.R. Del Castillo, L. Benítez-Bribiesca, DNA damage in peripheral blood lymphocytes in patients during combined chemotherapy for breast cancer, Mutat. Res., 640 (2008) 8–15.
[211] C. Benitez-Buelga, L. Sanchez-Barroso, M. Gallardo, M. Apellániz-Ruiz, L. Inglada-Pérez, K. Yanowski, J. Carrillo, L. Garcia-Estevez, I. Calvo, R. Perona, M. Urioste, A. Osorio, M.A. Blasco, C. Rodriguez-Antona, J. Benitez, Impact of chemotherapy on telomere length in sporadic and familial breast cancer patients, Breast Cancer Res. Treat., 149 (2015) 385–394.
[212] H. Su, S. Lee, C.S. Ha, Prevention of radiation-induced telomere shortening, a novel mechanism underlying low-dose arsenic-mediated protection of normal T-lymphocytes, Int. J. Radiat. Oncol., 99 (2017) 618–619.
[213] T. Maeda, K. Nakamura, K. Atsumi, M. Hirakawa, Y. Ueda, N. Makino, Radiation-associated changes in the length of telomeres in peripheral leukocytes from inpatients with cancer, Int. J. Radiat. Biol., 89 (2013) 106–109.
[214] A. Fattorossi, A. Battaglia, G. Ferrandina, A. Buzzonetti, F. Legge, V. Salutari, G. Scambia, Lymphocyte composition of tumor draining lymph nodes from cervical and endometrial cancer patients, Gynecol. Oncol., 92 (2004) 106–115.

[215] C. Wang, T. Zhang, Y. Wang, Y. Li, C. Liu, H. Liu, L. Li, K. Ding, T. Wang, H. Wang, Z. Shao, R. Fu, The shortening telomere length of T lymphocytes maybe associated with hyper-function in servere aplastic anemia, Mol. Med. Rep., 17 (2018) 1015–1021.
[216] K. Najarro, H. Nguyen, G. Chen, M. Xu, S. Alcorta, X. Yao, L. Zukley, E.J. Metter, T. Truong, Y. Lin, H. Li, M. Oelke, X. Xu, S.M. Ling, D.L. Longo, J. Schneck, S. Leng, L. Ferrucci, N. Weng, Telomere length as an indicator of the robustness of B- and T-cell response to influenza in older adults, J. Infect. Dis., 212 (2015) 1261–1269.
[217] E. Jeanclos, A. Krolewski, J. Skurnick, M. Kimura, H. Aviv, J.H. Warram, A. Aviv, Shortened telomere length in white blood cells of patients with IDDM, Diabetes, 47 (1998) 482–486.
[218] K.D. Salpea, S.E. Humphries, Telomere length in atherosclerosis and diabetes, Atherosclerosis, 209 (2010) 35–38.
[219] J. Zhao, K. Miao, H. Wang, H. Ding, D.W. Wang, Association between telomere length and type 2 diabetes mellitus: a meta-analysis, PLoS ONE, 8 (2013) e79993.
[220] M.J. Sampson, M.S. Winterbone, J.C. Hughes, N. Dozio, D.A. Hughes, Monocyte telomere shortening and oxidative DNA damage in type 2 diabetes, Diabetes Care, 29 (2006) 283--289.
[221] H. Jia, Z. Wang, Telomere length as a prognostic factor for overall survival in colorectal cancer patients, Cell. Physiol. Biochem., 38 (2016) 122–128.

Svoluji k zapůjčení této práce pro studijní účely a prosím, aby byla řádně vedena evidence vypůjčovatelů.

Jméno a příjmení s adresou	Číslo OP	Datum vypůjčení	Poznámka